Charles University
Faculty of Science

Study programme: Biology
Branch of study: Immunology

Bc. Klára Hrabánková

Use of polymer prodrugs containing cucurbitacin D for the treatment of experimental tumours
Využití polymerních proléčiv s cucurbitacinem D pro léčbu experimentálních nádorů

Diploma thesis

Supervisor: RNDr. Milada Šírová, Ph.D.

Prague, 2021

Prohlášení

Prohlašuji, že jsem závěrečnou práci zpracovala samostatně a že jsem uvedla všechny použité informační zdroje a literaturu. Tato práce ani její podstatná část nebyla předložena k získání jiného nebo stejného akademického titulu.

V Praze, 26. 4. 2021 Bc. Klára Hrabánková

Acknowledgements

I would like to thank my supervisor RNDr. Milada Šírová, Ph.D., for patient guidance and valuable advice needed to successfully process my diploma thesis. I would like to thank all my colleagues from the Laboratory of Tumour Immunology for their practical help. Last but not least, my family and friends also deserve huge thanks for their support throughout the years of my studies.

Abstract

Chemotherapy is still the most widely used anti-cancer treatment. The majority of chemotherapeutics inhibit proliferating cells generally, not selectively cancer cells. The side effects associated with chemotherapy can be partly limited by conjugating a cytotoxic drug with a polymer nanocarrier. Such binding facilitates solubility in aqueous solutions, reduces systemic toxicity; and passively targets the drug directly into the tumour through the enhanced permeability and retention (EPR) effect.

This thesis focuses on testing polymer conjugates based on N-(2-hydroxypropyl)methacrylamide (HPMA) carrying cucurbitacin D (CuD), a naturally occurring compound with potential anti-cancer activity. The mechanism of action is not elucidated yet, but several studies have depicted the inhibitory effect on signal transducer and activator of transcription 3 (STAT3) transcription factor. A STAT3 signalling pathway is overexpressed in several cancer cell lines and is also involved in the differentiation of myeloid-derived suppressor cells (MDSCs).

We examined the therapeutic effect of the HPMA copolymers based on CuD in combined therapy with other polymer chemotherapeutics. CuD conjugates have shown in vitro cytotoxic effect on several model cancer cell lines. The combination with conjugates carrying doxorubicin (Dox) reduced tumour growth in the course of *in vivo* therapy. Moreover, the effect of CuD-based conjugates on blocking the MDSC-mediated immunosuppression over the course of the Dox-based combined therapy was studied.

Keywords: cancer; immune-oncotherapy; cucurbitacin D; STAT3 signalling pathway; MDSCs; HPMA copolymers

Abstrakt

Chemoterapie je stále nejběžněji používaný typ protinádorové terapie. Většina chemoterapeutik obecně inhibuje proliferující buňky a necílí selektivně na nádorové buňky. Chemoterapie je spojena s vedlejšími účinky, které lze částečně omezit využitím polymerních nosičů konjugovaných s nízkomolekulárními léčivy. Vazba léčiva na polymer zlepšuje jeho rozpustnost ve vodných roztocích, snižuje systémovou toxicitu a pasivně jej cílí přímo do nádoru prostřednictvím efektu zvýšené propustnosti a retence.

Práce je zaměřena na testování polymerních konjugátů založených N-(2-hydroxypropyl)methacrylamidu (HPMA) nesoucího cucurbitacin D (CuD), přirozeně se vyskytující sloučeninu s potenciální protinádorovou aktivitou. Mechanismus účinku dosud není objasněn, ale několik studií popisuje inhibici fosforylace a dimerizace signal transducer and activator of transcription 3 (STAT3) transkripčního faktoru, který je overexprimován u řady nádorových linií a hraje roli v diferenciaci myeloidních supresorových buněk (MDSCs).

V této diplomové práci jsme zkoumali terapeutický účinek HPMA kopolymerů na bázi CuD v kombinované terapii s jinými polymerními chemoterapeutiky. Cytotoxický účinek polymerních konjugátů s CuD byl patrný *in vitro* u několika modelových nádorových linií. *In vivo* léčebné experimenty ukázaly, že kopolymery s CuD v kombinaci s konjugáty nesoucími doxorubicin (Dox) snižují růst nádoru. Polymery nesoucí CuD byly též studovány v kontextu blokování imunosuprese zprostředkované MDSCs za účelem zlepšení terapeutických výsledků léčby společně s jinými polymerními chemoterapeutiky.

Klíčová slova: nádorová onemocnění; imunoonkoterapie; cucurbitacin D; STAT3 signalizační ndráha; MDSCs; HPMA kopolymery

List of abbreviations

APC	Antigen presenting cell
ARG1	Arginase 1
CAR	Chimeric antigen receptor
CCL	Chemokine (C–C motif) ligand
CD	Cluster of differentiation
CTLA-4	Cytotoxic T lymphocyte antigen-4
CuD	Cucurbitacin D
DC	Dendritic cell
Dox	Doxorubicin
Dtx	Docetaxel
EPR effect	Enhanced permeability and retention effect
FACS	Fluorescence-activated cell sorting
FDA	Food and drug administration
GM-CSF	Granulocyte-macrophage colony-stimulating factor
HER2	Human epidermal receptor 2
HLA	Human lymphocyte antigen
HPMA	N-(2-Hydroxypropyl)methacrylamide
IDO	Indolamine-2,3-dioxygenase
IκB	Inhibitor of κB
IKK	Inhibitor of κB kinase
IL	Interleukin
iNOS	Inducible nitric oxide synthase
i.p.	Intraperitoneal
i.t.	Intratumoural
i.v.	Intravenous
Jak	Janus kinase
LP	Linear polymer
MDSC	Myeloid-derived suppressor cell
MHC	Major histocompatibility complex
MP	Micellar polymer
NF-κB	Nuclear factor kappa-light-chain-enhancer of activated B cells
NK cell	Natural killer cell

NO	Nitric oxide
NOX2	NADPH oxidase 2
PD-1	Programmed cell death-1
PD-L1/2	Programmed cell death ligand-1/2
PEG	Polyethylene glycol
RNS	Reactive nitrite species
ROS	Reactive oxygen species
s.c.	Subcutaneously
STAT	Signal transducer and activator of transcription
TAM	Tumour associated macrophage
TCR	T cell receptor
TGF-β	Transforming growth factor-beta
TIL	Tumour infiltrating T cell
Treg	Regulatory T cell
VEGF	Vascular and endothelial growth factor

Table of contents

1 Introduction

In countries with a developed socio-economic structure, cancer is regularly one of the most prominent causes of death. According to the statistics, every third citizen of the Czech Republic has encountered cancer and the incidence is steadily increasing. The causes could be the ageing and lifestyle of the population, better diagnostic protocols or regularly done screenings. The most common tumour types are skin, colorectal, prostate, breast or lung cancers. Although the number of oncological patients increases, the percentage of successfully treated patients with significantly prolonged survival is also growing. It is a result of early diagnostics, increasing progress in general healthcare and newly developed therapeutic protocols. During the last few decades, the field of cancer therapy has significantly progressed from the classical approaches such as surgical removal, radiotherapy and chemotherapy towards targeted personalized therapies. Cancer immunotherapy has been one of the most outstanding advancements made in cancer treatment in recent years. The combination of immunotherapy with conventional treatment enhances the initiation of anti-tumour responses and helps to increase therapeutic success rates.

The basis of conventional chemotherapy is to prevent the proliferation of rapidly dividing tumour cells. Chemotherapeutic agents inhibit mitosis or affect DNA replication. Such cytotoxic agents target all dividing cells and their effect is non-specific, therefore causing severe side effects. The attachment of a cytotoxic drug to a polymer nanocarrier can prevent some of the adverse effects while bringing benefits such as improvement of water solubility or prolonged half-time in the circulation. Polymer conjugates are passively accumulated in the tumour microenvironment due to the EPR effect. High molecular weight polymers do not pass through the wall of normal healthy vessels. The vessels associated with the solid tumours are widely fenestrated, which allows the polymer-conjugated drug to leave the bloodstream passing directly into the tumour microenvironment.

HPMA belongs to the most studied types of polymer nanocarriers so far. Cucurbitacins are a class of tetracyclic triterpenoids naturally occurring in the plant family of Cucurbitaceae. Cucurbitacins have been known in traditional medicine for their beneficial anti-inflammatory properties. Cucurbitacin D (CuD) represents a potential novel drug with a potent anti-cancer effect demonstrated on several tumour cell lines. The attachment of CuD onto a suitable nanocarrier, in this case, HPMA, could improve its solubility and delivery specifically into the tumour tissue and could serve as a useful tool to improve the efficacy of systemic anti-cancer chemotherapy.

2 Literature review

2.1 Tumorigenesis and anti-tumour immune response

Cancer remains one of the leading causes of death globally, with more than 10 million new cases per year and incidence rapidly growing all over the world.[1] The immune system interacts with tumour cells very closely to create an immune-suppressive milieu within the tumour microenvironment. The communication between the immune system and malignant cells has been first described in the 1970s by Frank Macfarlane Burnet. He came with the idea that tumour-specific neoantigens or tumour-associated antigens induce an immune response against cancer cells via the process of tumour immune surveillance.[2]

A few years later, the concept of three phases, the so-called three Es of cancer immunoediting, was formulated by two colleagues, Gavin Dunn and Robert Schreiber. In the first elimination phase, tumour cells are successfully destroyed by both innate and adaptive immunity. Nonetheless, due to genetic instability and constant cell division, tumours can generate clones with reduced immunogenicity that can evade immune elimination. In the second phase, the host immune system and tumour cells that have survived the elimination process enter a dynamic equilibrium. If the immune system fails to destroy the tumour cells, the malignant process proceeds to its third, escape phase, which results in the clinically detectable tumour.[3] *(Fig.1)*

Growing tumours adopt several strategies to escape immune surveillance to successfully develop in the body. In the early 2000s, Hanahan and Weinberg came up with the idea of six biological capabilities acquired during the development of human tumours. Those processes enable tumour cells to become malignant and tumour mass to grow and spread through metastasis. The original six hallmarks of cancer include sustaining proliferative signalling, evading growth suppressors, resisting cell death, enabling replicative immortality, inducing angiogenesis, and activating invasion and metastasis. An increasing body of research suggests that two additional hallmarks are involved in the pathogenesis of cancer. The first one includes the capability to modify cellular metabolism to reinforce neoplastic proliferation. The second allows cancer cells to evade immunological destruction by adaptive and innate immune cells such as T and B lymphocytes, macrophages or natural killer (NK) cells.[4]

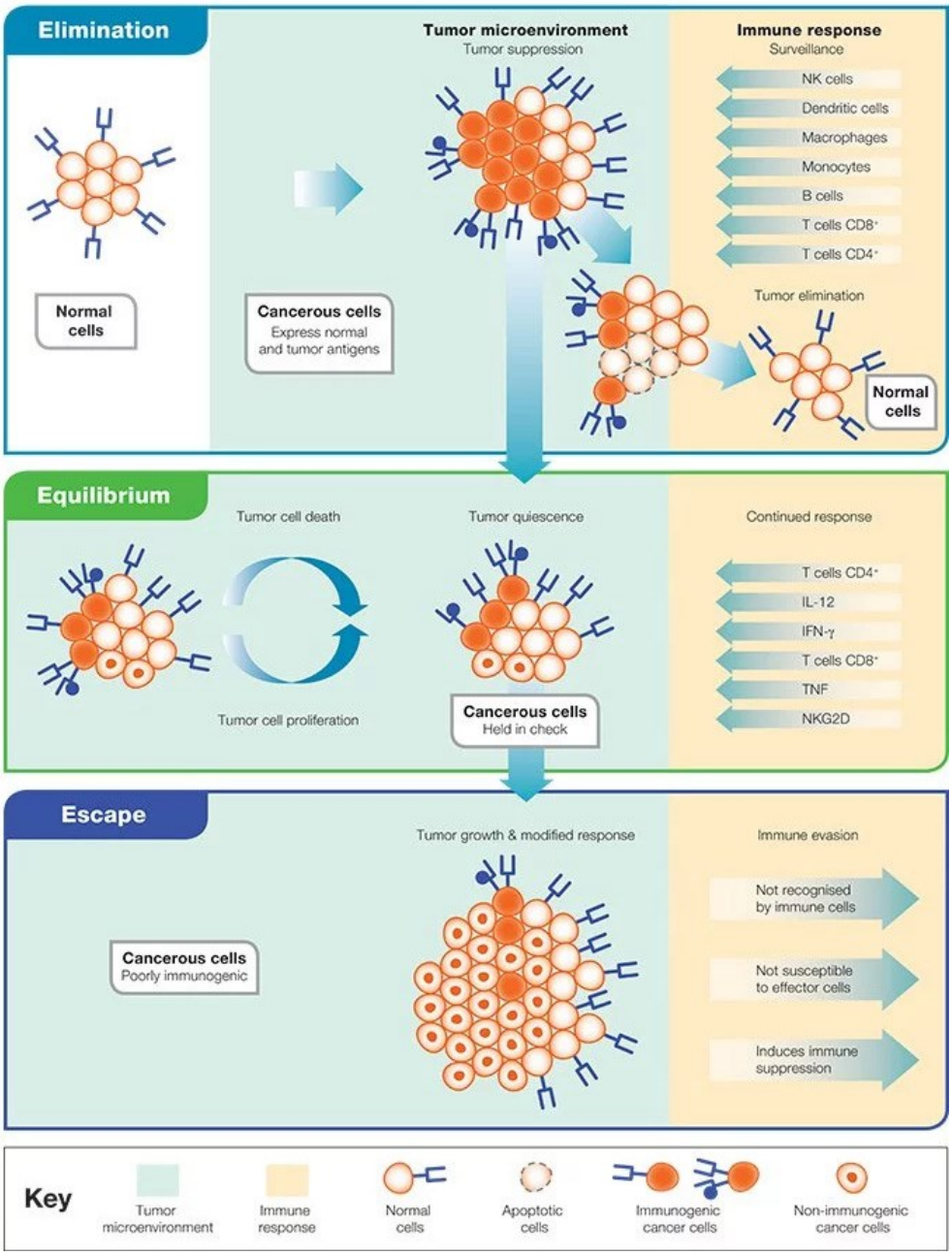

Figure 1 | An illustration of cancer immunoediting. The process is divided into three stages; elimination, equilibrium and escape. During the elimination phase, tumour cells are successfully destroyed by the immune system. In the equilibrium phase, the surviving cancer cells are held under control in the state of tumour dormancy. The escape phase manifests as a clinically visible tumour. IFN – Interferon; IL – Interleukin; NK – Natural killer; NKGD2 – Natural killer group 2D; TNF – tumour necrosis factor. Adapted from [3]

Despite the intensive research, the role of the immune system in the formation, progression and eradication of malignant cells remains to be more thoroughly elucidated. The increased risk of cancer after immunosuppression and subsequent organ transplantation highlights the importance of immunological surveillance.[5] Additionally, some immunosuppressed organ transplant recipients have been observed to develop donor-derived cancers, suggesting that in healthy donors, the cancer cells are held under the control of a fully functional immune system and the defence falls once transplanted to the immunocompromised recipient.[6]

In mouse models genetically engineered to be deficient in different components of the immune system, tumours arise more frequently and grow more rapidly compared to the immunocompetent controls. Impaired development and function of $CD8^+$ T lymphocytes, $CD4^+$ T lymphocytes, or NK cells increase cancer incidence. Moreover, mice with combined immunodeficiencies in both T and NK cells are even more susceptible to cancer development, which indicates that both innate and adaptive components of the immune system contribute to immune surveillance and thus tumour eradication.[3] Although considerable knowledge has been accumulated on how tumours avoid destruction, discovering effective cancer immunotherapies remains a challenging task.

2.2 Tumour immune evasion strategies

The molecular mechanisms by which cancer cells evade the host immune system have been investigated both in mouse models and human clinical samples for years. Rather than creating novel innovative strategies, tumour cells hijack the body's regulatory circuits that control tolerance and homeostasis. In the past decades, several important immune evasion mechanisms have been described.

2.2.1 Defective antigen presentation and lack of costimulation

A typical and well-documented mechanism by which tumour cells evade immune surveillance is the downregulation or complete loss of expression of tumour antigens on the cell surface.[7] Moreover, malignant cells can modulate the antigen processing machinery and affect the MHC I antigen-presenting pathway. Losing the human leukocyte antigen (HLA) decreases the ability to present tumour neoantigens and facilitates the process of immune evasion. For instance, in approximately half of the human non-small cell lung cancer patients, there is a loss of heterozygosity in HLA molecules, cancer cells present fewer antigens and therefore evade the control of the immune system.[8]

Moreover, most tumour cell lineages lack the expression of positive costimulatory molecules B7-1 (CD80) and B7-2 (CD86). T cell activation occurs through the recognition of a specific peptide presented on MHC molecules by $CD8^+$ or $CD4^+$ T cells bearing antigen-specific T cell receptor (TCR). However, the first signal for the activation of naive T cells is insufficient to initiate an effective immune response and additional signals from costimulatory molecules are needed. Therefore, the absence of costimulatory signal provided by the CD28 molecule on $CD8^+$ or $CD4^+$ T cells bound to CD80/86 on the surface of APCs leads to T cell unresponsiveness and anergy.[9]

2.2.2 Expression of inhibitory checkpoint molecules

Besides the absence of costimulation, tumour cells can also use negative regulatory pathways to terminate ongoing immune responses. One of the pathways includes a programmed cell death-1 (PD-1) molecule that was originally isolated from T cells undergoing apoptosis.[10] PD-1 is a negative costimulatory receptor that can be expressed on the cell surface of activated T and B cells, NKT cells, monocytes, or dendritic cells (DC). The PD-1 receptor has two known ligands. PD-L1 (B7-H1, CD274) is expressed on many cell types and

is important for the maintenance of immunological tolerance at immunologically privileged sites. PD-L2 (B7-DC, CD273) is a ligand expressed mainly on APCs and is involved in the negative regulation of the adaptive immune response. It has been observed that both ligands can be expressed on many types of tumour cells causing deletion or anergy of tumour reactive cells.[11]

Another coinhibitory receptor, cytotoxic T lymphocyte antigen-4 (CTLA-4), was described as a member of the immunoglobulin superfamily and the CD28 homologue. Unlike the constitutively expressed CD28 molecule, the expression of CTLA-4 is inducible with peak expression approximately two days after T cell activation. CTLA-4 binds CD80/86 molecules with much greater affinity than CD28. Such competitive binding limits T cell proliferation and survival, resulting in suppression of immune responses. CTLA-4 expressed by Treg cells can bind to CD80/86 molecules, thereby inhibit costimulatory signals and suppress the function of APCs in the tumour microenvironment.[11]

2.2.3 Secretion of immunosuppressive mediators

The production of immunosuppressive molecules strongly contributes to maintaining an immune tolerant milieu within the tumour microenvironment. Suppressive cytokines are secreted either by the cancer cells themselves or by the non-cancerous cells present in the tumour microenvironment. Main immunosuppressive cytokines include TGF-β and IL-10.

Mutations in the TGF-β pathway are observed in many human cancers, and overactivation of this pathway is associated with rapid tumour progression and poor prognosis of patients. It has been described that TGF-β stimulates tumorigenesis by promoting angiogenesis and suppressing the innate and adaptive anti-tumour immune responses.[12]

Production of IL-10, another immunosuppressive cytokine, correlates with disease aggressiveness in many types of tumour cells, such as non-small cell lung or gastrointestinal cancer. Several studies have reported that a high level of serum IL-10 corresponds with worse clinical outcome in cancer patients in both solid and haematological malignancies.[13]

In addition to immunosuppressive cytokines, tumour cells secrete various types of immunomodulatory and growth factors. Vascular endothelial growth factor (VEGF), for instance, is released by many human cancer cell lines and plays a critical role in the development of tumour vasculature. However, VEGF is known to inhibit the differentiation of hemopoietic progenitor cells into mature DCs, thus preventing the antigen uptake and efficient tumour antigen presentation.[14]

2.2.4 Recruitment of immunosuppressive cells

Immune suppression in the tumour microenvironment, mediated by various types of suppressive cells, seems to be a major mechanism of tumour immune escape and can be a crucial hurdle in the path to successful immunotherapy. The immunosuppressive tumour microenvironment is filled with immunosuppressive cells, including Treg cells, myeloid-derived suppressor cells (MDSCs) and tumour-associated macrophages (TAMs). These cells are drawn into the tumour microenvironment via tumour produced chemokine gradient including chemokine (C–C motif) ligand 17 (CCL17) or chemokine (C–C motif) ligand 22 (CCL22).[15]

2.2.4.1 T regulatory cells

Treg cells are essential for maintaining homeostasis, establishing peripheral tolerance and preventing autoimmune diseases. However, they can also act to prevent beneficial responses and diminish anti-tumour immunity. Tregs are characterized by the expression of one key transcription factor, the forkhead box P3 (*Foxp3*), which is needed for their development, function and maintenance. Murine, as well as human Treg cells, are identified by several surface markers such as CD4, CD25, also known as interleukin-2 (IL-2) receptor-α, and CD127, known as the interleukin-7 receptor.[16] Treg cells suppress immune functions through various mechanisms that can be divided into four general modes of actions. These include the production of immunosuppressive molecules, direct suppression by cytolysis, metabolic disruption and inhibition of the APCs.[17]

In the tumour microenvironment, Tregs typically produce inhibitory cytokines, such as TGF-β or IL-10, to inhibit the activation of effector T cells. Cytotoxic substances, such as perforin and granzyme, directly kill tumour-specific $CD8^+$ T lymphocytes. Another immunosuppressive mechanism is mediated by CD25, high-affinity IL-2 receptor-α, which rapidly consumes IL-2 and thereby limits the amount of IL-2 needed for the effector T cell to proliferate. Moreover, Tregs express integral membrane enzymes, such as CD39 and CD73, which metabolize extracellular ATP to adenosine, which consequently binds adenosine A2a receptor and inhibits effector T cell activation.

Additionally, the interaction between CTLA-4, expressed by Treg cells and CD80/86 on the surface of APCs, impairs their maturation and promotes secretion of IDO.[17] The activity of this enzyme inhibits the activation of effector T cells through depletion of the essential amino acid tryptophan and promotes differentiation and activation of Tregs through

the production of cytotoxic tryptophan metabolites called kynurenines. It is not surprising that the upregulation of IDO in tumours has been associated with poor prognosis of patients in several types of cancer.[18] IDO has been found to promote the recruitment of another immunosuppressive cell type, MDSCs, into the tumour tissue of experimental animal models, as well as human melanoma patients.[19] Moreover, Tregs control the differentiation and function of MDSCs via the production of immunomodulatory cytokine TGF-β. Tregs genetically engineered to lack the expression of TGF-β are not able to regulate the activation and function of MDSCs. Besides, adoptive transfer of wild-type Tregs, not TGF-β-deficient Treg cells, restored the immune-modulatory functions of MDSCs, as illustrated on the model of experimentally induced murine colitis. Aside from chronic inflammatory conditions such as colitis, the interaction between Tregs and MDSCs via the production of TGF-β may also play an important part in the coordination of the anti-tumour immunity.[20]

2.2.4.2 Myeloid-derived suppressor cells

One of the most prominent populations contributing to the immunosuppressive milieu within the tumour microenvironment are MDSCs, defined as a heterogeneous population of immature myeloid cells at different stages of differentiation. Under physiological condition, myeloid progenitors differentiate into mature mononuclear cells including monocytes, macrophages and DCs; as well as into polymorphonuclear cells such as neutrophils, eosinophils, basophils and mast cells. In contrast, under pathological condition, during chronic inflammation or tumour progression, these cells remain undifferentiated. Although similar to neutrophils and monocytes in morphology and phenotype, their functional characteristic lays in the ability to foster tumour progression by suppressing immune responses, promoting tumour cell survival and invasiveness to normal healthy tissues.[21]

2.2.4.2.1 Immunomodulatory properties of MDSCs

MDSCs exploit plenty of mechanisms to influence both innate and adaptive immune responses. Broadly speaking, these mechanisms can be divided into four distinct classes. *(Fig.2)* Firstly, MDSCs in the tumour microenvironment execute their role via the secretion of suppressive cytokines. It has been described that membrane-bound TGF-β1 on MDSCs is responsible for the inhibition of NK cell function via cell-to-cell contact mechanism.[22] Moreover, MDSCs producing IL-10 decrease the production of IL-12 by pro-inflammatory M1 macrophages and skew them toward a suppressive M2 phenotype.[23]

The second immune-suppressive strategy is to eliminate the key nutrition factors for activated T cells within the tumour microenvironment. L-arginine is a substrate for the enzyme arginase-1 (ARG1) highly expressed by MDCSs. Low arginine concentrations decrease T cell proliferation and activation, cytokine production, and eventually lead to complete loss of the TCRζ chain.[24] Similarly, MDSCs consume L-cysteine from the tumour microenvironment, limiting the availability of this essential amino acid needed for T cell activation.[25] Additionally, MDSCs express high levels of IDO, an enzyme that metabolizes essential amino acid L-tryptophan. The reduction of local tryptophan levels and generation of cytotoxic metabolites called kynurenines leads to impairment of immune responses initiated by effector T cells and a reciprocal increase in infiltration of Tregs into the tumour microenvironment.[26]

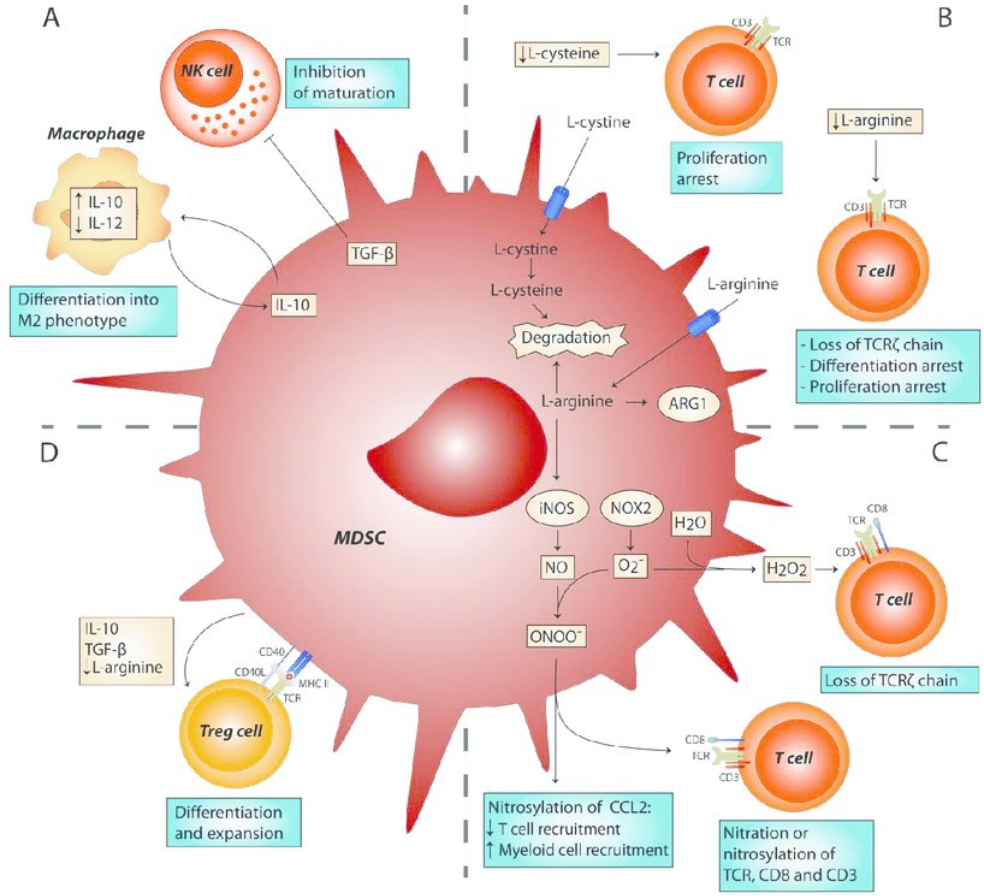

Figure 2 | Immunosuppressive mechanisms used by MDSCs. (A) Secretion of TGF-β and IL-10. (B) Deprivation of L-cysteine and L-arginine. (C) Production of hydrogen peroxide and peroxynitrite. (D) Induction of development and expansion of Treg cells. ARG1 – arginase 1; CCL – chemokine (C–C motif) ligand; IL – interleukin; iNOS - inducible nitric oxide synthase; NK – natural killer; NOX2 – NADPH oxidase 2; TCR – T cell receptor; TGF – transforming growth factor. Adapted from [27]

Thirdly, MDSCs produce reactive oxygen species (ROS) and reactive nitrogen species (RNS). The increased ROS production by MDSC is mediated by the upregulated activity of NADPH oxidase (NOX2), which produces superoxide anions reacting with water to form hydrogen peroxide.[28] RNS are generated by inducible nitric oxide synthase (iNOS). Production of nitric oxide in combination with superoxide anion results in the formation of peroxynitrite.[29] It has been documented that peroxynitrite causes nitration and nitrosylation of components of the TCR signalling complex and, together with hydrogen peroxide, induces modification of TCR molecules. $CD8^+$ T cells with defective TCRs lose the ability to bind peptides presented on MHC molecules and as result, antigen-specific non-responsiveness is established.[30] Moreover, MDSC-derived peroxynitrite causes modification of chemokine (C-C motif) ligand 2 (CCL2) resulting in decreased infiltration of effector $CD8^+$ T cells into the tumour microenvironment.[31]

At last, MDSCs induce differentiation of Tregs from naive $CD4^+$ T cells, as well as activation and expansion of already existing Treg populations. MDSC-mediated Treg expansion is found to be mediated via the interaction of the TCR with MHC-II and CD40 with CD40 ligand.[32, p. 40] Furthermore, the production of soluble factors such as IL-10 or TGF-β, and deprivation of L-arginine from the environment may also contribute to the polarization towards Treg cell phenotype.[33], [34]

2.2.4.2.2 MDSCs in mice

At present, it is well known that there are at least two main subsets of MDSCs, as identified in tumour-bearing mice as well as in humans. The first is the polymorphonuclear subset (PMN-MDSCs), which phenotypically and morphologically resembles neutrophils. The second is the monocytic subset (Mo-MDSC), which is similarly close to monocytes. As a heterogeneous population of cells, MDSCs can express several markers, which overlap with other myeloid lineage cells involving DCs, neutrophils or monocytes. MDSCs are not a subset of cells defined by the expression of a single specific marker. In mice, they were first characterised by the co-expression of myeloid lineage differentiation antigen Gr-1 and myeloid cell marker CD11b. Later on, more detailed phenotyping by two epitopes of myeloid differentiation antigen Gr-1, Ly-6G and Ly6C was added. Taken together, MDSCs in tumour-bearing mice can be distinguished as $CD11b^+Ly6C^{high}Ly6G^-$ monocytic MDSCs, and $CD11b^+Ly6C^{low}Ly6G^+$ polymorphonuclear MDSCs.[35]

For further identification, MDSCs were defined as lacking the surface markers of fully differentiated mononuclear phagocytes, CD11c and MHCII. Mo-MDSCs express very low levels of mature monocytic and macrophage marker F4/80, but its surface expression is insignificant when compared to TAMs.[36] At normal steady-state conditions in naïve mice, MDSCs are commonly found in bone marrow, and sporadically in the spleen, blood, pancreas or liver. Numerous studies have shown an increase in the frequency of MDSCs early in tumour development in the peripheral blood, which further advances upon tumour progression. When analysed in different models of tumour-bearing mice, almost all models demonstrated a preferential expansion of PMN-MDSCs over Mo-MDSC phenotype.[35], [37] In contrast, PMN-MDSCs were identified as less immunosuppressive compared to Mo-MDSCs, whether demonstrated using *in vitro* assays or as observed *in vivo*, following adoptive cell transfer.[38], [39]

2.2.4.2.3 MDSCs in humans

In recent years, a large body of research has documented a significant increase in MDSCs in human cancer patients. The increase in MDSCs both circulating in peripheral blood as well as infiltrating the tumour tissue has been described in various types of tumours, for instance melanoma, non-small lung cancer or renal carcinoma.[24], [40], [41]

Unlike mice, human MDSCs cannot be characterized based on the myeloid lineage differentiation antigen Gr-1 because of the absence of a homologous gene in humans. Therefore, human MDSCs are generally defined as cells that express CD11b and the common myeloid marker CD33. At the same time, human MDSCs lack the expression of markers of mature myeloid and lymphoid cells and the MHCII molecule HLA-DR.

The subsequent characterisation into the two main MDSC subsets is done using the expression of CD14 and CD15 surface markers. The human equivalent of PMN-MDSC is defined as $CD11b^{+}CD14^{-}CD15^{+}$ and often expresses an activation marker of human granulocytes, CD66b. On the other hand, human Mo-MDSCs are identified as having $CD11b^{+}CD14^{+}HLA\text{-}DR^{-/lo}CD15^{-}$ phenotype.[36] The frequency of each MDSC subset appears to be influenced by the type of cancer. For instance, studies have shown that while patients with metastatic melanoma demonstrate an increase of Mo-MDSCs, the main immunosuppressive subset in patients suffering from renal cancer is the PMN-MDSCs.[24], [40]

2.2.4.2.4 STAT3 signalling in MDSCs

STAT3 belongs to the signal transducer and activation (STAT) family of signal-responsive transcription factors. The STAT family of transcription factors mediates signals from various cytokine and growth factor receptors. Upon engagement of a ligand, receptors dimerize and activate receptor-associated Janus kinases (Jak), which phosphorylate both each other and the intracellular tails of their receptors. Jak-mediated phosphorylation activates STAT proteins, which then form either homo or heterodimers, translocate to the cell nucleus, bind directly to DNA, and regulate gene expression of multiple target genes.[42] Previously published reports suggest that STAT3 is overexpressed in various tumour types, such as human ovarian or prostate cancer cells.[43]–[45]

Moreover, it has been described that the STAT3 signalling pathway plays a major role in MDSC expansion and activation of suppressive mechanisms within the tumour microenvironment. Recent studies provide evidence documenting the STAT3 overexpression in MDSCs infiltrating the tumour microenvironment in mice and humans. For example, genetic deletion of suppressor of cytokine signalling 3 (SOCS3) protein, a negative regulator of STAT3 activation, leads to an accumulation of MDSCs in murine models of prostate cancer.[46] The central role of this signal-transducing molecule in human MDSCs was first described as an increase of overall STAT3 phosphorylation in MDSCs found in the blood of patients with advanced melanoma.[47]

STAT3 pathway in MDSCs is activated in response to several tumour-derived factors, for example, GM-CSF or VEGF. Such signals stimulate the expression of distinct proteins, including c-Myc, Bcl-XL, cyclin D1 and survivin. These proteins promote the proliferation of immature myeloid cells while preventing apoptosis and differentiation into mature cells, resulting in increased numbers of MDSCs.[48] Tumour-induced STAT3 upregulation of S100A9 protein in myeloid progenitors inhibits their differentiation into fully mature DCs and macrophages while expanding MDSCs. In the absence of S100A9 protein, MDSCs accumulation is suppressed and anti-tumour immune responses are restored.[49] It has been described that high levels of phosphorylated STAT3 found in MDSCs correlate with upregulation of ARG1 expression and activity.[50] Moreover, STAT3 directly regulates suppressive mechanisms in MDSCs by inducing higher expression of NOX2 subunits. Upregulation of NOX2 leads to increased ROS production, which contributes to the impaired myeloid cell differentiation.[49], [51]

Targeting the STAT3 signalling pathway could prevent the expansion and recruitment of MDSCs, inhibit their suppressive functions, and induce the differentiation of MDSCs into the mature myeloid cells. Indeed, there are several targeted cancer therapies that affect directly MDSCs. For instance, administration of axitinib, a selective inhibitor of VEGF receptor, exerts an anti-cancer effect in renal cell carcinoma by inhibition of STAT3 signalization and reducing the numbers of MDSCs.[52] Treatment of tumour-bearing mice with kinase inhibitors such as sorafenib or sunitinib reduces the frequency of tumour-infiltrating MDSCs in murine liver and renal cell carcinoma models.[53], [54] Moreover, several natural compounds such as cucurbitacin I, enhance the differentiation of immature myeloid cells into mature DCs by direct inhibition of the STAT3 pathway.[55] Taken together, pharmacological inhibition of the Jak2/STAT3 pathway may be a potentially useful tool in improving cancer immunotherapy.

2.3 Immune therapeutic strategies

Most cancer treatments include classical approaches how to eliminate malignant cells. These include typically surgery, radiation therapy and chemotherapy. In light of recent findings, an increasing number of clinical trials is currently focused on enhancing the anti-cancer mechanisms of the immune system. Following many initial clinical failures, the field of cancer immunotherapy has been one of the most progressive advancements made in cancer therapeutics in recent years and the combination of immunotherapy with conventional therapies is the leading path to the enhancement of anti-tumour responses and increased therapeutic success. Cancer immunotherapies include various approaches, ranging from stimulating effector mechanisms to counteracting inhibitory and suppressive mechanisms.

2.3.1 Nonspecific immune stimulation

This immunotherapeutic strategy gives the immune system an overall boost and can be used alone or in combination with other treatments to support long-lasting immune responses. Nonspecific immune stimulation treatments include the therapeutic administration of recombinant cytokines. Cytokine treatment enhances the activation and communication among immune cells. On the other hand, cytokines have a short biological half-life in the bloodstream and relatively low patient response rates. Besides, the administration of cytokines at high doses carries a risk of systemic toxicity accompanied by several adverse effects.

Administration of IL-2 was the first clinical immunotherapy approved for the treatment of metastatic melanoma and renal carcinoma, although high doses of IL-2 can cause many side effects including capillary leak syndrome.[56], [57] IFN-α has only limited effects when used as a single cancer treatment, but it is used as an adjuvant in melanoma therapy.[58]

2.3.2 Cancer vaccines

The aim of therapeutic cancer vaccination is to prime tumour-specific immune responses via induction of $CD4^+$ and $CD8^+$ T cells capable of recognizing tumour-expressed antigens. There are several types of cancer vaccines currently being evaluated as a treatment of diverse types of tumours. Vaccines are based on tumour cell lysates, purified or recombinant tumour antigens, recombinant DNA or RNA molecules, as well as DCs or viral vectors. Unfortunately, the main obstacle in the development of successful cancer vaccines remains the identification of suitable tumour neoantigens.[59]

Aside from therapeutic vaccines, there are several prophylactic vaccines approved for prevention against cancer-causing viral infections, including hepatitis B virus and human papillomavirus.[59] Despite initial clinical failures, therapeutic cancer vaccine research has succeeded with the approval of sipuleucel-T (Provenge) for the treatment of metastatic castration-resistant prostate cancer. The vaccine is created by isolating DCs from the peripheral blood of each patient. Isolated DCs are activated *ex vivo* in the presence of recombinant antigen, the prostatic acid phosphatase, which is specifically expressed on prostate cancer cells. As an immune activator, the granulocyte-macrophage colony-stimulating (GM-CSF) factor is used. Eventually, those DCs are returned to the patient to potentiate the anti-tumour T cell response.[60]

2.3.3 Adoptive cell transfer

Adoptive cell transfer is yet another promising type of immunotherapeutic strategy involving the improvement of T cell anti-tumour properties. There are two main types of adoptive cell transfer strategies; one relies on collecting the patient´s tumour-infiltrating lymphocytes (TIL); the other is based on engineering new chimeric antigen receptor (CAR) on T cells to recognize specific tumour antigens on the surface of cancer cells. TIL are firstly isolated from patients' resected metastatic tumour tissue, expanded *ex vivo* in the presence of a high dosage of IL-2, and infused back into the patient. This approach attempts to reverse the functional impairment of T cells residing within the tumour caused by the immune suppressive mechanisms described above (Chapter 2.2). The adoptive transfer of TILs is therefore preceded by lymphodepleting chemotherapy eliminating immunosuppressive cells such as Tregs and MDSCs. Moreover, TIL infusion is accompanied by the administration of IL-2 to achieve durable clinical responses after the transfer of TILs.[61]

The second advanced technique of adoptive cell transfer is based on the isolation of T cells from a patient's peripheral blood and their subsequent genetic modification. Genetically engineered CARs consist of an antibody-derived immunoglobulin variable domain fused with CD3ζ domains of TCR complex. Retroviral or lentiviral recombinant vectors containing cloned DNA plasmids are transfected into target cells creating T cells bearing TCRs that can be potentially targeted against any cell surface antigen. CD19-targeted CAR T cell treatment of patients with hematologic malignancies have demonstrated to be beneficial. On the contrary, CAR T cell therapy of solid tumours has yielded only limited efficacy, therefore, it needs to be further optimized.[62]

2.3.4 Monoclonal antibodies

Humanized or chimeric monoclonal antibodies that are designed to target specific tumour antigens work in various ways. Monoclonal antibodies can either block growth factors and their receptors, cross-link surface antigens resulting in cell death by antibody-dependent cellular cytotoxicity, or deliver other therapeutic agents such as cancer drugs or radiation particles directly to targeted cancer cells.

An example of a blocking humanized monoclonal antibody is bevacizumab. It was found to potently neutralize VEGF, a critical angiogenic factor involved in pathological alternations of tumour vasculature.[63] Bevacizumab has been evaluated in clinical trials as a treatment for various types of tumours, such as metastatic colorectal cancer or advanced non-small-cell lung carcinoma.[64], [65] Rituximab is a chimeric monoclonal antibody with a specific affinity for the B lymphocyte transmembrane protein, CD20, which is expressed on normal and most malignant B cells. Rituximab was first approved by Food and Drug Administration (FDA) for the treatment of Non-Hodgkin's lymphoma. Since then, it has become a standard in the treatment of several types of B cell malignancies.[66] Another humanized monoclonal antibody used in cancer treatment is trastuzumab, which targets the extracellular domain of human epidermal growth factor receptor 2 (HER2). It has been described that overexpression of HER2 in breast cancer is associated with worse clinical outcome. Therefore, the treatment with trastuzumab in combination with chemotherapy significantly improves survival among women with HER2-positive breast cancer.[67]

An example of a drug-conjugated monoclonal antibody is trastuzumab emtansine approved for the treatment of HER2-positive metastatic breast cancer. Trastuzumab binds to the extracellular domain of the HER2 molecule and, after the internalization, it inhibits microtubule polymerization causing apoptosis of the targeted cell.[68] Brentuximab vedotin is an antibody-drug conjugate that has been approved for the treatment of Hodgkin's lymphoma. The antibody targets CD30 surface antigen expressed on malignant cells and carries a microtubule-disrupting agent causing the apoptosis of lymphoma cells.[69]

2.3.5 Immune checkpoint inhibitors

Immune checkpoint inhibitors are monoclonal antibodies that block inhibitory pathways from being engaged and prevent tumour cells from inducing tolerance in tumour-specific T cells. The most significant is the clinical success of the monoclonal antibodies blocking CTLA-4 and PD-1/PD-L1 inhibitory checkpoint molecules. The blockade of the CTLA-4 and PD-1 inhibitory signalling pathways allows the recovery of effector T cell functions and reduces the immune suppression mediated by Tregs, therefore improves the clinical outcome of patients with metastatic tumours.[11] Ipilimumab, an anti-CTLA-4 antibody, acts to upregulate anti-tumour immunity and has been the first to achieve an improvement in overall survival after treatment of patients bearing metastatic melanoma.[70] Subsequently, the anti-PD-1 antibodies – nivolumab and pembrolizumab, and anti-PD-L1 antibodies – atezolizumab, avelumab and durvalumab; were approved by the FDA for the treatment of multiple advanced cancers.[71]

The combination therapy with Ipilimumab and Nivolumab antibodies has been also clinically tested in patients with chemotherapy-resistant metastatic melanoma. It has been described that progression-free survival and the therapeutic response of patients was significantly better when treated with the combination therapy compared to Nivolumab or Ipilimumab antibody alone.[72]

2.4 Polymer prodrugs in cancer therapy

Immunotherapeutic protocols used as a sole cancer therapy are not sufficient, however, they can be effective when used in combination with other types of treatment, in particular chemotherapy. On the other hand, conventional chemotherapy is accompanied by several disadvantages. The efficacy of classical chemotherapy is reduced by the non-specific distribution within the body and causes adverse effects due to the toxicity towards healthy tissues. Moreover, cancer cells often develop multidrug resistance to existing chemotherapeutic agents. Therefore, the development of new nanoparticle drug carriers could be the path to overcoming the major drawbacks of conventional cancer chemotherapy.[73]

The idea to attach a cytotoxic drug to polymer nanocarrier was initiated about fifty years ago and has significantly advanced since then. Macromolecular carriers protect the drug from degradation and activation in the bloodstream. The half-life of a nanocarrier-conjugated drug is increased and the overall systemic toxicity is reduced because of the controlled release from the polymer. Moreover, nanocarriers improve the bioavailability and solubility of drugs insoluble in water. A polymer carrier suitable for drug delivery has to be biocompatible, meaning that it has to be biodegradable or small enough to be cleared from the body by renal filtration or excreted by the liver and bile. The macromolecule should not interact non-specifically with cell membranes to prevent the accumulation of the drug in other than the targeted cells. The anti-cancer drug is bound to the carrier via a spacer, which provides its specific controlled release.[74]

The bond between the drug and its carrier is stable in the bloodstream. However, the drug needs to be released once it enters the tumour microenvironment or inside lysosomes after its engulfment by the tumour cells. One option is to bind the drug via a pH-sensitive bond and exploit the pH difference between blood and tumour microenvironment or lysosomes. An example of such a bond could be a hydrazone spacer that is stable under physiological conditions (pH 7,4) and hydrolytically degradable in a mildly acidic environment (pH 6-5).[75] There is also an option to design spacers that could be proteolytically cleaved by the lysosomal enzymes. For instance, a lysosomal enzyme called cathepsin B secures the controlled release of anti-cancer drug by the proteolytic cleavage of the bond formed between the drug and tetrapeptide spacer composed of glycine, phenylalanine, leucine and glycine.[76]

Lastly, macromolecular carriers have a distinct architecture that has an important impact on the biological activity of the conjugates. The studies have shown that the polymer structure, hydrodynamic radius and molecular weight significantly influence the elimination of the carrier

by glomerular filtration. Different structures of polymer nanocarriers include linear or branched conjugates, micellar conjugates, as well as dendrimer-based star conjugates. The results of whole-body biodistribution analysis showed that linear polymers with the lower molecular weights were excreted faster and more efficiently, followed by the higher molecular weight fractions with the threshold around 40 000 g/mol. More complex start conjugates with comparable molecular weights to the linear polymers were eliminated much slower. On the other hand, the treatment of tumour-bearing mice with star polymer conjugates with higher molecular weights exhibited longer blood circulation and yielded a significantly higher number of long-term survivors in comparison with the linear polymer conjugate treatment.[77]

2.4.1 Principles of nanocarrier tumour delivery

The targeting of polymer-drug conjugates is dependent on two key aspects: the type of tumour and the structure of the macromolecular drug carrier. Active targeting of polymer-drug conjugates can be achieved by adding target-specific antibodies or antibody fragments. An example of an active targeting approach is the synthesis of polymer carrier conjugated with CD20-specific antibody, which has been assessed for the treatment of B cell malignancies such as non-Hodgkin's lymphoma.[78]

Passive polymer-drug targeting benefits from the increased permeability of blood vessels and poor lymphatic drainage within the tumour microenvironment. This phenomenon known as the enhanced permeability and retention (EPR) effect was originally described by Maeda and Matsumura in 1986.[79] The majority of solid tumours have a chaotic and imperfect vasculature due to the abnormal production of various pro-angiogenic factors, such as VEGF. Newly generated blood vessels in the solid tumours have increased permeability as they are widely fenestrated and are often lacking smooth muscle layer and pericytes. Moreover, tumour endothelial cells do not form a monolayer connected with tight junctions. All those aspects contribute to the extravasation of macromolecules ranging up to hundreds of nanometres in diameter into tumour tissue. This, together with the absence of properly functioning lymphatic drainage allows selective accumulation of high molecular weight drug carriers in tumours less affecting the healthy tissues.[80]

In recent years, several studies have depicted the heterogeneity in EPR-based nanoparticle drug carrier treatments. The uptake of polymer prodrugs into solid tumours varies in patients with different types of cancer and among individuals bearing tumours of the same origin.[81] A growing body of research suggests that the EPR effect varies in humans and

mouse models, and may change over the time of tumour progression. As it may seem that the heterogeneous outcomes of clinical trials with polymer-drug conjugates are often not as promising as results of preclinical animal studies, it is important to highlight that multiple passively tumour-targeted nanocarrier prodrugs have been successfully translated to the clinic. For instance, liposome-encapsulated doxorubicin (Dox) attached to polyethylene glycol (PEG) prevents the accumulation of the cardiotoxic drug in the heart while improving the delivery specifically into the tumour microenvironment.[82]

Overall, while EPR-based nanomedicines might be a tool to improve the efficacy of systemic anti-cancer chemotherapy, there is a necessity to better understand the heterogeneity of the EPR effect in patients. The development of diagnostic protocols and imaging agents that facilitate the visualization of EPR-mediated tumour targeting on the individual level is the future of personalized nanocarrier drug delivery in the field of cancer therapy.[83]

2.4.2 HPMA-based polymer drug carriers

Various polymer-drug conjugates, based for instance on the structure of PEG or *N*-(2-hydroxypropyl)methacrylamide (HPMA), are being synthesized and evaluated to be suitable for use in cancer therapy. PEG belongs to the most widely used hydrophilic carriers for the delivery of biologically active proteins and low molecular weight drugs. However, it must be considered that the structure of the nanocarrier should provide enough suitable chemical groups available for the incorporation of cytotoxic drugs. Despite its good solubility and biocompatibility, the structure of PEG offers only one or two end-chain functional groups available for polymer modification and binding of a drug.[84]

In contrast to PEG, drug carriers based on HPMA have functional groups available for drug incorporation distributed along the whole polymer chain. The first synthesis of HPMA structure was published in the early 1970s by Jindřich Kopeček and his colleagues and has further advanced since then.[85] HPMA-based copolymers have proven to be biocompatible, nontoxic and nonimmunogenic. Therefore, they are suitable carriers for biologically active cytotoxic and immunomodulatory agents. The multivalency of the HPMA backbone offers attachment of more types of cytotoxic agents via a biodegradable spacer. [86], [87] The anti-tumour activity of polymer prodrugs containing cytostatics, such as Dox, docetaxel (Dtx) or paclitaxel, has been documented repeatedly.[88]–[90] The structure of a spacer is important for drug release and activation; peptide spacers are cleaved by specific lysosomal enzymes while low pH-sensitive spacers undergo chemical hydrolysis. *(Fig.3)*

The degradable polymer conjugates have various architectures, whether it is a linear polymer, star-shaped conjugate based on a dendrimer core or polymeric micelles. Carrier micelles are formed by the self-assembly of amphiphilic copolymers with a molecular weight above the limit of a renal threshold. After drug release by hydrolysis of the pH-sensitive spacer in the acidic conditions of tumour tissue, micelles are disassembled and unimers are removed by glomerular filtration from the body.[86], [87] HPMA-drug conjugates have proven to be nonimmunogenic because HPMA is not recognized by the immune system as an antigen. Conversely, HPMA copolymers reduce the immunogenicity of substances they carry, probably via masking the attached molecule by creating a hydrophilic capsule around the transported substances and sterically hindering their accessibility to the cells of the immune system.[91]

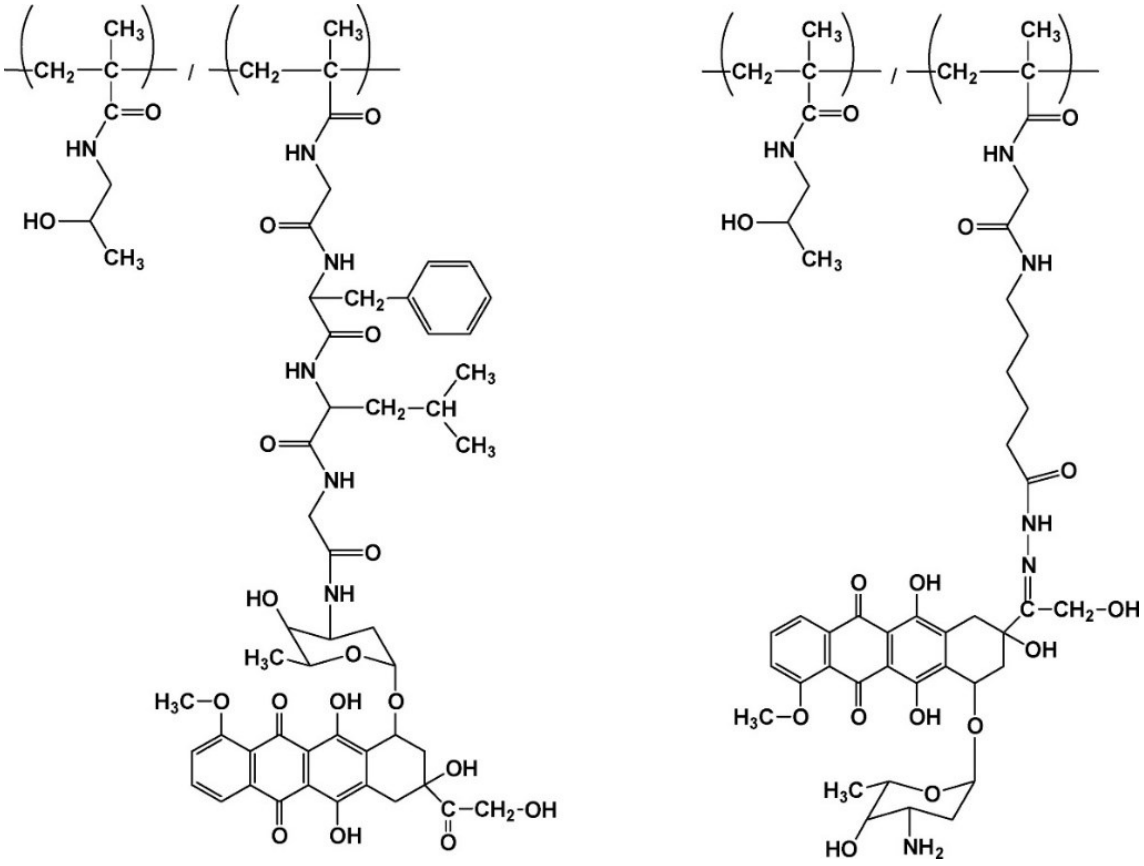

Figure 3 | Example of HPMA conjugates with Dox. (Left) Polymer conjugate with doxorubicin (Dox) bound via enzymatically degradable oligopeptide sequence. (Right) Polymer prodrug carrying Dox attached via a pH-sensitive hydrazone bond. Adapted from [92]

A large body of information has been collected concerning the effectiveness of *in vivo* HPMA-based nanomedicine treatment in murine models, as well as humans.[88], [89], [93] HPMA nanocarriers have shown prolonged blood circulation and enhanced transport to the tumour tissue due to the EPR effect followed by controlled release of the drug. Polymer prodrugs based on HPMA and Dox or Dtx have a potent anti-cancer effect and immunomodulating activity. The treatment of mouse tumour models using distinct HPMA polymer conjugates with Dox induces treatment-dependent cancer resistance and long-lasting immunological memory.[94] This was documented by re-inoculating cured, long-term surviving mice with a lethal dose of the original tumour cells as late as six months after the primary therapy. Mice re-challenged by the tumours were protected and survived without tumour progression, unlike the controls, which developed tumours and died. Further investigations have highlighted the importance of $CD8^+$ T cell responses in the development of cancer resistance, in rejecting re-transplanted tumours and in maintaining immunological memory.[94]–[96] Moreover, HPMA-Dox conjugates have shown the capacity to induce immunogenic cancer cell death.[97] Immunogenic cancer cell death activates the anti-tumour immune responses by releasing danger-associated molecular pattern molecules that are engulfed by DCs, which undergo maturation and activate $CD8^+$ and $CD4^+$ T cells.[98], [99]

2.5 General characteristics of cucurbitacins

Cucurbitacins are a class of highly oxidized tetracyclic triterpenoids originally extracted from the plant family of *Cucurbitaceae*. Historically, cucurbitacins have been known in traditional folk medicine for their anti-inflammatory, antipyretic and analgesic properties. Structurally, cucurbitacins are characterized by the tetracyclic cucurbitane nucleus composed of thirty carbon atoms with a variety of oxygen substitutions at different positions. According to the characteristics of their structures and side-chain variations, cucurbitacins are grouped into twelve distinct categories. The classes range from cucurbitacin A to cucurbitacin T, including hundreds of different derivates. Among those, the cucurbitacins B, D, E and I have been studied most thoroughly and proved to have strong anti-cancer activities.[100]–[102] *(Fig.4)* At room temperature, cucurbitacins are crystalline substances with prominent hydrophobicity. Therefore an attachment of cucurbitacins to a suitable nanocarrier could improve their solubility and delivery into specific tissues. Indeed, polymer micelles have been evaluated for the solubilization and delivery of cucurbitacin B and I; inhibitors of the STAT3 pathway. When studied in mouse melanoma models, polymer micellar cucurbitacins exhibited similar anti-cancer activity compared to the free drugs. Moreover, the systemic toxicity of cucurbitacins bound to nanocarriers was significantly lower. These results reveal the potential of polymeric nanocarriers as suitable vehicles for the delivery of cucurbitacins in cancer therapy.[103]

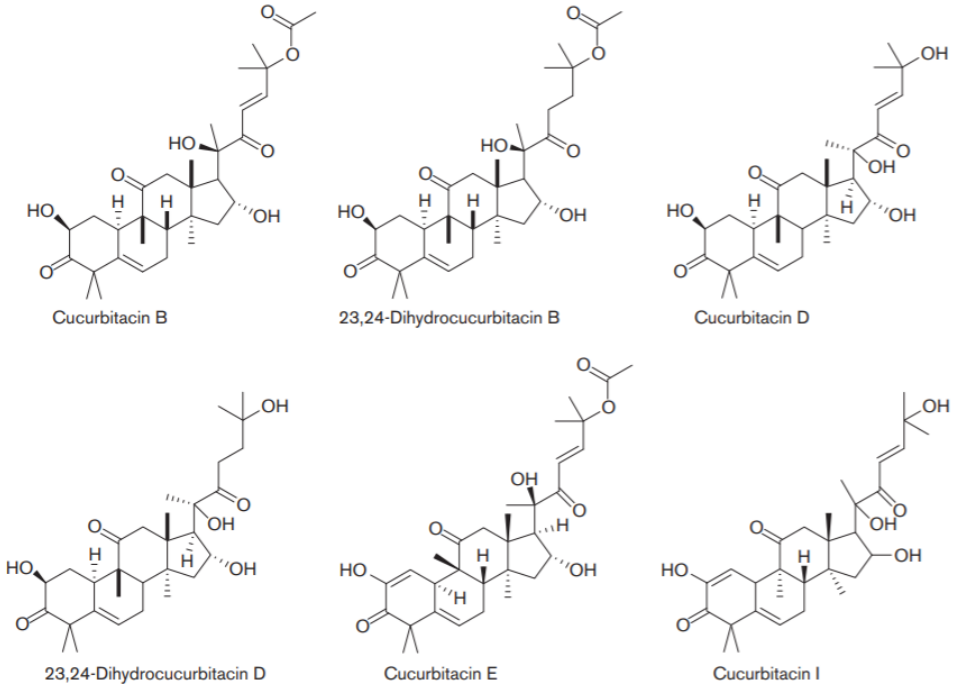

Figure 4 | Chemical structures of several widely studied cucurbitacins. Most intensive research is being done on cucurbitacins B, D, E, I and their derivates. Adapted from [102]

2.5.1 Cucurbitacin D as a promising anti-cancer agent

Several types of cucurbitacins are currently studied due to their possible beneficial effects in cancer therapy. The following chapter is focused on one of them, namely cucurbitacin D (CuD); also known as elatericin A. The anti-cancer properties of cucurbitacins were first discovered in the 1960s. In the series of experiments, elatericin A and B (CuD and E) were found to inhibit cancer cell proliferation *in vitro* and following tumour inoculation *in vivo*.[104], [105] Since then, CuD has shown a potent inhibitory effect on many cell lines including hepatocellular carcinoma, leukaemia, breast, colon, lung, pancreatic or prostate cancer.[106]–[110]

Lately, the emerging evidence describe significant synergistic effects of cucurbitacins with clinically approved chemotherapeutics. An example of such could be the combination of cucurbitacins with Dox, Dtx, gemcitabine or methotrexate.[100]–[102], [111] Unfortunately, the few studies published on the topic of CuD describe mainly the overall effects on cancer cells rather than specific mechanisms and molecules standing behind its anti-tumour activity. Therefore, further research regarding CuD is much needed. The effects of CuD described in tumour cells include for example cell cycle arrest and triggering of programmed cell death by affecting STAT3 or nuclear factor kappa-light-chain-enhancer of activated B cells (NF-κB) signalling pathways.

2.5.1.1 CuD-induced cell cycle arrest and apoptosis

The induction of cell cycle arrest and apoptosis is one of the main effects of cucurbitacins on cancer cells. Different cucurbitacins can induce stopping in different phases. It has been described that human ovarian and endometrial cancer cells are susceptible to the growth-inhibitory effect of CuD. *In vitro* cultivation of malignant cells in the presence of CuD induced arrest in the G2/M phase of the cell cycle. Upregulated level of $p21^{WAF1}$ and $p27^{KIP1}$, cyclin-dependent kinases that play important roles in blocking the cell cycle, was observed. Furthermore, CuD decreased the expression of other important cell cycle regulators, cyclins A and B. In line with these findings, CuD significantly increased the number of apoptotic cells via down-regulating the anti-apoptotic proteins Bcl-2 and Bcl-xL. Moreover, treatment with CuD stimulated the activity of caspase-3 and caspase-9, which initiate apoptosis by cleavage of many substrates such as poly-ADP ribose polymerase.[112]

Another study documented the effect of CuD on neurofibromatosis type 2-deficient mouse schwannoma and human benign meningioma cells. Treatment with CuD inhibited the

growth of malignant cells and induced cell cycle arrest at G2/M via decreasing the levels of cyclin A, B, and E. Additionally, CuD inhibited the phosphorylation of pro-survival serine/threonine kinase Akt. The lack of phospho-Akt in treated cells led to reduced cell survival and apoptosis.[113]

Analysis of human hepatocellular carcinoma cells after cultivation with CuD has shown increased activity of caspase-3, which plays a central role in the initiation of apoptosis. The results suggest that CuD activates the apoptotic pathway through proteolytic cleavage of procaspase-3, an inactive form of initiator caspase-3 that subsequently activates apoptotic effector caspases.[108] In human leukaemia cells, CuD markedly reduced anti-apoptotic proteins Bcl-2 and Bcl-xL and induced programmed cell death through the inhibition of the proteasome. The proteasome is a catalytic complex responsible for the degradation of most cellular proteins, therefore its inhibition led to an accumulation of ubiquitinated proteins in the cytoplasm, which resulted in apoptosis. More importantly, proapoptotic and proteasome inhibitory activity of CuD was demonstrated also *in vivo* using severe combined immunodeficiency mice inoculated with human T-cell leukaemia cells.[107]

Interestingly, recent evidence showed that CuD-induced apoptosis in human leukemic cells might be closely associated with autophagy. However, the researchers observed rather contradicting results using different autophagosome inhibitors on distinct human leukaemia T cell lines. Further work would be required to evaluate the involvement of autophagy concerning anti-cancer drug sensitivities.[114]

2.5.1.2 CuD and its molecular mechanisms of action

Mechanisms by which CuD controls the cell cycle arrest, apoptosis, and growth suppression can vary, as mentioned in the chapter above. At the molecular level, one of the most prominent CuD targets is the STAT3 transcription factor, one of the seven members of the STAT protein family. Activated STAT3 triggers tumour progression by regulating gene expression through cross-talk with other transcription factors, and it plays a major role in the oncogenesis of many cancer cell lineages. Therefore, the inhibition of constitutive STAT3 activity could serve as prevention and treatment of various human tumour types.[115]

When studied in human breast cancer cells, CuD suppressed proliferation while also inducing apoptosis and G2/M cell cycle arrest via inhibition of the STAT3 pathway. The experiments have shown inhibition of phosphorylation and nuclear translocation of STAT3 in treated cells. Moreover, CuD repressed STAT3-dependent reporter gene activity illustrating

potent inhibition of the constitutive transcriptional activity of STAT3.[114] CuD-induced apoptosis associated with the inhibition of STAT3 was also observed in human cervical cancer. CuD inhibited phosphorylation of STAT3 at Ser^{727} and Tyr^{705} residues. This resulted in the downregulation of STAT3 downstream target genes such as c-Myc and matrix metalloproteinase 9. These effects were confirmed also *in vivo* using athymic nude mice. The researchers described that the intratumoural administration of CuD reduced cervical cancer-derived xenograft tumour growth when compared to control mice without any treatment.[117]

Interestingly, other studies done on breast cancer cells describe the combined effect of CuD both on STAT3 and on NF-κB signalling pathways. NF-κB is another important signalling pathway playing part in human cancer initiation, progression and metastasis. NF-κB is a family of five transcription factors that form different homo or heterodimers. Upon engagement of diverse stimuli such as cytokines or growth factors, the cytoplasmic inhibitor of κB (IκB) kinase (IKK) complex is activated. The activated IKK complex is responsible for the phosphorylation of IκB, which triggers its degradation. NF-κB dimers are released and translocate to the nucleus, bind to DNA and regulate transcription of various target genes.[118]

When studied in doxorubicin-resistant breast cancer cells, CuD increased IκB level in the cytosol and suppressed the nuclear translocation of phosphorylated NF-κB, resulting in apoptosis. At the same time, CuD disrupted constitutive STAT3 signalling and nuclear translocation, therefore promoting changes in the cell cycle resulting in apoptosis. The subsequent luciferase reporter gene assay performed in CuD-treated cancer cells confirmed reduced STAT3 and NF-κB transcriptional activity.[119] Further investigations have focused on the synergism of two chemotherapeutic agents, Dox and CuD, in the treatment of human breast cancer cells. The combined treatment with CuD and Dox was significantly more efficient in cell growth suppression than CuD alone. Further analysis has shown that the anti-cancer effect was mediated via decreased phosphorylation and activity of both STAT3 and NF-κB transcription factors.[120]

When all of the above is taken into account, several studies demonstrate the potential of CuD as a useful therapeutic agent for the treatment of human breast or cervical cancer as well as other types of tumours. In summary, the accumulated studies have clearly illustrated that CuD has notable anti-cancer potential. STAT3 and NF-κB appear to be the most crucial CuD targets, although their exact contributions call for further study to achieve a complete understanding of the CuD-mediated pharmacological properties.

3 Aims of the thesis

The general aim of the work was the definition of cytostatic activity of polymer conjugates based on CuD, yet unused drug with potential anti-cancer activity. Its molecular mechanism of action remains unclear, however, several studies suggest that CuD affects phosphorylation and dimerization of STAT3 transcription factor. STAT3 is overexpressed in many human cancer cell lines and plays an important role in the differentiation of myeloid cells. The work should benefit from the use of polymer conjugates based on HPMA that are suitable for targeted delivery of drugs specifically to the solid tumour tissue.

The main aims of the work are:

- To assess the biological activity of HPMA copolymers bearing CuD in selected human and murine cell lineages *in vitro*
- To define the therapeutic effect of polymer-bound CuD in combination with other polymer chemotherapeutic prodrugs *in vivo*
- To study the effect of the HPMA conjugates carrying CuD on the frequencies of MDSCs expanded *in vitro* as well as during *in vivo* tumour therapy

4 Materials and methods

4.1 Solutions and buffers

Phosphate buffered saline (PBS)

9 g NaCl

1.2 g $Na_2HPO_4 \times 12H_2O$

0.2 g $Na_2H_2PO_4 \times H_2O$

The buffer filled with deionized H_2O to a total volume of 1 L with the pH adjusted to value 7,4.

Flow cytometry (FACS) buffer

PBS supplemented with 2 % foetal calf sera (FTS, Invitrogen) and 2 mM EDTA (Invitrogen).

Trypsin-EDTA solution

2,5 g/L porcine trypsin and 0,2 g/L EDTA•4Na in Hank's Balanced Salt Solution with phenol red with pH adjusted to value 7,4.

Media for the cultivation of isolated bone marrow cells

RPMI 1640 (Sigma-Aldrich) supplemented with 10% FTS, 50 mM 2-mercaptoethanol (Sigma-Aldrich), 100 U/mL penicillin, 100 µg/mL streptomycin (Pen/strept; Gibco), 2 mM glutamine (Sigma-Aldrich), 0.1 mM Non-Essential Amino Acids (Sigma-Aldrich).

Media for the cultivation of EL4 cell line

RPMI 1640 (Sigma-Aldrich) supplemented with 10 % FTS, 100 U/mL penicillin, 100 µg/mL streptomycin (Pen/strept; Gibco), 2 mM glutamine (Sigma-Aldrich), 4,5 g/l glucose (Sigma-Aldrich), 1 mM sodium pyruvate (Sigma-Aldrich).

Media for the cultivation of 4T1 and CT26 cell lines

RPMI 1640 (Sigma-Aldrich) supplemented with 10 % FTS, 100 U/mL penicillin, 100 µg/mL streptomycin (Pen/strept; Gibco), 2 mM glutamine (Sigma-Aldrich), 4,5 g/l glucose (Sigma-Aldrich), 1 mM sodium pyruvate (Sigma-Aldrich), 10 mM HEPES (Sigma-Aldrich).

Media for the cultivation of OVCAR-3 cell line

RPMI 1640 (500mL) supplemented with 20% FTS, 100 U/mL penicillin, 100 µg/mL streptomycin (Pen/strept; Gibco), 2mM glutamine (Sigma-Aldrich), 4,5 g/l glucose (Sigma-Aldrich), 1mM sodium pyruvate (Sigma-Aldrich), 10 mM HEPES (Sigma-Aldrich), 0,01 mg/mL bovine insulin (Sigma-Aldrich).

Media for the cultivation of SK-OV-3 cell line

McCoy's 5A Medium (Sigma-Aldrich) supplemented with 10 % FTS, 100 U/mL penicillin, 100 µg/mL streptomycin (Pen/strept; Gibco), 2 mM glutamine (Sigma-Aldrich), 7,5% sodium bicarbonate (Sigma-Aldrich), 10 mM HEPES (Sigma-Aldrich).

Media for the cultivation of DU-145 cell line

Minimum Essential Medium (Sigma-Aldrich) supplemented with 10% FTS, 100 U/mL penicillin, 100 µg/mL streptomycin (Pen/strept; Gibco), 2 mM glutamine (Sigma-Aldrich), 1 mM sodium pyruvate (Sigma-Aldrich), 0.1 mM Non-Essential Amino Acids (Sigma-Aldrich), 7,5% sodium bicarbonate (Sigma-Aldrich).

4.2 Cells

Tumour cell lines

Following murine and human cell lines that were used in the experiments were purchased from ATCC: murine EL4 T-cell lymphoma (ATCC TIB-39), murine 4T1 mammary carcinoma (ATCC CRL-2539), murine CT26 colon adenocarcinoma (ATCC CRL-2638), human ovarian carcinoma SK-OV-3 (ATCC HTB-77) and human ovarian carcinoma OVCAR-3 (ATCC HTB 161). Human prostate cancer DU-145 were obtained from Dr. Hodný from the Institute of Molecular Genetics of the Czech Academy of Sciences, Prague, Czech Republic. The cells were maintained as recommended by the provider. All cell lines were checked for the presence of mycoplasma contamination (MycoAlert Mycoplasma Detection Kit, Lonza).

Cell cultivation

Cells were cultured in complete media in culture flasks (Nunc, Thermo Fisher Scientific) and kept in a CO_2 incubator in a stable atmosphere containing 5% CO_2 at temperature 37°C. Cells were manipulated in a laminar flow cabinet under sterile conditions. The first passage of cells was used for all experiments. Cell viability and cell numbers were evaluated using automatic cell counter Countess (Invitrogen) and trypan blue staining (Invitrogen).

4.3 Experimental mice

BALB/c female mice were obtained from a breeding facility at the Institute of Physiology of the Czech Academy of Sciences, v.v.i. Mice were housed under conventional conditions, food and water *ad libitum*, at the laboratory animal experimental facility at the Institute of Microbiology of the Czech Academy of Sciences, v.v.i. and used for experiments at 2-5 months of age.

4.4 Therapeutic agents

All HPMA polymer-bound drugs for the experiments were synthesized in the Institute of Macromolecular Chemistry of the Czech Academy of Sciences, v.v.i... Polymer–drug conjugates were prepared via the reaction of the hydrazide groups of linear and micellar carriers based on HPMA with the keto group from carbon three of CuD, providing pH-sensitive drug delivery systems through the use of the hydrazone bond. Some results presented in this diploma thesis including the physicochemical characterization of CuD-bearing polymer prodrugs have already been published.[121]

Polymer conjugates carrying CuD

Four batches of linear conjugates of HPMA copolymer carrying CuD (8,5 wt.%; 6,2 wt.%; 7,7 wt.% and 9,3 wt.%) bound to the polymer by pH-sensitive hydrazone bond were prepared. Besides, one batch of a micellar conjugate of amphiphilic HPMA copolymer bearing cholest-4-en-3-one (2 mol.%) and CuD (6,7 wt.%) bound to the polymer by pH-sensitive hydrazone bond was tested.

Polymer conjugates carrying Dox

For *in vivo* therapy, the micellar conjugate of amphiphilic HPMA copolymer bearing cholest-4-en-3-one (2 mol.%) and Dox (8,1 wt.%) bound by hydrazone bond was used.

Table 1 | Physicochemical properties of hydrophilic or amphiphilic copolymer precursors (LP or MP) and their conjugates with CuD or Dox.[121]

Compound	Content of hydrazide [mol. %]	Content of hydrophobic moiety [mol. %]	Content of drug [wt. %]	Mn [g/mol]	Mw [g/mol]	Đ	Dh ± SD [nm]
LP	4,0	-	-	25 100	26 500	1,05	8,8 ± 0,2
LP-CuD	-	-	6,2	27 000	36 200	1,34	12,4 ± 1,0
MP	5,0	2,1	-	21 500	26 400	1,23	19,8 ± 0,4
MP-CuD	-	2,1	6,7	25 700	39 000	1,51	32,2 ± 1,6
MP-Dox	-	2,0	8,1	14 200	25 500	1,80	29,6 ± 1,0

LP – linear polymer; MP – micellar polymer; Mn – number-average molecular weight; Mw – weight-average molecular weight; Đ – dispersity; Dh – hydrodynamic diameter.

Free drugs

In several *in vitro* experiments, free CuD (Tocris Bioscience) was used.

Checkpoint inhibitors

For *in vivo* treatment, anti-mouse PD-1 monoclonal Ab (RMP1-14; BioXcell) was used.

4.5 *In vitro* cellular drug sensitivity assay

To test the cytostatic effect of the drugs, the cancer cells were washed and cell viability and counts were estimated. Cells were seeded in 96-well flat-bottom tissue plates (Nunc, Thermo Fisher Scientific) in the culture medium at concentrations of 5 000 cells per well, or 2 500 cells in the case of the 4T1 cell line. In each well, 200 μL of cell suspension was pipetted and different concentrations of polymer-drug samples were added to reach a final volume of 250 μL. Four parallel samples were used for each experimental condition. Free CuD (Tocris Bioscience) was used as a control, dissolved in DMSO at 4 mM concentration, and further diluted in the culture medium. Besides the wells containing polymer-bound or free drug, control wells containing only cells in media were seeded. The cells were cultivated for 72 hours at standard conditions in a CO_2 incubator. At the end of the cultivation, ^{3}H-thymidine was added at a concentration of 0.4 μCi/mL for 6 hours. Afterwards, the plates were frozen at −20 °C. The final processing was done using a Tomtec Mach III harvester, and the radioactivity was measured on the filter plate with a solid Meltilex scintillator using the Microbeta Trilux beta counter (Perkin Elmer).

Because EL4 T-cell lymphoma cells do not incorporate ^{3}H-thymidine in a sufficient quantity, the metabolic activity and cytotoxic effect of polymer-bound or free drug were evaluated using the standard 3-(4,5-dimethylthiazol-2-yl)-2,5-diphenyltetrazolium bromide (MTT) assay. After cultivation, the plates were centrifuged (250 g, 5 min, 4 °C) and 100 μL of complete medium and 20 μL of 3-(4,5-dimethylthiazol-2-yl)-2,5-diphenyltetrazolium bromide (solution 5 mg/mL in PBS) were added to each well. The plates were incubated in a CO_2 incubator. After 1-2 hours, 200 μL of DMSO was added to each well and the plates were left for another 15 minutes in the dark. The absorbance was measured using a plate spectrophotometer Infinite M200 Pro (Tecan) at 540 nm, reference wavelength 690 nm. The cytotoxicity towards normal murine spleen cells was also tested using the MTT assay. Cells were seeded at a density of 100 000 cells per well and for polyclonal stimulation, 5 μg/mL concanavalin A (Sigma-Aldrich) was added.

The cytotoxicity towards isolated bone marrow cells was determined by Alamar blue cell viability reagent (Invitrogen). The cells were seeded at concentrations of 50 000 cells per well and for stimulation toward MDSC phenotype, 20 ng/mL GM-CSF (Sigma-Aldrich) was added. Different concentrations of polymer-drug samples were added to each well to reach a final volume of 250 μL. After cultivation, the plates were centrifuged (250 g, 5 min, 4 °C) and 100 μL of media with 10 μL of Alamar blue cell viability reagent (Invitrogen) was added to

each well. Plates were left in a CO_2 incubator for 2 hours. The fluorescence was measured using a plate spectrophotometer Infinite M200 Pro (Tecan) using an excitation wavelength of 550 nm and an emission wavelength of 590 nm. The *in vitro* cytostatic/cytotoxic effects were expressed as half-maximal inhibitory concentration (IC_{50}) value, which is the concentration of drug that inhibits the proliferation or metabolic activity by 50%. All IC_{50} values were a mean of at least three independent experiments.

4.6 Bone marrow isolation and *in vitro* MDSCs expansion

Bone marrow cells were extracted from the femur and tibia of BALB/c mice, washed in a culture medium, and cell viability and cell numbers were evaluated. Cells were seeded at a concentration of 5×10^6 bone marrow cells per well in 6-well flat-bottom tissue plates (Nunc, Thermo Fisher Scientific). Cells were cultured in complete media in the presence of 20 ng/mL GM-CSF (Sigma-Aldrich) and different concentrations of polymer or free drug samples in the total volume of 5 mL. The cells were cultivated in a CO_2 incubator for 72 hours. After the cultivation, cells were collected and flow cytometry analysis was performed (Chapter 4.9).

4.7 *In vitro* detection of STAT3 signalling pathway

DU-145 human prostate cancer cells were washed with EDTA and a trypsin-EDTA mixture (Sigma-Aldrich) was added until cells detached from the bottom of the culture flask. The cells were harvested, washed with serum-free media and viability and cell numbers of the suspension were evaluated. The cells were seeded at a concentration of 1×10^6 cells per well in 12-well flat-bottom tissue plates (Nunc, Thermo Fisher Scientific). The cells were left overnight in a CO_2 incubator. The next day, the plates were centrifuged (250 g, 5 min, 4 °C) and the supernatant was discarded. Then, 20 μM Stattic (Sigma-Aldrich), a selective STAT3 inhibitor; or different concentrations of free CuD (Tocris Bioscience) in serum-free media in a total volume of 1 mL were added. The plates were left in a CO_2 incubator for 1 hour. After that, 50 ng/mL of human recombinant interleukin-6 (IL-6) (Peprotech) was added to each well and the plates were left stimulated in a CO_2 incubator for another 30 minutes.

Next, the cells were harvested and seeded into 96-well U-bottom plates (TPP), in 200 μL of FACS buffer at 1×10^6 cells per well, the plates were centrifuged (250 g, 5 min, 4 °C) and the supernatant was discarded. FoxP3 Transcription Factor Staining Buffer Set (eBioscience) was used to fix and permeabilize cells for staining of intracellular markers. The cell pellet was resuspended in 100 μL of the prepared Fix/Perm solution (eBioscience; Fix/Perm Concentrate

+ Diluent 1:3). The plates were incubated for 30 minutes in the dark at room temperature. After the incubation, 100 µL of Perm Wash (eBioscience, diluted 1:10 in deionized water) was added to each well and plates were centrifuged (250 g, 5 min, 4 °C). The plates were washed once more with 200 µL Perm Wash. The pellet was resuspended in a 50 µL mixture of fluorochrome-conjugated monoclonal Abs (diluted in Perm Wash) for labelling intracellular markers. PE-conjugated anti-STAT3 (Invitrogen; clone: 232209) and APC-conjugated anti-pSTAT3 (Tyr705) (Invitrogen; clone: LUVNKLA) was used. The plates were incubated on ice in the dark for 1 hour. The cells were washed twice with 200 µL Perm Wash, the pellet was resuspended in 100 µL FACS buffer and analysed by flow cytometry. The analysis was performed on LSRII cytometer (BD Biosciences). The data were analysed using FlowJo 10.6 software (Tree Star).

4.8 *In vivo* experimental tumour therapy

Tumour cells were harvested from the culture flasks, washed with serum-free media and cell viability and counts were defined. The 4T1 mammary carcinoma cells (ATCC CRL-2539) or CT26 colon adenocarcinoma cells (ATCC CRL-2638) were injected subcutaneously (s.c.) with 2×10^5 cells in 100 µL volume per mouse. The mice were treated after tumours developed to a measurable size (diameter around 6–7 mm). The mice were treated intravenously (i.v.) according to the therapeutic scheme. One group of mice was left untreated and served as a control. Tumour size was regularly monitored by measuring its length and width by calliper. Survival of experimental mice was recorded. Moreover, body weight and signs of systemic toxicity were scored following the treatment, considered toxic if the body weight dropped by more than 15%. For FACS analysis, mice were treated according to the selected therapeutic scheme and the blood was collected from the tail vein on day 9, day 15 and day 21 after therapy and further processed and analysed using FACS (Chapters 4.9-10).

4.9 Isolation of cells from mice and preparation of single-cell suspensions

The blood was collected in round-bottom 15 mL tubes (Falcon) and centrifuged (250 g, 5 min, 4 °C). The supernatant was discarded, and the cell pellet was resuspended in 1 mL of ACK lysing buffer (Gibco) to achieve the lysis of red blood cells. The reaction was stopped after 10 mins by adding the FACS buffer to the total volume of 10 mL. The cells were then

centrifuged (250 g, 10 min, 4°C) and the process of lysis was repeated, if needed. After erythrocyte lysis, the cells were centrifuged (250 g, 10 min, 4°C) and resuspended in cold FACS buffer and kept on ice from this point on.

Spleens and tumours were harvested. Spleens were placed into C Tubes (Milteyi Biotec) with 5 mL of cell media and homogenized using gentleMACS Tissue Dissociator (Miltenyi Biotec). Tumours were placed into C Tubes (Milteyi Biotec) with 5 mL of an enzymatic mixture (Tumor Dissociation Kit, mouse; Miltenyi Biotec), homogenized using gentleMACS Tissue Dissociator according to the manufacturer's instructions and incubated for 40 min at 37 °C. After the end of incubation, the suspension was homogenized twice more using gentleMACS Tissue Dissociator. The cell suspensions were filtered through a 70 µm filter (BD Falcon) and centrifuged (250 g, 10 min, 24°C). The supernatant was discarded, and the cell pellet was resuspended in 2 mL of ACK lysing buffer (Gibco). The reaction was stopped after 10 mins by adding FACS buffer to the total volume of 20 mL. The cells were then centrifuged (250 g, 10 min, 4°C), resuspended in 5 mL of ice-cold FACS buffer and filtered through a 30 µm filter (BD Falcon). The cells were kept on ice from this point on and labelled for the flow cytometry analysis.

4.10 Flow cytometry

Single-cell suspensions of cells from blood, spleen, tumour or the bone marrow of mice were prepared as described in the chapters above. The number of cells in suspension was determined and the cells were seeded into 96-well U-bottom plates (TPP) in 200 µL of FACS buffer at 1×10^6 cells per well. Plates were centrifuged (250 g, 5 min, 4°C), the supernatant discarded and each well was resuspended in 20 µL of the prepared mixture containing Fc block (anti-mouse CD16/CD32; eBiosceince, diluted 1:50) and 10% normal mouse sera. Plates were kept on ice for 10 min; 200 µL of FACS buffer was added to each well and the plates were centrifuged (250 g, 5 min, 4°C). The supernatant was discarded and the cells were then stained with 20 µL of the prepared mixture containing fluorochrome-conjugated monoclonal Abs for surface cell antigens *(Table 2)* and kept on ice in dark for 30 min. Fixable viability dye was used to stain dead cells. After the staining, the cells were twice washed with 200 µL FACS buffer and centrifuged (250 g, 5 min, 4°C). The pellet was resuspended in 100 µL FACS buffer and analysed by flow cytometry. The analysis was performed on an LSRII cytometer. The data were analysed using FlowJo 10.6 software and gated as shown on one representative dot-blot. *(Fig.5)*

Table 2 | The list of monoclonal Abs with conjugated fluorochrome used in FACS analysis.

Marker	Clone	Fluorochrome	Dilution	Manufacturer
CD11b	M1/70	PE-Cy7	1:1200	eBioscience
CD11c	N418	eF450	1:150	eBioscience
CD45	30-F11	FITC	1:200	eBioscience
CD45	30-F11	PE-Cy7	1:1200	eBioscience
CD45	30-F11	eF450	1:150	eBioscience
CD45.2	104	AF700	1:80	eBioscience
CD45.2	104	PE	1:200	eBioscience
CD45.2	104	APC	1:1000	eBioscience
F4/80	BM8	PE	1:200	eBioscience
Gr-1	RB6-8C5	APC	1:1000	eBioscience
Ly6C	HK1.4	AF488	1:200	eBioscience
Ly6G	1A8	AF700	1:80	BD Pharmigen
FVD	-	eF780	1:200	eBioscience

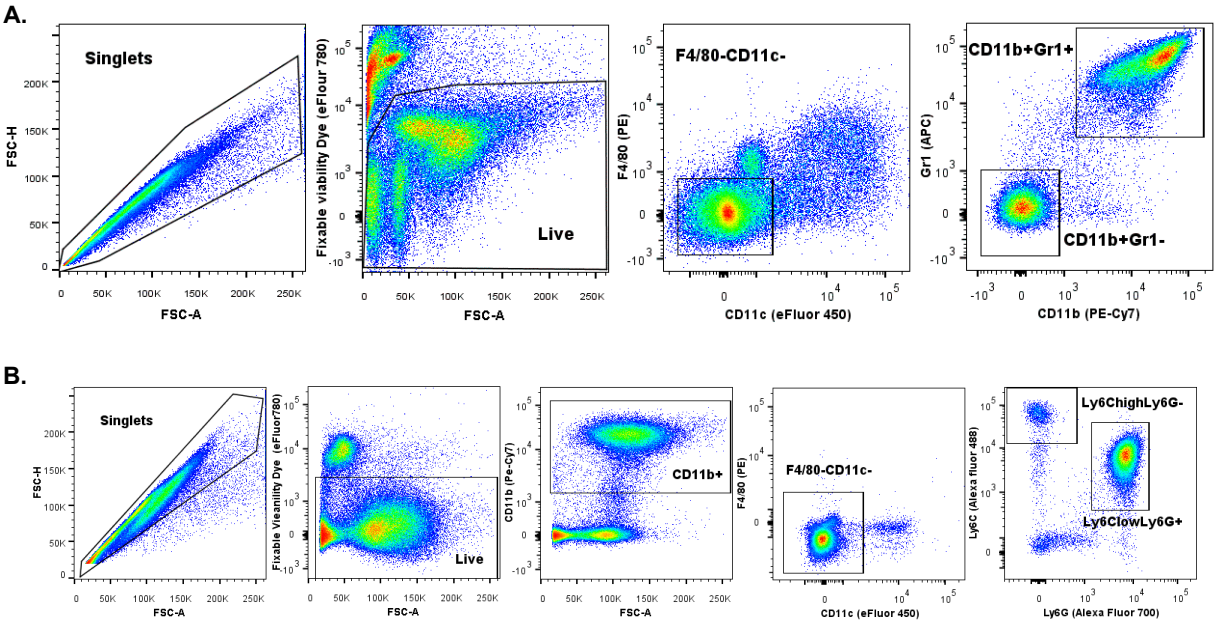

Figure 5 | Gating strategy applied in the experiments. The basic gating strategy comprised of exclusion of doublets and FVD^+ dead cells. (A) $F4/80^-CD11c^-$ and $CD11b^+Gr1^+$ were gated. (B) First, $CD11b^+$ and $F4/80^-CD11c^-$ cells were gated. Then, $Ly6C^{high}Ly6G^-$ monocytic MDSCs and $Ly6C^{low}Ly6G^+$ polymorphonuclear MDSCs were gated.

4.11 Statistical analysis

The data was processed using Graph-Pad Prism8 software. The data are presented as means +/- standard deviation unless stated otherwise. Analysis of significance was conducted using Student's t-test. Statistical significance of mice survival experiments was determined by log-rang Mantel-Cox test. P values of *$p < 0.05$, **$p < 0.01$ and ***$p < 0.001$ were considered statistically significant.

5 Results

5.1 *In vitro* anti-cancer activity of CuD-based conjugates

The *in vitro* biological activity of both linear and micellar CuD-based polymer conjugates was tested on several murine and human cancer cell lines. Some results presented in this diploma thesis including the characterization of CuD-bearing polymer prodrugs have already been published.[121] The cytostatic activity was determined by the ^{3}H-thymidine incorporation assay. In the case of the EL4 cell line, cytotoxic activity was determined using the MTT assay as EL4 do not incorporate ^{3}H-thymidine in sufficient quantity.

As already seen in other HPMA-based conjugates carrying various cytotoxic drugs, the free drug CuD was more toxic than its polymer conjugates. The half-maximal inhibitory concentration (IC_{50}) of CuD polymer conjugates has proven to be four to six times higher compared to the free CuD. *(Table 3)* Free drug enters the cell mainly via diffusion. The internalization of HPMA copolymers into the cell occurs via endocytosis, which is a significantly slower process. As a result, a higher drug amount is required within a given time to produce a comparable cytotoxic effect as a free low molecular weight drug. Therefore, polymer conjugates carrying anti-cancer drugs are *in vitro* less toxic than the free parent drugs.

Table 3 | Cytostatic/cytotoxic effect of CuD-based polymer conjugates in murine and human cancer cell lines *in vitro*. [121]

Cell line	CuD-LP	CuD-MP	Free CuD
4T1	0,512 ± 0,258	0,293 ± 0,033	0,175 ± 0,025
CT26	0,521 ± 0,226	0,386 ± 0,037	0,125 ± 0,020
EL4*	0,175 ± 0,002	0,380 ± 0,189	0,048 ± 0,013
SK-OV-3	0,183 ± 0,009	0,185 ± 0,037	0,025 ± 0,007
OVCAR-3	0,190 ± 0,057	0,277 ± 0,099	0,053 ± 0,014
DU-145	0,272 ± 0,057	0,517 ± 0,155	0,062 ± 0,022

IC_{50} values ± SD are expressed as a concentration equivalent of CuD (μM). Cytostatic/cytotoxic activity was determined by ^{3}H-thymidine incorporation assay and (*) the MTT assay. The experiments were repeated 3-5 times. 4T1 – murine mammary carcinoma; CT26 – murine colon adenocarcinoma; EL4 – murine T-cell lymphoma; SK-OV-3, OVCAR-3 – human ovarian carcinoma; DU-145 – human prostate carcinoma.

The selected human tumour cell lines were notably more susceptible to the activity of CuD polymer conjugates compared to murine tumour cell lineages. This could be due to overexpression of the STAT3 transcription factor, which has been documented in many human tumours of various origins. We have chosen to examine the cytostatic effect on human ovarian carcinoma SC-OV-3 and OVCAR-3, and prostate DU-145 cells; based on the previously described overexpression of the STAT3 transcription factor.[43]–[45] Indeed, SC-OV-3, OVCAR-3, and DU-145 cells showed a rather high susceptibility to CuD *in vitro*. Lower IC_{50} values in these cell lines were in good agreement with the hypothesis that CuD could act as a STAT3 inhibitor, although additional mechanisms of toxicity are probably involved in this process.[117], [119], [120]

Subsequently, four batches of linear polymer CuD conjugates were tested in selected murine and human cancer cell lines, all with reproducible results and comparable IC_{50} values. The biological activity of different batches of linear conjugates was similar, therefore the synthesis and preparation of HPMA prodrugs containing CuD proved to be reproducible. Moreover, we did not find significant differences between the cytotoxicity of the linear and micellar CuD-based conjugates. This could be partly due to the extracellular release of the drug before the engulfment of the polymer conjugate by the tumour cells. In this case, the rate of pH-sensitive hydrolysis of the hydrazone bond in both types of polymer conjugates seems similar. On the other hand, the values expressed as a concentration equivalent of CuD might not reflect the behaviour of the polymer conjugate in the *in vivo* system. *(Fig.6A)*

Cytostatic and cytotoxic activity of CuD conjugates was also tested in normal murine cells isolated from the spleens of tumour-free BALB/c mouse. Upon addition of T-cell mitogen concanavalin A, spleen cells were stimulated to proliferate, therefore were quite sensitive to the cytotoxic activity of free CuD. On the other hand, spleen cells showed considerable durability to the cytotoxic effect of the linear CuD polymer conjugate. The IC_{50} values were calculated as $0{,}14 \pm 0{,}035$ μM CuD for the free drug and $2{,}6 \pm 0{,}055$ μM CuD equivalent for linear polymer conjugate. *(Fig.6B)* These results suggest that the cancer cells are generally more susceptible to polymer CuD conjugates in comparison to normal proliferating murine spleen cells.

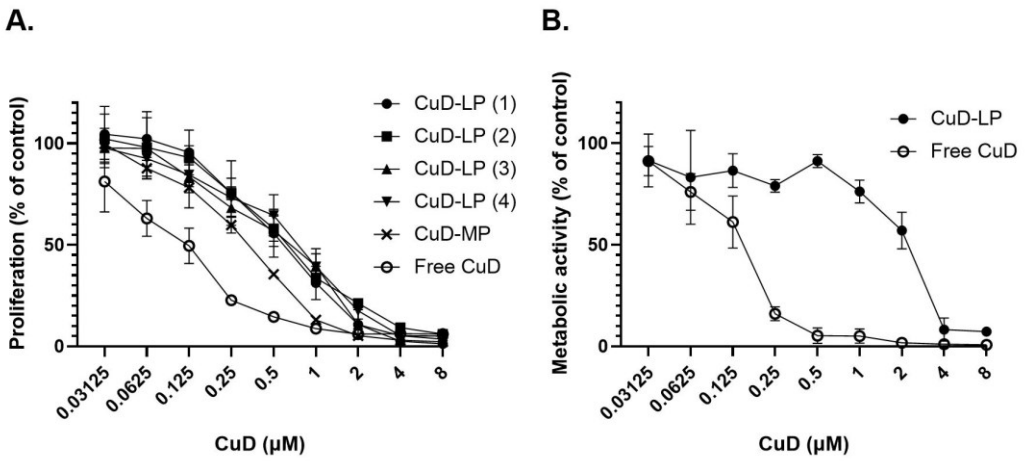

Figure 6 | *In vitro* cytostatic activity of the polymer CuD-based conjugates in murine CT26 colon adenocarcinoma and normal spleen cells. (A) Four batches of CuD-LP, one batch of CuD-MP and free CuD were tested on murine CT26 cancer cells. The values are expressed as a concentration equivalent of CuD (μM). The cytostatic activity of a drug was determined by a ^{3}H-thymidine incorporation assay. (B) Cytotoxic activity of CuD-LP and free CuD in mitogen-activated murine spleen cells. The cells were isolated from spleens of normal BALB/c mice and during cultivation stimulated by 5 mg/mL concanavalin A. Metabolic activity was determined using the MTT assay. Four parallel samples per condition were used.

5.2 Effect of CuD-based conjugates on MDSCs expanded *in vitro*

As described in Chapter 3.2.4.2, MDSCs play an important role in the development and progression of many cancer types. It has been suggested that CuD could act as a STAT3 transcription factor inhibitor. [117], [119], [120] Since STAT3 plays a crucial role in MDSC differentiation and immunosuppressive function [42], [46], [48], we aimed to investigate whether free CuD or CuD-based polymer conjugates have a biological effect on *in vitro* cultivated bone-marrow cells stimulated towards MDSC-like phenotype. Bone marrow cells extracted from tumour-free BALB/c mice were cultured in complete media in the presence of 20 ng/mL GM-CSF to stimulate their differentiation towards MDSC-like phenotype. Firstly, the cytostatic activity of polymer CuD conjugates and the parent free drug was assessed using Alamar blue cell viability reagents. The half-maximal inhibitory concentration (IC_{50}) values were calculated as 4,33 μM CuD equivalent for the linear polymer conjugate; 2,58 μM CuD equivalent for the micellar polymer conjugate and 0,56 μM CuD equivalent for the free drug. *(Fig.7A, Fig.7B)* CuD polymer conjugates were characterized by approximately six times higher IC_{50} values compared to the free CuD, similarly to the results previously obtained from *in vitro* testing in murine and human cancer cell lineages.

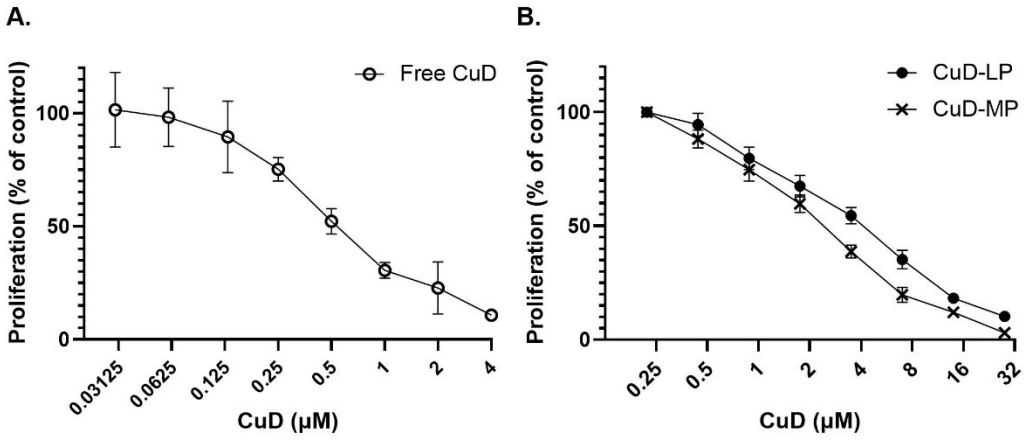

Figure 7 | *In vitro* cytotoxic activity of CuD-LP, CuD-MP and free CuD on bone marrow cells. The cells were isolated from the bone marrow of normal BALB/c mice and upon cultivation stimulated by 20 ng/mL GM-CSF. The values are expressed as a concentration equivalent of CuD (μM). The cytostatic activity of polymer conjugates and the free drug was determined by Alamar blue cell viability assay. IC_{50} values were 4,33 μM CuD equivalent for LP-CuD; 2,58 μM CuD equivalent for CuD-MP and 0,56 μM CuD equivalent for the free drug. Four parallel samples per condition were used.

Based on the results of *in vitro* proliferation assays, the isolated bone marrow cells were cultivated in the presence of various concentrations of free CuD; or the equitoxic dose of linear or micellar conjugate and 20 ng/mL GM-CSF. After 72 hours, the cells were collected and flow cytometry analysis was performed. Cells were gated to detect MDSC-like $CD11b^{+}Gr1^{+}$ phenotype as shown on the representative dot-blot. *(Fig.8A)* In the analysed samples, we could see a significant decrease of MDSC-like $CD11b^{+}Gr1^{+}$ phenotype with increased concentrations of free CuD compared to untreated controls. *(Fig.8B)* The equitoxic dose of linear polymer CuD conjugate had a similar effect on MDSC-like $CD11b^{+}Gr1^{+}$ cells as free CuD. Micellar polymer conjugate did not reduce the expansion of MDCS-like population to the same extent as the free drug or linear CuD conjugate. Conversely, the $CD11b^{+}Gr1^{-}$ population has significantly expanded with higher concentrations of free drug and linear polymer conjugate. *(Fig.8C)*

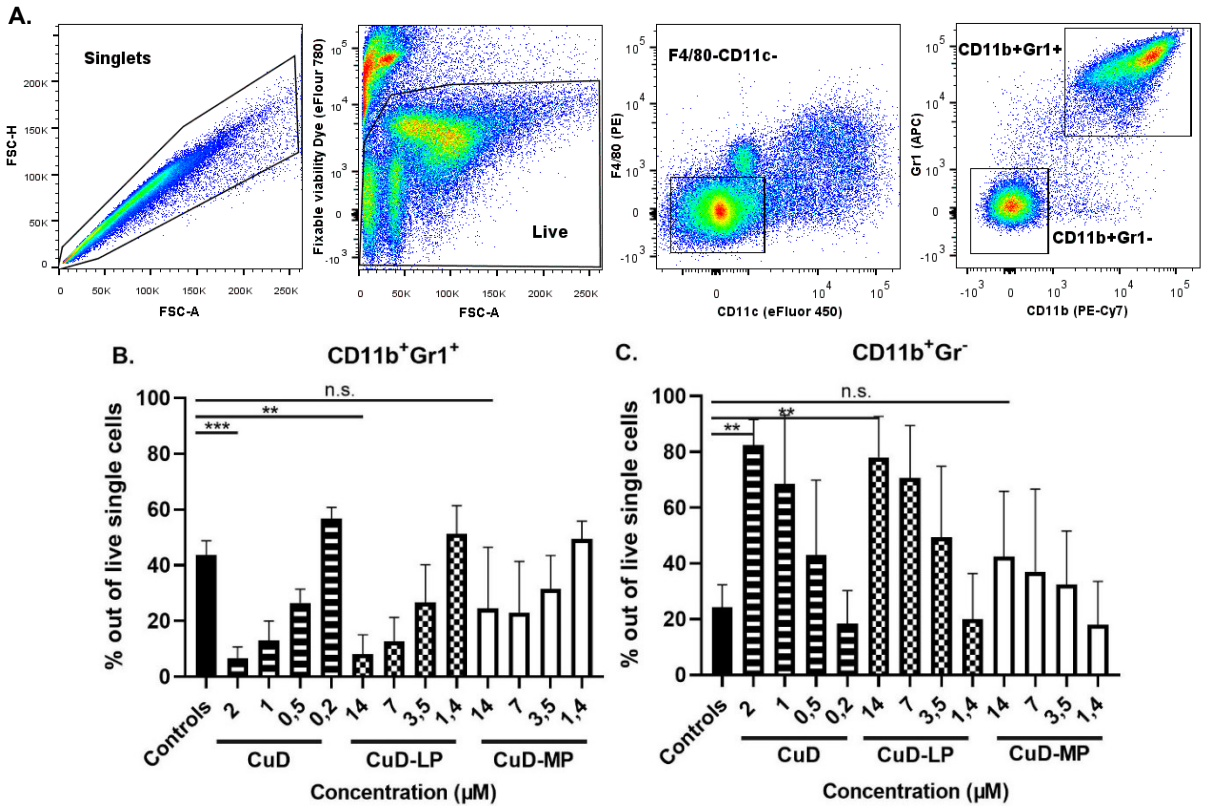

Figure 8 | The effect of CuD-based polymers and free CuD on MDSC-like cells *in vitro.* The cells were isolated from the bone marrow of tumour-free BALB/c mice and cultivated in the presence of 20 ng/mL GM-CSF. A gradient of concentrations of free CuD or polymer conjugates expressed as a concentration equivalent of CuD (μM) were added. (A) FACS analysis was performed as shown on one representative mouse. Percentage of (B) $CD11b^{+}Gr1^{+}$ and (C) $CD11b^{+}Gr1^{-}$ within all viable cells are presented as means of 3-4 mice +/- SD. Statistical significance was determined by two-tailed unpaired Student t-test, *p < 0,05, **p < 0,01 and ***p < 0,001.

5.3 Effect of CuD-based conjugates on STAT3 detected in DU-145 cells *in vitro*

In line with the *in vitro* cytotoxic activity of CuD-based polymer nanomedicines, we have decided to further illustrate the mechanism behind this phenomenon. Human prostate cancer cells DU-145 are known to express high levels of an active STAT3 transcription factor. It has been described, that overexpression of STAT3 promotes the growth and metastatic progression of prostate cancer cells and direct STAT3 inhibition induces apoptosis in several prostate cancer lines. [45], [122]

We evaluated the direct effect of low-molecular-weight CuD on the phosphorylation of the STAT3 transcription factor. We compared the effect of free CuD and Stattic, a selective STAT3 inhibitor reducing phosphorylation of STAT3 on Tyr^{705} residue. [123] DU-145 cells were cultivated with 20 μM Stattic or various concentrations of free CuD. Upon stimulation with IL-6, 20 μM Stattic significantly decreased the phosphorylated STAT3 but did not have any effect on overall levels of the STAT3 transcription factor. The concentration of 50 nM CuD (approximately IC_{50} value) was able to reduce the levels of pSTAT3 compared to the stimulation with IL-6 without any inhibition. Again, it did not influence the overall expression of STAT3. *(Fig.9)* These results suggest that CuD indeed acts as the STAT3 signalling pathway inhibitor, although additional mechanisms of toxicity are probably taking part in the anti-cancer activity of CuD-conjugated polymer nanomedicines.

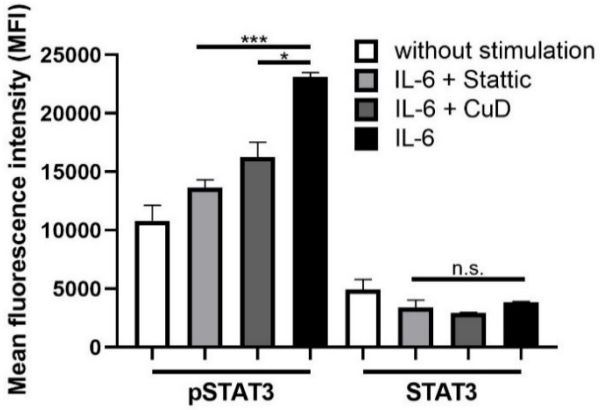

Figure 9 | The effect of free CuD on the phosphorylation of STAT3 detected in DU-145 human prostate cancer cells *in vitro*. The cells were incubated in the presence of 20 μM Stattic or 50 nM free CuD for 1 hour and stimulated with 50 ng/mL IL-6 for 30 mins. The levels of STAT3 and pSTAT3 transcription factor were detected using FACS. The mean fluorescence intensity was calculated. Data are presented as means of 3 experiments +/- SD. Statistical significance was determined by a two-tailed unpaired Student t-test, ***$p < 0{,}001$.

5.4 Evaluation of optimal dosing for *in vivo* CuD-based therapy

The hydrophobic nature and low bioavailability of CuD restrict its potential therapeutic application. Several studies have shown the anti-cancer activity of CuD in various tumour models when administered intraperitoneally (i.p.) or intratumorally (i.t.). [107], [109], [114], [117]. In our study, the mice that were s.c. inoculated with 5×10^5 4T1 mammary carcinoma cells were treated i.t. with CuD. The changes in the behaviour and body weight of the mice were monitored. The reduction of body weight by more than 15% was considered as a cut-off value for the determination of systemic toxicity. The treatment with 1 mg/kg CuD in six consecutive doses every other day led to the development of severe superficial lesions lined with an edge formed by growing tumour cells and no survival prolongation. The higher dosing scheme, 2 mg/kg CuD i.t. in six consecutive doses every other day, led to the observable systemic toxicity. Therefore, the free parent drug was not included in any further experiment as a control. To estimate the optimal therapeutic dose of polymer CuD-bearing prodrugs, we performed intravenous (i.v.) administration of the linear polymer CuD conjugate at three dosing schemes. Tumour-free BALB/c mice were injected i.v. with linear polymer CuD conjugate. Three dosing schemes were following: the single-dose equivalent of 2 mg CuD/kg, single dose equivalent of 5 mg CuD/kg, or three consecutive doses each equivalent of 2 mg CuD, injected in 3-day intervals. The conjugate was dissolved in PBS. The changes in the behaviour and body weight of the mice were monitored. *(Fig.10)*

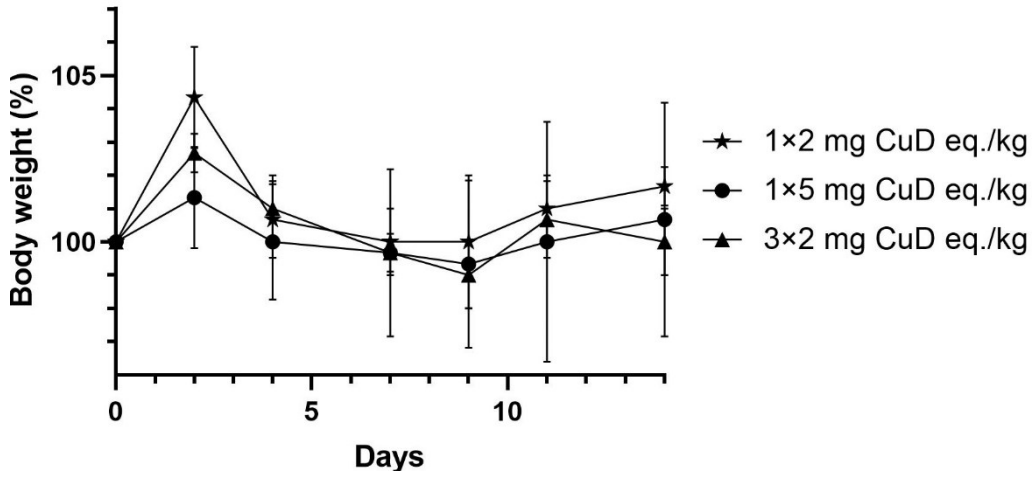

Figure 10 | Systemic toxicity of treatment with linear CuD-based conjugate. BALB/c mice (n=3 per group) received linear polymer CuD conjugate i.v according to three different therapeutic schemes. Potential systemic toxicity was monitored using the body weight as the measurable parameter; a reduction of more than 15 % was chosen as the cut-off value. The values are shown as means +/- SD.

As shown in *Fig.10*, linear polymer CuD conjugate did not induce any detectable systemic toxicity. As well, no other signs of systemic toxicity (e.g., hunched posture, bristle coat) were observed. As previously shown, linear and micellar CuD-bearing polymers had a comparable cytostatic effect *in vitro*. Therefore, we have decided to use a comparable therapeutic dosage of both conjugates also for *in vivo* treatment. Taken together, the results have confirmed the hypothesis that CuD transported by the HPMA polymer nanocarrier is suitable for drug delivery because it significantly reduces the systemic toxicity of i.t. administered free parent drug.

5.5 MDSC levels in CT26 and 4T1 tumour-bearing mice

Our next goal was to determine the significance of MDSCs in two well-established murine experimental models; CT26 colon adenocarcinoma and 4T1 mammary carcinoma. First, we assessed the levels of MDSCs in blood, tumours and spleens of CT26 tumour-bearing mice. BALB/c mice (n=5) were s.c. inoculated with 2×10^5 CT26 tumour cells on day 0. The blood, spleens and tumours were collected in 6-day intervals starting on day 9. Flow cytometry analysis was performed; MDSCs were distinguished as $CD11b^+Ly6C^{high}Ly6G^-$ Mo-MDSCs, and $CD11b^+Ly6C^{low}Ly6G^+$ PMN-MDSCs as shown on the representative dot blot. *(Fig.11A)* The analysis of peripheral blood has shown that the major MDSC subset circulating in the blood is PMN-MDSCs. The levels of PMN-MDSCs and Mo-MDSCs in the peripheral blood of CT26 tumour-bearing mice have not significantly changed with the ongoing progression of the tumour when compared to the tumour-free mice. *(Fig.11B)* Both subsets of MDSCs in the spleen had comparable frequencies and had mildly increased over the course of the tumour growth, even though the overall counts of MDSCs remained very low. *(Fig.11C)* Tumour analysis has shown that both subsets of MDSCs have remained at similar counts over the course of the tumour growth. *(Fig.11D)* Probably due to the significant turnover of the cells within the tumour microenvironment and rapid changes in MDCSs frequencies, detected MDCSs counts are low and relatively heterogeneous. Moreover, the tumour isolation process and the preparation of samples are rather difficult. For future experiments, we have decided to focus on the flow cytometric analysis of the peripheral blood, which allows repeated sample collection over the course of tumour progression accompanied by easier sample isolation, manipulation and analysis.

The second step was to detect the levels of MDSCs circulating in the blood of 4T1 tumour-bearing mice. BALB/c mice (n=5) were s.c. inoculated with 2×10^5 4T1 tumour cells on day 0. The blood was collected in 6-day intervals starting on day 9. The blood samples were analysed using flow cytometry. Again, MDSCs in tumour-bearing mice were gated as $CD11b^+Ly6C^{high}Ly6G^-$ Mo-MDSCs, and $CD11b^+Ly6C^{low}Ly6G^+$ PMN-MDSCs as shown on the representative dot blot. The analysis has shown a significant increase in the PMN-MDSC population in the peripheral blood of the experimental animals. PMN-MDSCs had gradually expanded over the course of the tumour progression. *(Fig.11E)* Our results suggest that MDSC-mediated immune suppression plays a considerable role in murine 4T1 mammary carcinoma. On the other hand, the immune modulation via MDCSs does not seem to a have similar impact on the tumour progression in CT26 colon adenocarcinoma tumour-bearing mice.

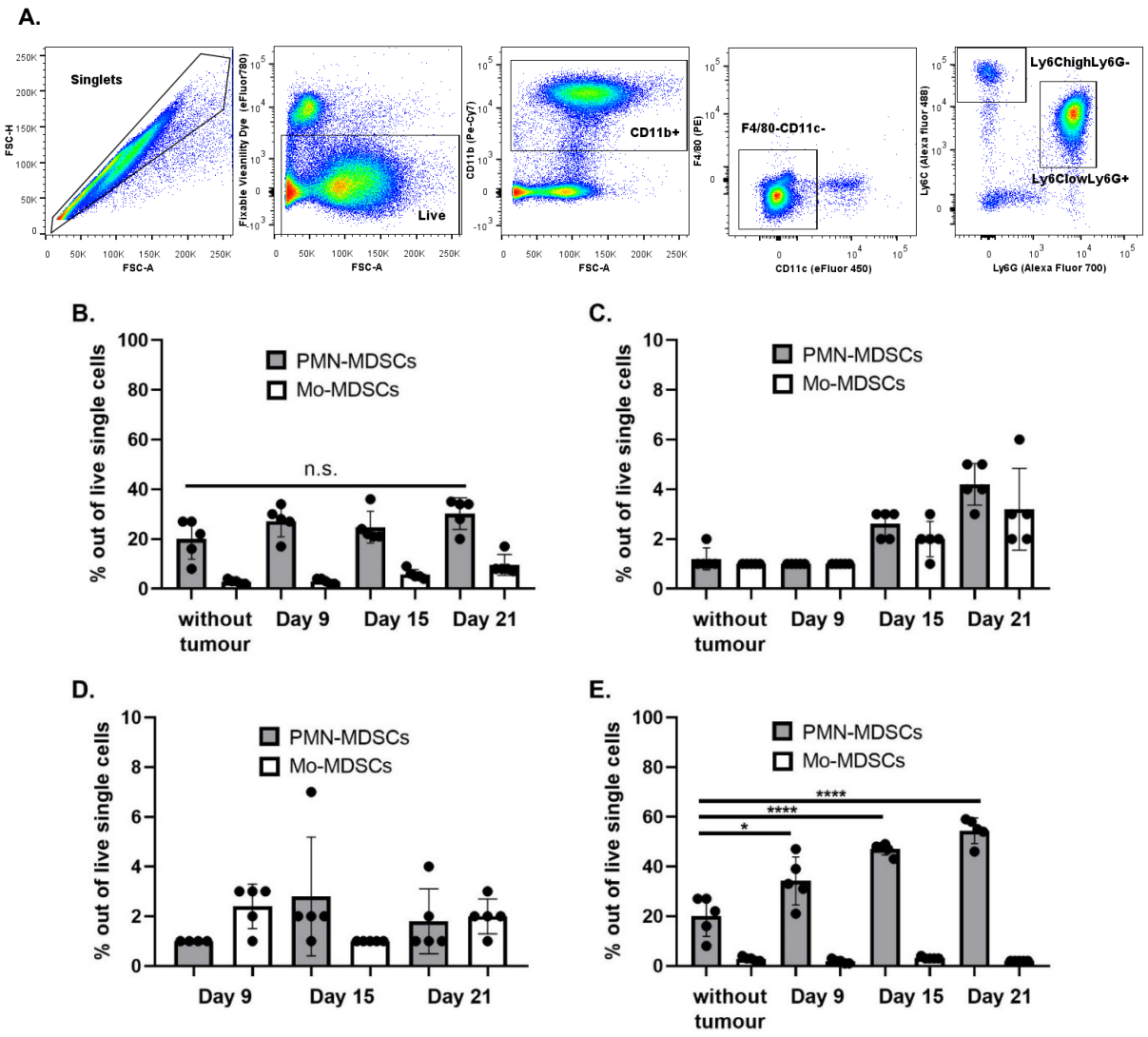

Figure 11 | The levels of MDSCs subsets in blood, spleen and tumour in CT26 colon adenocarcinoma and blood of 4T1 mammary carcinoma mouse model. BALB/c mice (n=5) were s.c. inoculated with 2×10^5 CT26 tumour cells on day 0. The blood, spleens and tumours were collected in 6-day intervals on day 9, day 15 and day 21. (A) FACS analysis was performed as shown on one representative mouse**.** Percentage of $CD11b^+Ly6C^{high}Ly6G^-$ and $CD11b^+Ly6C^{low}Ly6G^+$ populations in (B) peripheral blood, (C) spleen and (D) tumour within all viable cells are depicted. BALB/c mice (n=5) were s.c. inoculated with 2×10^5 4T1 tumour cells on day 0 and the blood was collected on day 9, day 15 and day 21. (E) FACS analysis was performed as shown on one representative mouse as shown in (A)**.** Percentage of $CD11b^+Ly6C^{high}Ly6G^-$ and $CD11b^+Ly6C^{low}Ly6G^+$ in the peripheral blood within all viable cells are depicted. The data are presented as means of 5 mice +/- SD. Statistical significance was determined by two-tailed unpaired Student t-test, *p < 0,05, **p < 0,01 and ***p < 0,001.

5.6 *In vivo* 4T1 murine mammary carcinoma therapy

5.6.1 Linear polymer CuD-based conjugate

Based on previously established therapeutic schemes using micellar Dox-bearing conjugate and our experimentally estimated safe dose of linear CuD conjugate, we conducted *in vivo* therapeutic experiment. We aimed to investigate whether linear polymer CuD-based prodrug brings benefit to the treatment of murine 4T1 mammary carcinoma, rapidly progressing and metastasizing type of cancer. Tumours derived from 4T1 carcinoma cells are rather difficult to treat, tumour-bearing mice left without any therapy live only around forty days. Based on our results of peripheral blood analysis and published data [124], we assumed that MDSCs have an important impact on the development of murine 4T1 mammary carcinoma. Therefore, we hypothesized that combined therapy composed of CuD-based conjugate blocking the STAT3 signalling pathway in MDSCs and classical Dox-based chemotherapeutic micellar conjugate targeted directly towards the malignant cells could bring significant benefit in the treatment of tumours derived from 4T1 carcinoma cells.

We investigated the anti-tumour activity of linear CuD-based conjugate as a sole therapy as well as in the combination with micellar Dox-bearing conjugate. BALB/c mice (n=8) were s.c. inoculated with 2×10^5 4T1 tumour cells on day 0. Mice were treated i.v. with linear CuD conjugate (3 mg CuD eq./kg) and/or micellar Dox conjugate (8 mg Dox eq./kg) in 3-day intervals starting on day 8. One control group was left without any treatment. The dosing scheme *(Fig.12A)* was chosen to prevent any systemic toxicity. The changes in body weight of the mice were regularly documented, no significant decrease was observed. The minor decrease in body weight during the combination therapy was within the 15% range that was considered as a cut-off value for the determination of systemic toxicity. We have confirmed that the combination of CuD-based and Dox-based prodrugs do not carry any risk of toxicity. *(Fig.12B)* Tumour growth was measured from day 8 after inoculation of cancer cells and measurements were terminated on day 32. Linear polymer CuD conjugate did not significantly reduce the tumour growth, although we could see a trend in the reduction of tumour size in the combined treatment together with micellar Dox conjugate. *(Fig.12C)* Sole CuD-based linear conjugate treatment had no observable effect on the survival of experimental animals. On the contrary, micellar polymer carrying Dox was efficient at prolonging the lifespan of experimental mice in comparison to the control group. Only a mild beneficial effect on the survival of mice treated with the combination of both conjugates was observed. *(Fig.12D)*

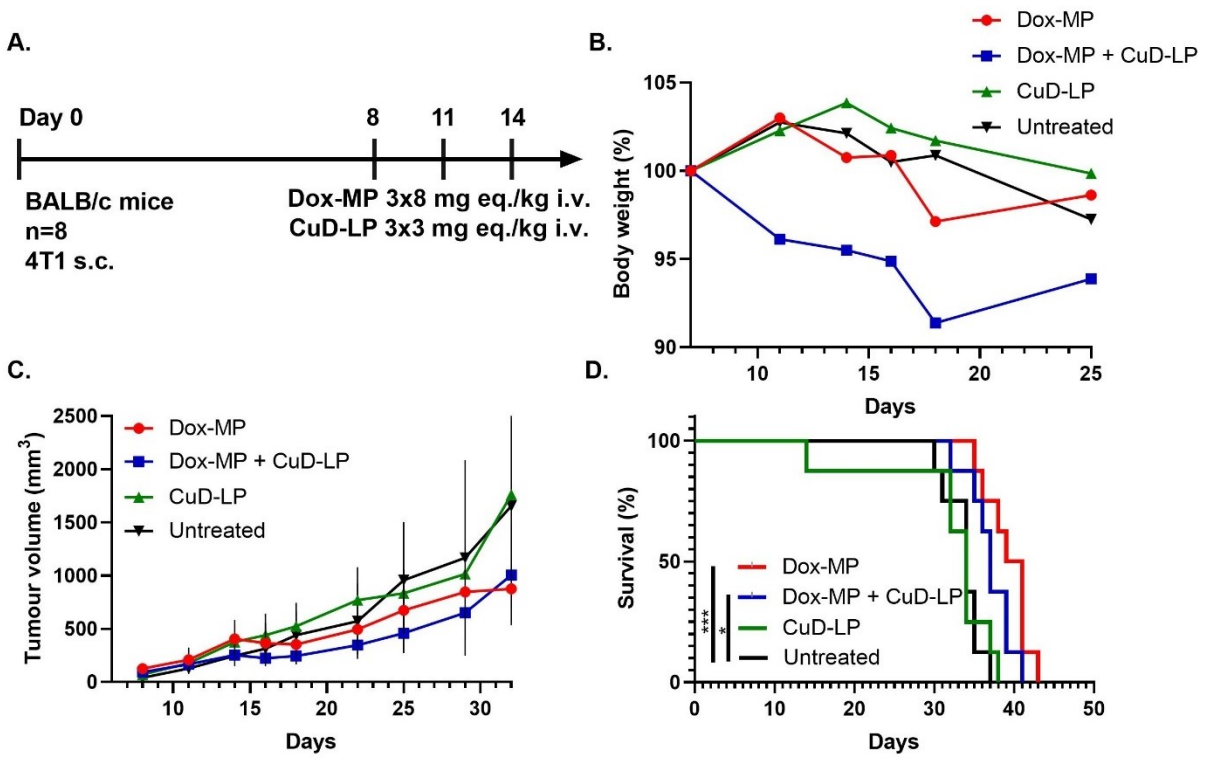

Figure 12 | *In vivo* therapeutic effect of linear CuD-based polymer conjugate combined with micellar polymer Dox conjugate in 4T1 mammary carcinoma tumour-bearing mice. (A) Therapeutic scheme of the experiment. BALB/c mice (n=8 per group) were s.c. inoculated with 2×10^5 4T1 tumour cells on day 0. Mice were treated i.v. with linear polymer CuD conjugate and/or micellar polymer Dox conjugate. (B) Potential systemic toxicity was monitored using the body weight as the measurable parameter; a reduction of more than 15 % was considered the cut-off value. (C) Tumour growth (means +/- SD) (D) and survival were recorded. Statistical significance was determined by a two-tailed unpaired Student t-test for tumour growth assessment and log-rang Mantel-Cox test for survival analysis, ***$p < 0{,}001$.

5.6.2 Micellar polymer CuD-based conjugate

Our next step was to assess the therapeutic effect of micellar CuD-bearing conjugate and to compare it with the linear CuD-based polymer. Micellar nanocarriers have different biological properties and the parent drug is sheltered by the micelle core which should provide more continuous drug release. We tested the activity of micellar polymer CuD conjugate in 4T1 mammary carcinoma. We used a similar therapeutic scheme as in the previous experiments with optimized doses to prevent any systemic toxicity. BALB/c mice (n=8) were s.c. inoculated with 2×10^5 4T1 tumour cells on day 0. Mice were treated i.v. with linear polymer CuD conjugate (2,5 mg CuD eq./kg); or micellar polymer CuD conjugate (2,5 mg CuD eq./kg.); and/or micellar polymer Dox conjugate (8 mg Dox eq./kg) in 3-day intervals starting on day 8. *(Fig.13A)* One control group was left without any treatment. Tumour growth and survival were monitored. *(Fig.13B, Fig.13C)*

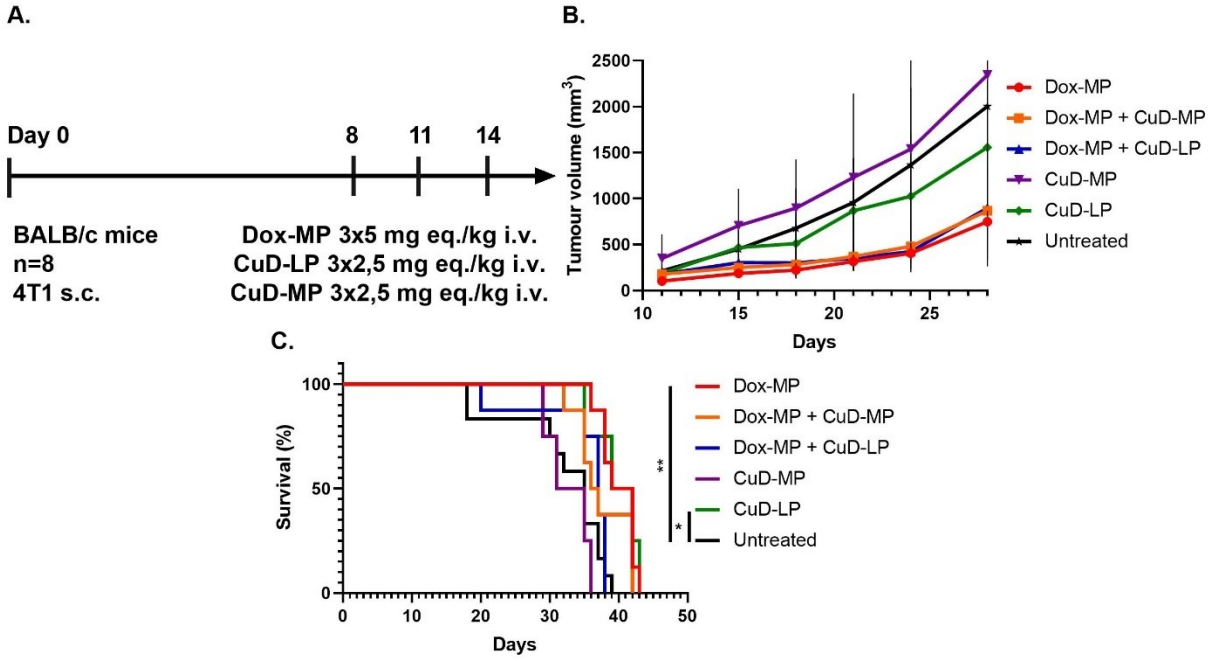

Figure 13 | Therapeutic effect of micellar and linear CuD-based polymer conjugates in combination with micellar Dox conjugate in 4T1 tumour-bearing mice. (A) Therapeutic scheme of the experiment. BALB/c mice (n=8 per group) were s.c. inoculated with 2×10^5 4T1 tumour cells on day 0. Mice were treated i.v. with linear polymer CuD conjugate, micellar polymer CuD conjugate; and/or micellar polymer Dox conjugate. (B) Tumour growth (means +/- SD) (C) and survival were monitored. Statistical significance was determined by two-tailed unpaired Student t-test for tumour growth assessment and log-rang Mantel-Cox test for survival analysis, *$p < 0,05$, **$p < 0,01$.

Tumour growth was measured from day 11 after inoculation of cancer cells until day 28. Anti-tumour activity of micellar polymer CuD conjugate was not detectable as a reduction of tumour growth when applied as a sole treatment. Linear polymer CuD conjugate did not significantly reduce the tumour growth, although we could see a mild reduction of tumour size when applied as a sole therapy. The combined treatment with both types of CuD-based polymer prodrugs together with micellar conjugate bearing Dox significantly reduced the tumour growth. However, we hypothesize that the effect was caused mainly due to the treatment with Dox-based polymer conjugate, because the sole Dox-based conjugate treatment had the same effect as the combination treatment with both CuD-bearing conjugates. *(Fig.13B)*

Sole CuD-based micellar conjugate treatment has failed to have any effect on the survival of experimental animals. On the contrary, micellar polymer carrying Dox moderately prolonged the lifespan of experimental mice in comparison to the control group. Interestingly, we could see that CuD-based linear polymer mildly prolonged the survival of experimental mice when compared to the untreated controls. The other therapeutic modalities failed to significantly extend the survival time of experimental mice. *(Fig.13C)*

We hypothesize that the key issue in such a low therapeutic efficacy of micellar polymer CuD conjugate lies in the release of CuD from the nanocarrier. The release of free parent drug entrapped in the micelle core surrounded by the micellar unimers may be very slow and CuD is not liberated from the conjugate in levels high enough to be therapeutically sufficient. Based on our experiments, the micellar polymer CuD conjugate does not seem to bring any advantage for *in vivo* treatment. This, together with the rather poor water solubility of micellar polymer CuD conjugate lead us to the decision to continue further only with the *in vivo* testing of linear CuD-based conjugate.

5.6.3 Linear CuD-based conjugate plus checkpoint blockade

Based on the results of previous experiments, we have decided to adjust the therapeutic scheme and optimize the dosing of linear polymer CuD conjugate. We have also decided to add the checkpoint inhibition by anti-PD-1 monoclonal antibody to further support the potential immunotherapeutic efficacy of the combined treatment. BALB/c mice (n=8) were s.c. inoculated with 2×10^5 4T1 tumour cells on day 0. Linear polymer CuD conjugate (2,5 mg CuD eq./kg) was administered to mice i.p. in five doses in 3-day intervals starting on day 7 and/or micellar polymer Dox conjugate (8 mg Dox eq./kg) was administered i.v. in three doses in 3-day intervals starting on day 8. Moreover, five consecutive doses of anti-mouse PD-1 monoclonal Ab (5 mg/kg) were administered i.p. in 2-day intervals starting on day 15. *(Fig.14A)* One control group was left without any treatment. Tumour growth and survival were monitored. *(Fig.14B, Fig.14C)*

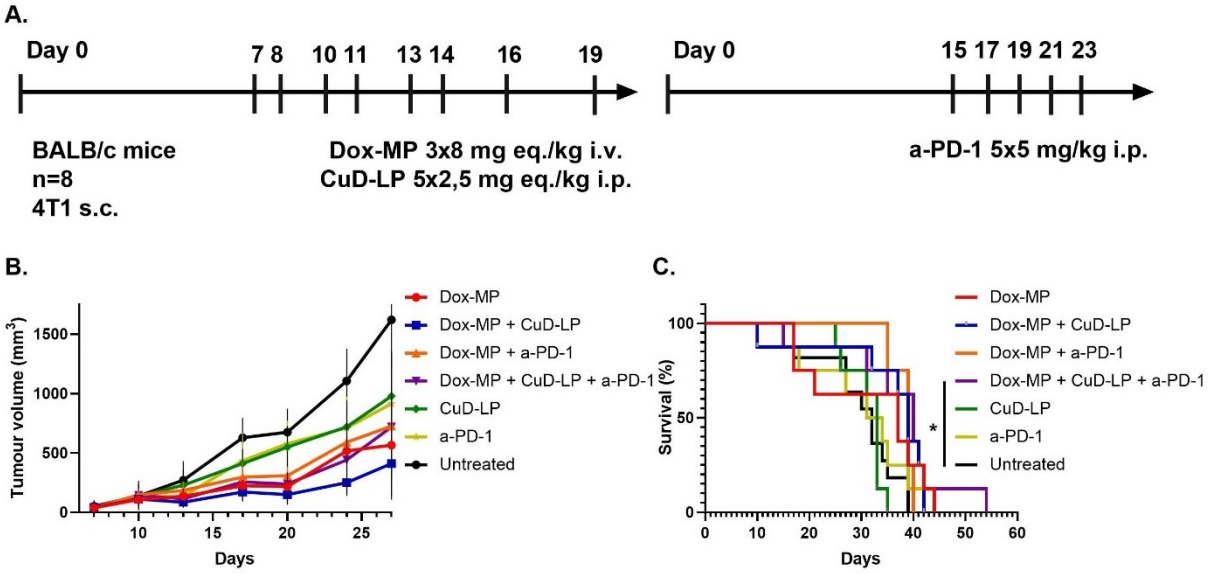

Figure 14 | Therapeutic effect of linear CuD-based conjugate combined with Dox-bearing micellar conjugate and checkpoint inhibition treatment in 4T1 tumour-bearing mice. (A) Therapeutic scheme of the experiment. BALB/c mice (n=8 per group) were s.c. inoculated with 2×10^5 4T1 tumour cells on day 0. Mice were treated i.p. with linear polymer CuD conjugate; and/or i.v. with micellar polymer Dox conjugate; and/or i.p. with an anti-mouse PD-1 checkpoint inhibitor. (B) Tumour growth (means +/- SD) and (C) survival were monitored. Statistical significance was determined by a two-tailed unpaired Student t-test for tumour growth assessment and log-rang Mantel-Cox test for survival analysis, *$p < 0,05$.

Tumour growth was measured from day 7 after inoculation of cancer cells until day 27. All the therapeutic strategies were able to significantly reduce the tumour growth compared to the untreated control group. The combined therapy with CuD-based linear conjugate and micellar polymer Dox conjugate has proven to be the most efficient. *(Fig.14B)*

Potentiation of combined treatment with PD-1 blockade significantly prolonged the survival time in one out of the eight animals in the group, whilst the other treatment modalities did not extend the lifespan of experimental mice. *(Fig.14C)* We can see that the addition of the checkpoint blockade did have a significant beneficial effect on the survival in the group treated with the combination of linear polymer CuD conjugate together with Dox-based nanomedicine.

5.7 *In vivo* CT26 murine colon adenocarcinoma therapy

We aimed to investigate whether linear CuD-based prodrug brings benefit to the treatment of murine CT26 colon adenocarcinoma. CT26 cells are slowly metastasizing and reveal a certain degree of multidrug resistance to various anti-cancer agents via upregulation of the P-glycoprotein expression.[125] Therefore, the treatment of tumours is rather difficult. Untreated tumour-bearing mice live around sixty days. The previous analysis of the peripheral blood has shown that the frequencies of MDSCs do not change upon the tumour progression so that MDSC-mediated immune suppression may not be crucial for the development of murine CT26 colon adenocarcinoma. Based on our *in vitro* results, we have decided to investigate the direct inhibitory effects of CuD-based conjugates on malignant cells during *in vivo* therapy. We investigated the anti-tumour activity of linear polymer CuD conjugate as a single therapy as well as in the combination with micellar Dox-based conjugate.

BALB/c mice (n=8) were s.c. inoculated with 2×10^5 CT26 tumour cells on day 0. Mice were treated i.v. with linear CuD conjugate (2,5 mg CuD eq./kg) and/or micellar polymer Dox conjugate (8 mg Dox eq./kg) in 4-day intervals starting on day 9. *(Fig.15A)* One control group was left without treatment. The therapeutic scheme was chosen based on our estimated safe dosage to prevent any systemic toxicity. The changes in body weight were regularly monitored, no significant decrease was observed. *(Fig.15B*) Tumour growth was measured from day 10 until day 38 after the inoculation of cancer cells. All the therapeutic strategies have failed to significantly reduce the tumour growth compared to the control group. Anti-tumour activity of linear polymer CuD conjugate was not observable and did not reduce the tumour growth at all. However, we could see a mild reduction of tumour size in the treatment with micellar Dox-bearing conjugate or when combined with linear CuD-based conjugate. *(Fig.15C)* Sole CuD-based linear conjugate treatment has failed to have any effect on the survival of experimental animals. Other therapeutic modalities failed to significantly extend the lifespan of experimental mice as well. *(Fig.15D)*

We hypothesize that the key issue for low therapeutic efficacy of CuD-containing nanocarriers in CT26 colon adenocarcinoma therapy lies in the low significance of MDSCs-mediated immune suppression for the tumour progression in this experimental tumour model. The direct cytotoxic effect of CuD-based conjugate is too low to improve either tumour growth or survival of the CT26 tumour-bearing mice.

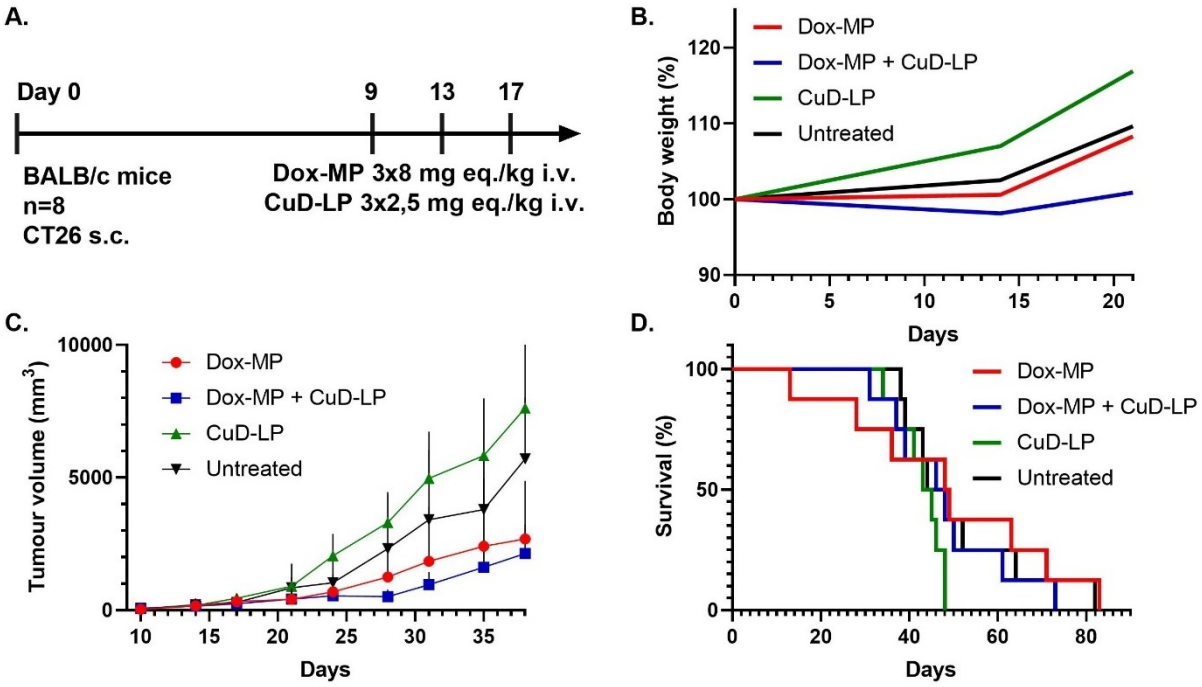

Figure 15 | Therapeutic effect of linear CuD-based polymer conjugate combined with micellar polymer Dox conjugate in CT26 colon adenocarcinoma tumour-bearing mice. (A) Therapeutic scheme of the experiment. BALB/c mice (n=8 per group) were s.c. inoculated with 2×10^5 CT26 tumour cells on day 0. Mice were treated i.v. with linear polymer CuD conjugate and/or micellar polymer Dox conjugate. (B) The changes in body weight were monitored; a reduction of more than 15 % was considered the cut-off value. (C) Tumour growth (means +/- SD) (D) and survival were recorded.

5.8 MDSCs levels during *in vivo* CuD-based conjugate therapy

Based on the results of *in vivo* experimental therapies and the peripheral blood analysis, we have decided to assess the effect of the CuD-based nanomedicine on the levels of MDCSs subsets in the peripheral blood of mice during the early stages of 4T1 murine mammary carcinoma development. BALB/c mice (n=5) were s.c. inoculated with 2×10^5 4T1 tumour cells on day 0. Mice were treated i.v. with linear polymer CuD conjugate (2,5 mg CuD eq./kg); and/or micellar Dox-bearing conjugate (8 mg Dox eq./kg) in 3-day intervals starting on day 8. *(Fig.16B)* The blood was collected in 6-day intervals, on day 9, day 15 and day 21. The blood samples were analysed using flow cytometry. MDSCs in tumour-bearing mice were gated as $CD11b^{+}Ly6C^{high}Ly6G^{-}$ Mo-MDSCs, and $CD11b^{+}Ly6C^{low}Ly6G^{+}$ PMN-MDSCs as shown on one representative dot blot. *(Fig.16A)*

Tumour growth was measured from day 8 until day 25 after the inoculation of cancer cells. We could see a trend in reduction of the tumour growth in all therapeutic modalities. The combination of CuD-based linear conjugate and micellar Dox-bearing conjugate has proven to be the most sufficient. *(Fig.16C)* All the therapeutic modalities failed to significantly extend the survival of experimental mice when compared to the control group. *(Fig.16D)*

The peripheral blood analysis has shown a reduction in levels of PMN-MDSCs in all the therapeutic modalities; starting to be apparent, but statistically insignificant, on day 9. *(Fig. 16E)* The most significant differences were observed on day 15. *(Fig 16F)* The combined therapy, as well as sole micellar Dox-bearing conjugate treatment, have significantly decreased the number of circulating PMN-MSDCs. Sole CuD-based conjugate treatment was not as efficient as the other two therapeutic strategies. *(Fig.16F)* The flow cytometry analysis on day 21 has shown, that the effect of polymer prodrugs on the levels of PMN-MDSCs a week after the last dose of therapy is almost nondetectable. *(Fig.16G)* This corresponds with the fact that the drug-conjugated polymers often reduce the tumour growth in earlier stages of tumour progression, but fail to significantly extend the survival of the experimental animals.

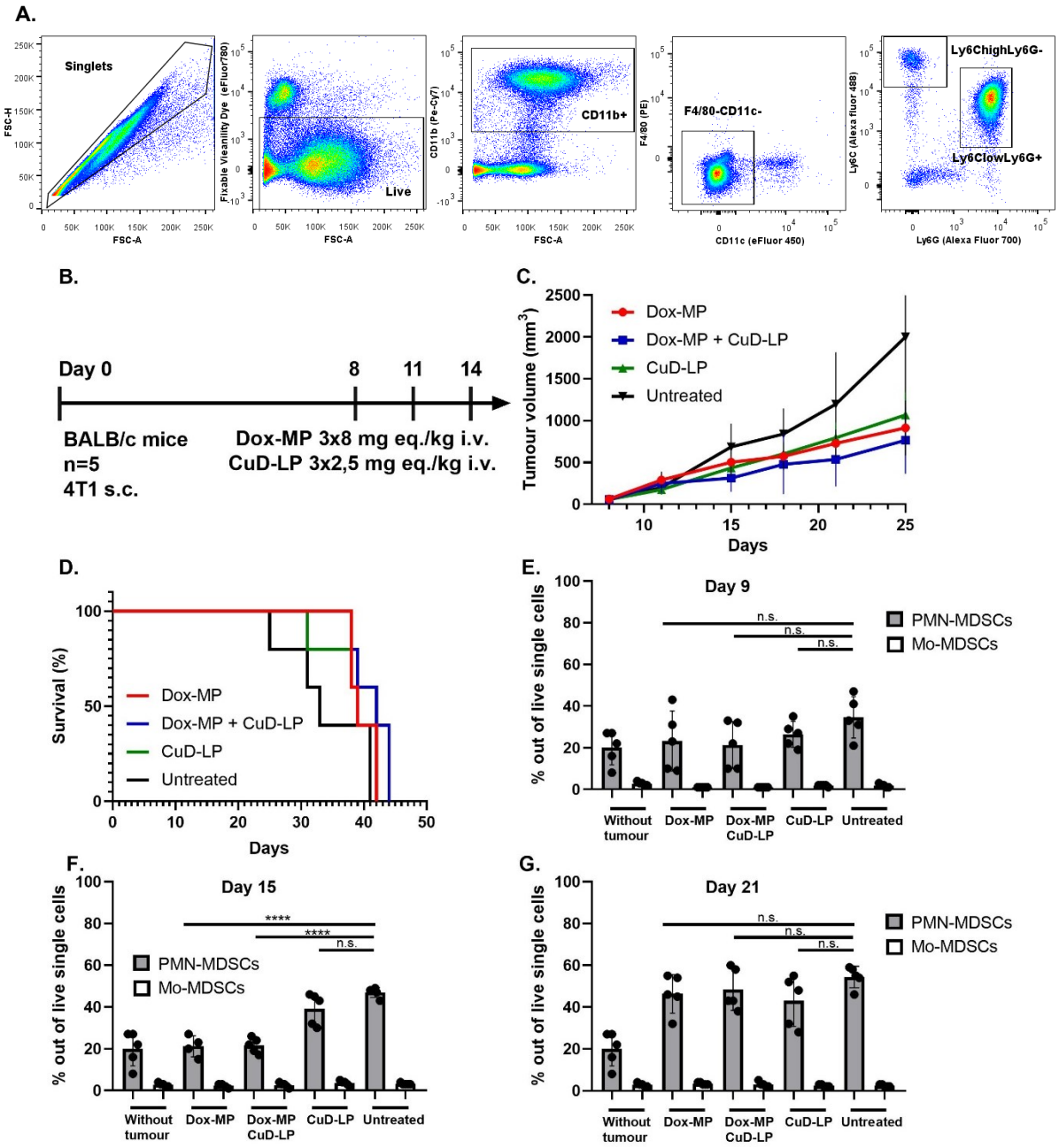

Figure 16 | MDSCs in the peripheral blood of 4T1 tumour-bearing mice during CuD-based conjugate therapy. BALB/c mice (n=5 per group) s.c. inoculated with 2×10^5 4T1 tumour cells on day 0 were treated i.v. with linear CuD conjugate and/or micellar Dox conjugate. The blood was collected on day 9, 15 and 21. (A) FACS analysis was performed as shown on the representative dot-blot. (B) Therapeutic scheme of the experiment. (C) Tumour growth (means +/- SD) (D) and survival are presented. Percentage of $Ly6C^{high}Ly6G^{-}$ and $Ly6C^{low}Ly6G^{+}$ populations within all viable cells on (E) day 9, (F) day 15 and (G) day 21 is shown. The data are presented as means of 5 mice +/- SD. Statistical significance was determined by a two-tailed unpaired Student t-test, ***p < 0,001.

6 Discussion

Despite the progressive development of the new immunotherapeutic protocols, chemotherapy is still one of the most commonly used anti-cancer treatments. Chemotherapy is based on the administration of cytotoxic drugs that generally inhibit the rapidly dividing cells by various mechanisms. Therefore, it is accompanied by characteristic side effects as it affects non-cancerous cells with fast proliferation rates; typically the bone marrow, gastrointestinal tract cells or hair follicles. Besides the overall systemic toxicity, conventional chemotherapeutics carry other disadvantages such as short biological half-life and circulation time in the blood or narrow therapeutic window. Moreover, cancer cells might develop multiple drug resistance, which is directly related to the repeated administration of low molecular weight cytotoxic drug.[73]

An essential task to achieve successful immune-oncotherapy is the preparation of an effective drug delivery system. An improvement of the pharmacological properties of classical chemotherapeutics could be accomplished by binding the drug to a polymer nanocarrier. For example, polymer nanocarrier based on HPMA, that has proven to be biocompatible, nontoxic and nonimmunogenic.[85], [91] HPMA copolymers are currently studied mostly in the context of low molecular weight cytotoxic drugs.[126] The binding of low molecular weight drug to HPMA increases its solubility in water, reduces systemic toxicity, prolongs the circulation time in the blood and increases the maximum tolerated dose. The drug is bound to the polymer backbone via a spacer. The nature of the spacer determines the specific release of the drug, whether it is liberated depending on the changes in pH or enzymatically.[127] In addition to the attachment of the cytotoxic drugs, the HPMA polymer backbone can be modified by molecules providing specific targeting of the conjugate, such as monoclonal Abs or their fragments.[128], [129] Besides the specifically targeted copolymers, HPMA conjugates accumulate in the tumour microenvironment passively via the so-called EPR effect.[79], [80]

The drug-polymer conjugate is then engulfed via endocytosis by tumour cells and the cytotoxic agent is released in the low pH of the lysosomal compartments of the cell. The pH-sensitive hydrolysis of the hydrazone bond and release of the parent drug may to some extent occur also in the tumour microenvironment where the pH is lower compared to normal tissues. Polymer prodrugs based on HPMA conjugated with established anti-cancer chemotherapeutics have a potent anti-cancer effect and immunomodulating activity. It has been described, that the treatment of experimental tumours using distinct HPMA polymer conjugates

with Dox induces treatment dependent resistance of the host towards the same cancer cells and establishes immunological memory.[94]–[96]

This diploma thesis describes the biological evaluation of novel polymer therapeutics based on HPMA copolymers and immunomodulatory agent CuD, intended for tumour-targeted immune-oncotherapy. Several studies have reported that cucurbitacins exhibit potent pharmacological effects, including anticancer activity.[106], [110], [117], [130] Among cucurbitacin derivatives, CuD showed an inhibitory effect on the proliferation of several tumour cell lineages mediated mainly via inhibition of the JAK/STAT3 signalling pathway.[116], [117] Reports also suggested that cucurbitacins together with other chemotherapeutic agents can promote a synergism and may support the effect of chemotherapy via the suppression of STAT3 transcription factor.[111], [120]

On the other hand, there are notable limitations concerning the potential clinical application of cucurbitacins such as their poor water solubility, considerable toxicity, low selectivity, and narrow therapeutic window for treatment.[103], [130], [131] We have assumed that binding an immunomodulatory compound, such as CuD, to a hydrophilic nanocarrier, such as HPMA, would provide a conjugate that could be easily administered to the body without the risk of systemic toxicity. Moreover, the polymer-drug conjugate would improve the pharmacokinetic profile and bioavailability of the free highly hydrophobic drug. Besides, the CuD-based conjugate would enable selective targeting directly to the solid tumour tissue through the EPR effect. Based on the previous results from our laboratory, polymer drug delivery systems can be used to elicit a targeted and localized effect directly in the tumour microenvironment. For instance, we have described that polymer nitric oxide donors, which alone do not exhibit antitumor effect, allow higher accumulation of polymer cytostatics via augmenting the passive accumulation of nanomedicines in tumours induced by the EPR effect. We have demonstrated, that the combination of polymer nitric oxide donors and polymer-bound Dox increased Dox accumulation in the tumour microenvironment, thereby increased the effect of treatment which led to a better therapeutic outcome in the mouse EL4 T-cell lymphoma tumour model.[132]

This thesis is based on the hypothesis that CuD as a STAT3 inhibitor could exert a dual effect, killing directly the tumour cells as well as inhibiting tumour-infiltrating MDSCs. The use of CuD-based nanomedicine could also work as an adjuvant therapy complementary to the treatment with other polymer-bound cytostatic, necessary for the direct anti-tumour responses. The polymer conjugate would allow us to target the immunomodulatory effect of CuD specifically into the tumour microenvironment and attenuate the immune-suppressive functions

of MDSCs that are crucial for the suppression of the anti-tumour immune responses via inhibiting effector T cells by direct cell-to-cell contact or secreted mediators.

Our first goal was to assess the biological activity of HPMA copolymers bearing CuD *in vitro*. Cytostatic/cytotoxic activity tested in selected human and murine cell lineages proved that the binding of CuD to the polymer nanocarrier, whether linear or micellar, retains the functional capacity of the drug. As previously seen in other HPMA-based prodrugs, polymer conjugates were *in vitro* less toxic than the free parent drug; with four to six times lower IC_{50} values. The human cancer cells were more sensitive to CuD-bearing conjugates compared to murine tumour cell lines. The results correspond with the fact that human ovarian carcinoma cells SC-OV-3 and OVCAR-3, and prostate DU-145 cells have been reported to have high expression of the STAT3 transcription factor.[43]–[45] Moreover, the cytotoxic activity of CuD conjugates was checked in normal murine spleen cells proving that tumour cells are significantly more susceptible to polymer CuD-based conjugates, which seems beneficial for the potential *in vivo* applications.

We have tested four batches of linear CuD-bearing conjugates with well-defined physicochemical parameters (*Table 1)*, that corresponded when compared within the individual batches. We have obtained results with corresponding IC_{50} values proving that the synthesis and preparation of HPMA prodrugs containing CuD were reproducible. We did not find significant differences between *in vitro* cytotoxicity of the linear and micellar CuD-based conjugates. We believe that this could be partly due to the pH-sensitive extracellular release of the drug before the engulfment of the polymer conjugate by the tumour cells. The results suggest that the rate of extracellular pH-sensitive hydrolysis of the hydrazone bond in both types of polymer conjugates is similar. However, IC_{50} values expressed as a concentration equivalent of CuD might not reflect the biological activity of different types of polymer conjugates that may show different behaviour observed during *in vitro* and *in vivo* experiments.

Based on the cytotoxicity assays results, we wanted to investigate the hypothesis that CuD acts as the STAT3 signalling pathway inhibitor in DU-145 cells *in vitro.* We have decided to compare the effect of free CuD and Stattic, a selective inhibitor of phosphorylation of STAT3 on Tyr^{705} residue.[123] Indeed, we could see that Stattic as well as the concentration of CuD corresponding with the IC_{50} value significantly decreased the phosphorylated STAT3 in IL-6 stimulated cells while not affecting the total levels of the STAT3 transcription factor. In this case, CuD-bearing conjugate would not work similarly because of the short incubation times used in the experiments. Free parent drug enters the cell via diffusion, meanwhile, HPMA copolymers are engulfed via endocytosis, which is significantly slower.

As MDSCs play an important role in the progression of various tumour types, one of our goals was to study the effect of the HPMA conjugates with CuD on the frequencies of MDSCs expanded *in vitro* as well as over the course of *in vivo* experiments. It has been suggested that the cytotoxic activity of CuD could be mediated via the inhibition of the STAT3 signalling pathway.[117], [119], [120] As previously described in several studies [52]–[55], targeting the STAT3 signalling pathway could prevent the expansion of MDSCs and enhance their differentiation towards immature myeloid cell populations. On the other hand, many investigators have used the Gr-1-specific Ab to deplete MDSCs in tumour-bearing mice and the results were quite controversial. The efforts to eliminate MDSC with an anti-Gr-1 antibody have shown only limited effect because eliminated MDSCs are rapidly supplemented by the increased recruitment of precursors from the bone marrow.[133]–[135] Thus, administration of a low molecular weight drug that inhibits MDSCs function is likely to have only limited efficacy. On the contrary, the administration of a polymer-drug conjugate could prolong the effect of eliminating or reducing the number of MDSCs over a longer period of time due to the prolonged blood circulation and targeted accumulation in the tumour tissue.

Based on the literature describing STAT3 as essential for MDSCs differentiation and immunosuppressive function [42], [46], [48]; we aimed to investigate whether polymer-bound CuD or free drug for comparison affects bone-marrow cells *in vitro* stimulated into expansion towards MDSC-like cells. Indeed, flow cytometry analysis of MDSC-like bone-marrow cells after cultivation with different concentration of free CuD and the equitoxic dose of its linear polymer conjugate has shown a significant decrease of MDSC-like $CD11b^{+}Gr1^{+}$ phenotype with increased concentrations of the drug compared to untreated controls. Conversely, the $CD11b^{+}Gr1^{-}$ population has significantly expanded with higher concentrations of the drug. Micellar CuD-based conjugate did not reduce the expansion of MDCS-like population to the same extent as a free or linear polymer-bound CuD, possibly due to the slow release of CuD from the hydrophobic micellar core. CuD may not be liberated from the conjugate in levels high enough to prevent $CD11b^{+}Gr1^{+}$ cell expansion during the 72-hour cultivation.

Following the *in vitro* experiments, we intended to define the therapeutic effect of polymer-bound CuD in combination with other polymer chemotherapeutic prodrugs *in vivo*. The hydrophobic nature and low bioavailability of CuD restrict its therapeutic application. Some studies have described an anti-cancer activity of i.p. or i.t. administered free CuD.[107], [109], [114], [117] Polymer-bound CuD brings the possibility to inject the conjugates i.v. which is in contrast to the devastating effect of i.t. administration of free CuD. Our results have proven the hypothesis that CuD transported by the HPMA nanocarriers is applicable and suitable for

the targeted drug delivery because it significantly reduces systemic toxicity when compared with the i.t. administration of free parent drug. We do not have exact data describing the targeted accumulation of CuD in the tumour microenvironment, normal tissues or its blood clearance as the direct detection of CuD in the tissue samples is not reliable. From our previous experience with conjugates based on Dox [77], [136]; we know that the accumulation of the drug is controlled mainly by the size and structure of the polymer nanocarrier. Therefore, we assume that the accumulation of CuD-bearing polymer conjugates could be similar to other nanomedicines based on other low molecular weight drugs.

For our experiments, we have chosen two distinct types of murine tumours; CT26 colon adenocarcinoma and 4T1 mammary carcinoma. At first, we have performed a flow cytometry analysis of MDSCs levels in tumour-bearing mice in both. Our results together with published literature [124] suggest, that MDSC-mediated immune suppression plays a considerable role in murine 4T1 mammary carcinoma, but might not have such a great impact on the tumour progression in the CT26 colon adenocarcinoma tumour-bearing mice. In line with these findings, the anti-tumour activity of linear CuD-based conjugate in CT26 tumour-bearing mice was not observable as it did not reduce the tumour growth. A mild reduction of tumour size observable in the treatment with linear CuD-based conjugate together with micellar Dox-bearing conjugate was caused probably by the Dox-based nanocarrier as Dox-based micellar conjugate reduced the tumour growth by itself. CuD-based linear conjugate therapy has failed to have any effect on the survival of experimental animals. We hypothesize that the reason for the poor therapeutic efficacy of linear CuD-containing nanocarrier in CT26 treatment lies in the disputable significance of MDSCs-mediated immune suppression in this experimental cancer model. The *in vitro* described cytotoxic effect of CuD-based conjugate on CT26 cells is probably too low to improve either tumour growth or survival of the CT26 tumour-bearing mice. On top of that, CT26 tumour cells have a naturally increased upregulation of the P-glycoprotein expression. [125] It seems that this mechanism, which plays a major role in the difficult-to-treat characteristic of CT26 tumours, is not influenced by the activity of CuD-based conjugates.

On the contrary, the treatment of mice with 4T1 mammary carcinoma showed the potential of the CuD-containing polymer conjugates in combination with targeted Dox-based therapy. We aimed to assess and compare the therapeutic efficacy of linear and micellar CuD-bearing conjugates used as a single therapy or together with Dox-bearing conjugate. As previously documented, the molecular weight and structure of conjugates have an important impact on their biological activity.[77] Micellar nanocarriers are typically formed by the

self-assembly of amphiphilic copolymers and the parent drug is sheltered by the micelle core.[86], [87] CuD-based micellar conjugate was prepared to investigate whether it could mediate a higher accumulation of CuD in the tumour microenvironment as it is known that polymer transport systems with higher molecular weight and larger hydrodynamic radius have prolonged blood circulation, provide more specific tumour localization and yield higher therapeutic efficacy.[137], [138] Unfortunately, the anti-tumour activity of micellar CuD-bearing conjugate was not detectable as a reduction of tumour growth when applied as a sole treatment. The combined treatment together with micellar conjugate bearing Dox significantly reduced the tumour growth, but we hypothesize that the effect was caused mainly by Dox-based polymer conjugate as the sole Dox conjugate treatment yielded similar results. Sole CuD-based micellar conjugate treatment has failed to have any effect on the survival of experimental animals when compared to the untreated control group. Based on the significant hydrophobic nature of CuD, we assume that CuD could remain partially entrapped in the hydrophobic micellar core even after the release from the hydrazone bond. A similar effect has been recently documented in other micellar HPMA-based systems.[139] Based on our results, it seems that the release of the parent drug from the micellar conjugate is not fast enough to be therapeutically efficient therefore the micellar polymer CuD conjugate does not bring any advantage for *in vivo* experimental tumour therapy. Linear CuD conjugate improved the *in vivo* activity of micellar conjugate containing Dox as evidenced by a significant reduction in tumour growth in several experiments. However, the survival prolongation is a parameter better reflecting the potential clinical applicability. Sole linear CuD-based conjugate treatment was not highly efficient in prolonging the lifespan of experimental animals. On the other hand, the addition of checkpoint inhibition by anti-PD-1 monoclonal antibody did have a significant beneficial effect on the survival in the group treated with the combination of linear polymer CuD conjugate together with Dox-based nanomedicine.

Based on the results of *in vivo* experimental therapies and the flow cytometry blood analysis, we investigated the effect of CuD-based linear conjugate on the levels of MDCSs during the early stages of 4T1 tumour development. The peripheral blood analysis one day after the last therapeutic dose has shown a reduction in levels of PMN-MDSCs in the combined therapy, as well as in the sole micellar Dox-bearing conjugate treatment. Single CuD-based conjugate treatment was not as efficient as the other two therapeutic strategies. The effect of polymer prodrugs on MDSCs in the blood a week after the last dose of therapy was not observable. It has been described that Dox can inhibit the expansion and functions of MDSCs and induce their apoptosis.[140], [141] From our results, it may seem that the addition of

CuD-bearing conjugates brings only mild benefit to the inhibition of MDSCs caused by Dox-based therapy. Since the turnover of MDSCs within the tumour microenvironment is very rapid, we hypothesize that CuD-conjugated polymers succeed in the reduction of the tumour growth in the early stages of the tumour development, but fail to significantly extend the survival of the experimental animals. We cannot rule out that we could achieve better therapeutic efficacy via optimizing the therapeutic and dosing scheme of conjugates, but we do not consider it as highly likely.

7 Conclusion

In this diploma thesis, we provide the biological evaluation of linear and micellar HPMA conjugates bearing the immunomodulatory agent CuD bound by the pH-sensitive hydrazone bond. Both types of CuD-based polymer conjugates were characterized by significant cytotoxic activity in several murine and human cancer lines *in vitro*. *In vivo* results suggest only mild therapeutic efficacy of the combined therapy with newly developed CuD-based nanomedicines and micellar HPMA copolymers containing Dox. The proper and optimized dosing of the conjugates remains a task for future investigations. With CuD being probable STAT3 inhibitor, the combination of chemotherapy with immunotherapy targeted on the inhibition of STAT3 signalization could be the path for improving the outcome of cancerous diseases.

The main conclusions of the thesis include:

- Linear and micellar CuD-bearing conjugates exhibit potent cytostatic/cytotoxic activity tested *in vitro* on murine 4T1, CT26 and EL4 cancer cells and human SK-OV-3, OVCAR-3 and DU-145 cancer cells
- The binding of free CuD to an HPMA nanocarrier retains its functional capacity while improving the solubility of the hydrophobic parent drug
- Linear polymer-bound CuD prevents the expansion of MDSC-like $CD11b^{+}Gr1^{+}$ phenotype cultivated *in vitro* as well as the free parent drug
- We confirmed that CuD reduces the levels of phosphorylated STAT3 detected *in vitro* in IL-6 stimulated DU-145 prostate cancer cells
- Polymer-bound CuD brings the advantage to inject the conjugates i.v. which improves its therapeutic applicability in contrast to the i.t. administration of free parent drug
- As a sole treatment, the anti-cancer activity of linear CuD conjugate during *in vivo* CT26 therapy is neither observable as a reduction of tumour growth nor prolongation of survival
- Similarly, the anti-tumour activity of micellar CuD conjugate during *in vivo* 4T1 tumour therapy is neither detectable as a reduction of tumour growth nor survival prolongation
- Linear CuD conjugate improves the activity of micellar Dox-based conjugate as evidenced by a significant reduction in 4T1 tumour growth in several *in vivo* experiments
- Sole linear CuD-based conjugate therapy is not efficient in prolonging the survival of 4T1 tumour-bearing mice and does not bring a significant benefit in prolonging the survival of mice treated with micellar Dox-bearing conjugate
- Linear CuD-based conjugate brings mild benefit to the inhibition of MDSCs caused by Dox-bearing micellar conjugate during *in vivo* 4T1 tumour therapy

8 List of references

[1] F. Bray, J. Ferlay, I. Soerjomataram, R. L. Siegel, L. A. Torre, and A. Jemal, 'Global cancer statistics 2018: GLOBOCAN estimates of incidence and mortality worldwide for 36 cancers in 185 countries', *CA. Cancer J. Clin.*, vol. 68, no. 6, pp. 394–424, 2018, doi: 10.3322/caac.21492.

[2] F. M. Burnet, 'The Concept of Immunological Surveillance', *Immunol. Asp. Neoplasia*, vol. 13, pp. 1–27, 1970, doi: 10.1159/000386035.

[3] G. P. Dunn, A. T. Bruce, H. Ikeda, L. J. Old, and R. D. Schreiber, 'Cancer immunoediting: from immunosurveillance to tumor escape', *Nat. Immunol.*, vol. 3, no. 11, Art. no. 11, Nov. 2002, doi: 10.1038/ni1102-991.

[4] R. Desai and J. Neuberger, 'Donor transmitted and de novo cancer after liver transplantation', *World J. Gastroenterol. WJG*, vol. 20, no. 20, pp. 6170–6179, May 2014, doi: 10.3748/wjg.v20.i20.6170.

[5] M. Hortlund, L. S. A. Mühr, H. Storm, G. Engholm, J. Dillner, and D. Bzhalava, 'Cancer risks after solid organ transplantation and after long-term dialysis', *Int. J. Cancer*, vol. 140, no. 5, pp. 1091–1101, 2017, doi: 10.1002/ijc.30531.

[6] R. Desai and J. Neuberger, 'Donor transmitted and de novo cancer after liver transplantation', *World J. Gastroenterol. WJG*, vol. 20, no. 20, pp. 6170–6179, May 2014, doi: 10.3748/wjg.v20.i20.6170.

[7] H. T. Khong and N. P. Restifo, 'Natural selection of tumor variants in the generation of "tumor escape" phenotypes', *Nat. Immunol.*, vol. 3, no. 11, pp. 999–1005, Nov. 2002, doi: 10.1038/ni1102-999.

[8] N. McGranahan *et al.*, 'Allele-Specific HLA Loss and Immune Escape in Lung Cancer Evolution', *Cell*, vol. 171, no. 6, pp. 1259-1271.e11, Nov. 2017, doi: 10.1016/j.cell.2017.10.001.

[9] G. Driessens, J. Kline, and T. F. Gajewski, 'Costimulatory and coinhibitory receptors in anti-tumor immunity', *Immunol. Rev.*, vol. 229, no. 1, pp. 126–144, May 2009, doi: 10.1111/j.1600-065X.2009.00771.x.

[10] Y. Ishida, Y. Agata, K. Shibahara, and T. Honjo, 'Induced expression of PD-1, a novel member of the immunoglobulin gene superfamily, upon programmed cell death.', *EMBO J.*, vol. 11, no. 11, pp. 3887–3895, Nov. 1992.

[11] E. I. Buchbinder and A. Desai, 'CTLA-4 and PD-1 Pathways: Similarities, Differences, and Implications of Their Inhibition', *Am. J. Clin. Oncol.*, vol. 39, no. 1, pp. 98–106, Feb. 2016, doi: 10.1097/COC.0000000000000239.

[12] S. Colak and P. ten Dijke, 'Targeting TGF-β Signaling in Cancer', *Trends Cancer*, vol. 3, no. 1, pp. 56–71, Jan. 2017, doi: 10.1016/j.trecan.2016.11.008.

[13] S. Zhao, D. Wu, P. Wu, Z. Wang, and J. Huang, 'Serum IL-10 Predicts Worse Outcome in Cancer Patients: A Meta-Analysis', *PLOS ONE*, vol. 10, no. 10, p. e0139598, Oct. 2015, doi: 10.1371/journal.pone.0139598.

[14] T. Oyama *et al.*, 'Vascular Endothelial Growth Factor Affects Dendritic Cell Maturation Through the Inhibition of Nuclear Factor-κB Activation in Hemopoietic Progenitor Cells', *J. Immunol.*, vol. 160, no. 3, pp. 1224–1232, Feb. 1998.

[15] Y. Mizukami *et al.*, 'CCL17 and CCL22 chemokines within tumor microenvironment are related to accumulation of Foxp3+ regulatory T cells in gastric cancer', *Int. J. Cancer*, vol. 122, no. 10, pp. 2286–2293, May 2008, doi: 10.1002/ijc.23392.

[16] D. A. A. Vignali, L. W. Collison, and C. J. Workman, 'How regulatory T cells work', *Nat. Rev. Immunol.*, vol. 8, no. 7, pp. 523–532, Jul. 2008, doi: 10.1038/nri2343.

[17] Y. Ohue and H. Nishikawa, 'Regulatory T (Treg) cells in cancer: Can Treg cells be a new therapeutic target?', *Cancer Sci.*, vol. 110, no. 7, pp. 2080–2089, 2019, doi: https://doi.org/10.1111/cas.14069.

[18] C. Uyttenhove *et al.*, 'Evidence for a tumoral immune resistance mechanism based on tryptophan degradation by indoleamine 2,3-dioxygenase', *Nat. Med.*, vol. 9, no. 10, pp. 1269–1274, Oct. 2003, doi: 10.1038/nm934.

[19] R. B. Holmgaard *et al.*, 'Tumor-Expressed IDO Recruits and Activates MDSCs in a Treg-Dependent Manner', *Cell Rep.*, vol. 13, no. 2, pp. 412–424, Oct. 2015, doi: 10.1016/j.celrep.2015.08.077.
[20] C.-R. Lee *et al.*, 'Myeloid-Derived Suppressor Cells Are Controlled by Regulatory T Cells via TGF-β during Murine Colitis', *Cell Rep.*, vol. 17, no. 12, pp. 3219–3232, Dec. 2016, doi: 10.1016/j.celrep.2016.11.062.
[21] D. I. Gabrilovich, 'Myeloid-derived suppressor cells', *Cancer Immunol. Res.*, vol. 5, no. 1, pp. 3–8, Jan. 2017, doi: 10.1158/2326-6066.CIR-16-0297.
[22] H. Li, Y. Han, Q. Guo, M. Zhang, and X. Cao, 'Cancer-Expanded Myeloid-Derived Suppressor Cells Induce Anergy of NK Cells through Membrane-Bound TGF-β1', *J. Immunol.*, vol. 182, no. 1, pp. 240–249, Jan. 2009, doi: 10.4049/jimmunol.182.1.240.
[23] P. Sinha, V. K. Clements, S. K. Bunt, S. M. Albelda, and S. Ostrand-Rosenberg, 'Cross-Talk between Myeloid-Derived Suppressor Cells and Macrophages Subverts Tumor Immunity toward a Type 2 Response', *J. Immunol.*, vol. 179, no. 2, pp. 977–983, Jul. 2007, doi: 10.4049/jimmunol.179.2.977.
[24] A. H. Zea *et al.*, 'Arginase-Producing Myeloid Suppressor Cells in Renal Cell Carcinoma Patients: A Mechanism of Tumor Evasion', *Cancer Res.*, vol. 65, no. 8, pp. 3044–3048, Apr. 2005, doi: 10.1158/0008-5472.CAN-04-4505.
[25] M. K. Srivastava, P. Sinha, V. K. Clements, P. Rodriguez, and S. Ostrand-Rosenberg, 'Myeloid-derived Suppressor Cells Inhibit T Cell Activation by Depleting Cystine and Cysteine', *Cancer Res.*, vol. 70, no. 1, pp. 68–77, Jan. 2010, doi: 10.1158/0008-5472.CAN-09-2587.
[26] J. Yu *et al.*, 'Myeloid-Derived Suppressor Cells Suppress Antitumor Immune Responses through IDO Expression and Correlate with Lymph Node Metastasis in Patients with Breast Cancer', *J. Immunol.*, vol. 190, no. 7, pp. 3783–3797, Apr. 2013, doi: 10.4049/jimmunol.1201449.
[27] N. de Haas, C. de Koning, L. Spilgies, I. J. M. de Vries, and S. V. Hato, 'Improving cancer immunotherapy by targeting the STATe of MDSCs', *Oncoimmunology*, vol. 5, no. 7, Jun. 2016, doi: 10.1080/2162402X.2016.1196312.
[28] C. A. Corzo *et al.*, 'Mechanism regulating reactive oxygen species in tumor induced myeloid-derived suppressor cells', *J. Immunol. Baltim. Md 1950*, vol. 182, no. 9, pp. 5693–5701, May 2009, doi: 10.4049/jimmunol.0900092.
[29] A. Mazzoni *et al.*, 'Myeloid Suppressor Lines Inhibit T Cell Responses by an NO-Dependent Mechanism', *J. Immunol.*, vol. 168, no. 2, pp. 689–695, Jan. 2002, doi: 10.4049/jimmunol.168.2.689.
[30] S. Nagaraj *et al.*, 'Altered recognition of antigen is a novel mechanism of CD8+ T cell tolerance in cancer', *Nat. Med.*, vol. 13, no. 7, pp. 828–835, Jul. 2007, doi: 10.1038/nm1609.
[31] B. Molon *et al.*, 'Chemokine nitration prevents intratumoral infiltration of antigen-specific T cells', *J. Exp. Med.*, vol. 208, no. 10, pp. 1949–1962, Sep. 2011, doi: 10.1084/jem.20101956.
[32] P.-Y. Pan *et al.*, 'Immune Stimulatory Receptor CD40 Is Required for T-Cell Suppression and T Regulatory Cell Activation Mediated by Myeloid-Derived Suppressor Cells in Cancer', *Cancer Res.*, vol. 70, no. 1, p. 99, Jan. 2010, doi: 10.1158/0008-5472.CAN-09-1882.
[33] B. Huang *et al.*, 'Gr-1+CD115+ Immature Myeloid Suppressor Cells Mediate the Development of Tumor-Induced T Regulatory Cells and T-Cell Anergy in Tumor-Bearing Host', *Cancer Res.*, vol. 66, no. 2, pp. 1123–1131, Jan. 2006, doi: 10.1158/0008-5472.CAN-05-1299.
[34] P. Serafini, S. Mgebroff, K. Noonan, and I. Borrello, 'Myeloid-Derived Suppressor Cells Promote Cross-Tolerance in B-Cell Lymphoma by Expanding Regulatory T Cells', *Cancer Res.*, vol. 68, no. 13, pp. 5439–5449, Jul. 2008, doi: 10.1158/0008-5472.CAN-07-6621.
[35] J.-I. Youn, S. Nagaraj, M. Collazo, and D. I. Gabrilovich, 'Subsets of Myeloid-Derived Suppressor Cells in Tumor Bearing Mice', *J. Immunol. Baltim. Md 1950*, vol. 181, no. 8, pp. 5791–5802, Oct. 2008.
[36] V. Bronte *et al.*, 'Recommendations for myeloid-derived suppressor cell nomenclature and characterization standards', *Nat. Commun.*, vol. 7, Jul. 2016, doi: 10.1038/ncomms12150.
[37] F. Zhao *et al.*, 'Increase in frequency of myeloid-derived suppressor cells in mice with spontaneous pancreatic carcinoma', *Immunology*, vol. 128, no. 1, pp. 141–149, Sep. 2009, doi: 10.1111/j.1365-2567.2009.03105.x.

[38] L. Dolcetti *et al.*, 'Hierarchy of immunosuppressive strength among myeloid-derived suppressor cell subsets is determined by GM-CSF', *Eur. J. Immunol.*, vol. 40, no. 1, pp. 22–35, 2010, doi: https://doi.org/10.1002/eji.200939903.
[39] K. Movahedi *et al.*, 'Identification of discrete tumor-induced myeloid-derived suppressor cell subpopulations with distinct T cell–suppressive activity', *Blood*, vol. 111, no. 8, pp. 4233–4244, Apr. 2008, doi: 10.1182/blood-2007-07-099226.
[40] P. Filipazzi *et al.*, 'Identification of a New Subset of Myeloid Suppressor Cells in Peripheral Blood of Melanoma Patients With Modulation by a Granulocyte-Macrophage Colony-Stimulation Factor–Based Antitumor Vaccine', *J. Clin. Oncol.*, vol. 25, no. 18, pp. 2546–2553, Jun. 2007, doi: 10.1200/JCO.2006.08.5829.
[41] P.-H. Feng *et al.*, 'CD14+S100A9+ Monocytic Myeloid-derived Suppressor Cells and Their Clinical Relevance in Non–Small Cell Lung Cancer', *Am. J. Respir. Crit. Care Med.*, vol. 186, no. 10, pp. 1025–1036, Nov. 2012, doi: 10.1164/rccm.201204-0636OC.
[42] T. Condamine, J. Mastio, and D. I. Gabrilovich, 'Transcriptional regulation of myeloid-derived suppressor cells', *J. Leukoc. Biol.*, vol. 98, no. 6, pp. 913–922, Dec. 2015, doi: 10.1189/jlb.4RI0515-204R.
[43] Z. Duan *et al.*, 'Signal Transducers and Activators of Transcription 3 Pathway Activation in Drug-Resistant Ovarian Cancer', *Clin. Cancer Res.*, vol. 12, no. 17, pp. 5055–5063, Sep. 2006, doi: 10.1158/1078-0432.CCR-06-0861.
[44] M. Huang, C. Page, R. K. Reynolds, and J. Lin, 'Constitutive Activation of Stat 3 Oncogene Product in Human Ovarian Carcinoma Cells', *Gynecol. Oncol.*, vol. 79, no. 1, pp. 67–73, Oct. 2000, doi: 10.1006/gyno.2000.5931.
[45] B. E. Barton, J. G. Karras, T. F. Murphy, A. Barton, and H. F.-S. Huang, 'Signal transducer and activator of transcription 3 (STAT3) activation in prostate cancer: Direct STAT3 inhibition induces apoptosis in prostate cancer lines', *Mol. Cancer Ther.*, vol. 3, no. 1, pp. 11–20, Jan. 2004.
[46] H. Yu *et al.*, 'SOCS3 Deficiency in Myeloid Cells Promotes Tumor Development: Involvement of STAT3 Activation and Myeloid-Derived Suppressor Cells', *Cancer Immunol. Res.*, vol. 3, no. 7, pp. 727–740, Jul. 2015, doi: 10.1158/2326-6066.CIR-15-0004.
[47] I. Poschke, D. Mougiakakos, J. Hansson, G. V. Masucci, and R. Kiessling, 'Immature Immunosuppressive CD14+HLA-DR−/low Cells in Melanoma Patients Are Stat3hi and Overexpress CD80, CD83, and DC-Sign', *Cancer Res.*, vol. 70, no. 11, pp. 4335–4345, Jun. 2010, doi: 10.1158/0008-5472.CAN-09-3767.
[48] T. Condamine and D. I. Gabrilovich, 'Molecular mechanisms regulating myeloid-derived suppressor cell differentiation and function', *Trends Immunol.*, vol. 32, no. 1, pp. 19–25, Jan. 2011, doi: 10.1016/j.it.2010.10.002.
[49] P. Cheng *et al.*, 'Inhibition of dendritic cell differentiation and accumulation of myeloid-derived suppressor cells in cancer is regulated by S100A9 protein', *J. Exp. Med.*, vol. 205, no. 10, pp. 2235–2249, Sep. 2008, doi: 10.1084/jem.20080132.
[50] D. Vasquez-Dunddel *et al.*, 'STAT3 regulates arginase-I in myeloid-derived suppressor cells from cancer patients', *J. Clin. Invest.*, vol. 123, no. 4, pp. 1580–1589, Apr. 2013, doi: 10.1172/JCI60083.
[51] C. A. Corzo *et al.*, 'Mechanism regulating reactive oxygen species in tumor induced myeloid-derived suppressor cells', *J. Immunol. Baltim. Md 1950*, vol. 182, no. 9, pp. 5693–5701, May 2009, doi: 10.4049/jimmunol.0900092.
[52] H. Yuan *et al.*, 'Axitinib augments antitumor activity in renal cell carcinoma via STAT3-dependent reversal of myeloid-derived suppressor cell accumulation', *Biomed. Pharmacother.*, vol. 68, no. 6, pp. 751–756, Jul. 2014, doi: 10.1016/j.biopha.2014.07.002.
[53] M. Cao *et al.*, 'Kinase Inhibitor Sorafenib Modulates Immunosuppressive Cell Populations in a Murine Liver Cancer Model', *Lab. Investig. J. Tech. Methods Pathol.*, vol. 91, no. 4, pp. 598–608, Apr. 2011, doi: 10.1038/labinvest.2010.205.
[54] H. Xin, C. Zhang, A. Herrmann, Y. Du, R. Figlin, and H. Yu, 'Sunitinib inhibition of Stat3 induces renal cell carcinoma tumor cell apoptosis and reduces immunosuppressive cells', *Cancer Res.*, vol. 69, no. 6, pp. 2506–2513, Mar. 2009, doi: 10.1158/0008-5472.CAN-08-4323.
[55] Y. Nefedova, S. Nagaraj, A. Rosenbauer, C. Muro-Cacho, S. M. Sebti, and D. I. Gabrilovich, 'Regulation of dendritic cell differentiation and antitumor immune response in cancer by

pharmacological selective inhibition of the Jak2/STAT3 pathway', *Cancer Res.*, vol. 65, no. 20, pp. 9525–9535, Oct. 2005, doi: 10.1158/0008-5472.CAN-05-0529.
[56] T. Achkar *et al.*, 'High-dose interleukin 2 in patients with metastatic renal cell carcinoma with sarcomatoid features', *PLOS ONE*, vol. 12, no. 12, p. e0190084, Dec. 2017, doi: 10.1371/journal.pone.0190084.
[57] R. Bright, B. J. Coventry, N. Eardley-Harris, and N. Briggs, 'Clinical Response Rates From Interleukin-2 Therapy for Metastatic Melanoma Over 30 Years' Experience: A Meta-Analysis of 3312 Patients', *J. Immunother.*, vol. 40, no. 1, pp. 21–30, Jan. 2017, doi: 10.1097/CJI.0000000000000149.
[58] A. A. Tarhini, H. Gogas, and J. M. Kirkwood, 'IFN-α in the Treatment of Melanoma', *J. Immunol. Baltim. Md 1950*, vol. 189, no. 8, pp. 3789–3793, Oct. 2012, doi: 10.4049/jimmunol.1290060.
[59] K. Yaddanapudi, R. A. Mitchell, and J. W. Eaton, 'Cancer vaccines', *OncoImmunology*, vol. 2, no. 3, p. e23403, Mar. 2013, doi: 10.4161/onci.23403.
[60] P. W. Kantoff *et al.*, 'Sipuleucel-T immunotherapy for castration-resistant prostate cancer', *N. Engl. J. Med.*, vol. 363, no. 5, pp. 411–422, Jul. 2010, doi: 10.1056/NEJMoa1001294.
[61] R. Andersen *et al.*, 'Long-Lasting Complete Responses in Patients with Metastatic Melanoma after Adoptive Cell Therapy with Tumor-Infiltrating Lymphocytes and an Attenuated IL2 Regimen', *Clin. Cancer Res.*, vol. 22, no. 15, pp. 3734–3745, Aug. 2016, doi: 10.1158/1078-0432.CCR-15-1879.
[62] B. Heyman and Y. Yang, 'Chimeric Antigen Receptor T Cell Therapy for Solid Tumors: Current Status, Obstacles and Future Strategies', *Cancers*, vol. 11, no. 2, Feb. 2019, doi: 10.3390/cancers11020191.
[63] Y. Wang, D. Fei, M. Vanderlaan, and A. Song, 'Biological activity of bevacizumab, a humanized anti-VEGF antibody in vitro', *Angiogenesis*, vol. 7, no. 4, pp. 335–345, Dec. 2004, doi: 10.1007/s10456-004-8272-2.
[64] H. Hurwitz *et al.*, 'Bevacizumab plus Irinotecan, Fluorouracil, and Leucovorin for Metastatic Colorectal Cancer', *N. Engl. J. Med.*, vol. 350, no. 23, pp. 2335–2342, Jun. 2004, doi: 10.1056/NEJMoa032691.
[65] T. Kato *et al.*, 'Erlotinib Plus Bevacizumab Phase ll Study in Patients with Advanced Non-small-Cell Lung Cancer (JO25567): Updated Safety Results', *Drug Saf.*, vol. 41, no. 2, pp. 229–237, 2018, doi: 10.1007/s40264-017-0596-0.
[66] G. Salles *et al.*, 'Rituximab in B-Cell Hematologic Malignancies: A Review of 20 Years of Clinical Experience', *Adv. Ther.*, vol. 34, no. 10, pp. 2232–2273, Oct. 2017, doi: 10.1007/s12325-017-0612-x.
[67] M. J. Piccart-Gebhart *et al.*, 'Trastuzumab after adjuvant chemotherapy in HER2-positive breast cancer', *N. Engl. J. Med.*, vol. 353, no. 16, pp. 1659–1672, Oct. 2005, doi: 10.1056/NEJMoa052306.
[68] I. Krop and E. P. Winer, 'Trastuzumab Emtansine: A Novel Antibody–Drug Conjugate for HER2-Positive Breast Cancer', *Clin. Cancer Res.*, vol. 20, no. 1, pp. 15–20, Jan. 2014, doi: 10.1158/1078-0432.CCR-13-0541.
[69] L. J. Scott, 'Brentuximab Vedotin: A Review in CD30-Positive Hodgkin Lymphoma', *Drugs*, vol. 77, no. 4, pp. 435–445, 2017, doi: 10.1007/s40265-017-0705-5.
[70] P. Gq *et al.*, 'Cancer regression and autoimmunity induced by cytotoxic T lymphocyte-associated antigen 4 blockade in patients with metastatic melanoma.', *Proc. Natl. Acad. Sci. U. S. A.*, vol. 100, no. 14, pp. 8372–8377, Jun. 2003, doi: 10.1073/pnas.1533209100.
[71] H. T. Lee *et al.*, 'Molecular mechanism of PD-1/PD-L1 blockade via anti-PD-L1 antibodies atezolizumab and durvalumab', *Sci. Rep.*, vol. 7, Jul. 2017, doi: 10.1038/s41598-017-06002-8.
[72] J. Larkin *et al.*, 'Combined Nivolumab and Ipilimumab or Monotherapy in Untreated Melanoma', *N. Engl. J. Med.*, vol. 373, no. 1, pp. 23–34, Jul. 2015, doi: 10.1056/NEJMoa1504030.
[73] E. Pérez-Herrero and A. Fernández-Medarde, 'Advanced targeted therapies in cancer: Drug nanocarriers, the future of chemotherapy', *Eur. J. Pharm. Biopharm.*, vol. 93, pp. 52–79, Jun. 2015, doi: 10.1016/j.ejpb.2015.03.018.

[74] J. Yang and J. Kopeček, 'MACROMOLECULAR THERAPEUTICS', *J. Control. Release Off. J. Control. Release Soc.*, vol. 0, pp. 288–303, Sep. 2014, doi: 10.1016/j.jconrel.2014.04.013.
[75] T. Etrych, M. Jelínková, B. Říhová, and K. Ulbrich, 'New HPMA copolymers containing doxorubicin bound via pH-sensitive linkage: synthesis and preliminary in vitro and in vivo biological properties', *J. Controlled Release*, vol. 73, no. 1, pp. 89–102, May 2001, doi: 10.1016/S0168-3659(01)00281-4.
[76] V. Šubr, J. Kopeček, J. Pohl, M. Baudyš, and V. Kostka, 'Cleavage of oligopeptide side-chains in N-(2-hydroxypropyl)meth-acrylamide copolymers by mixtures of lysosomal enzymes', *J. Controlled Release*, vol. 8, no. 2, pp. 133–140, Dec. 1988, doi: 10.1016/0168-3659(88)90039-9.
[77] T. Etrych, V. Šubr, J. Strohalm, M. Šírová, B. Říhová, and K. Ulbrich, 'HPMA copolymer-doxorubicin conjugates: The effects of molecular weight and architecture on biodistribution and in vivo activity', *J. Controlled Release*, vol. 164, no. 3, pp. 346–354, Dec. 2012, doi: 10.1016/j.jconrel.2012.06.029.
[78] R. N. Johnson, P. Kopečková, and J. Kopeček, 'Biological Activity of Anti-CD20 Multivalent HPMA Copolymer-Fab' Conjugates', *Biomacromolecules*, vol. 13, no. 3, pp. 727–735, Mar. 2012, doi: 10.1021/bm201656k.
[79] Y. Matsumura and H. Maeda, 'A New Concept for Macromolecular Therapeutics in Cancer Chemotherapy: Mechanism of Tumoritropic Accumulation of Proteins and the Antitumor Agent Smancs', *Cancer Res.*, vol. 46, no. 12 Part 1, pp. 6387–6392, Dec. 1986.
[80] S. K. Golombek *et al.*, 'Tumor Targeting via EPR: Strategies to Enhance Patient Responses', *Adv. Drug Deliv. Rev.*, vol. 130, pp. 17–38, May 2018, doi: 10.1016/j.addr.2018.07.007.
[81] K. J. Harrington *et al.*, 'Effective Targeting of Solid Tumors in Patients With Locally Advanced Cancers by Radiolabeled Pegylated Liposomes', *Clin. Cancer Res.*, vol. 7, no. 2, pp. 243–254, Feb. 2001.
[82] Y. (Chezy) Barenholz, 'Doxil® — The first FDA-approved nano-drug: Lessons learned', *J. Controlled Release*, vol. 160, no. 2, pp. 117–134, Jun. 2012, doi: 10.1016/j.jconrel.2012.03.020.
[83] T. Lammers, F. Kiessling, M. Ashford, W. Hennink, D. Crommelin, and G. Storm, 'Cancer nanomedicine: Is targeting our target?', *Nat. Rev. Mater.*, vol. 1, no. 9, Sep. 2016, doi: 10.1038/natrevmats.2016.69.
[84] G. Pasut and F. M. Veronese, 'State of the art in PEGylation: The great versatility achieved after forty years of research', *J. Controlled Release*, vol. 161, no. 2, pp. 461–472, Jul. 2012, doi: 10.1016/j.jconrel.2011.10.037.
[85] J. Kopeček and H. Bažilová, 'Poly[N-(2-hydroxypropyl)methacrylamide]—I. Radical polymerization and copolymerization', *Eur. Polym. J.*, vol. 9, no. 1, pp. 7–14, Jan. 1973, doi: 10.1016/0014-3057(73)90063-3.
[86] L. Kostka and T. Etrych, 'High-molecular-weight HPMA-based polymer drug carriers for delivery to tumor', *Physiol. Res.*, vol. 65, no. Suppl 2, pp. S179–S190, Oct. 2016, doi: 10.33549/physiolres.933420.
[87] P. Chytil, E. Koziolová, T. Etrych, and K. Ulbrich, 'HPMA Copolymer–Drug Conjugates with Controlled Tumor-Specific Drug Release', *Macromol. Biosci.*, vol. 18, no. 1, p. 1700209, 2018, doi: https://doi.org/10.1002/mabi.201700209.
[88] M. Sirova *et al.*, 'Preclinical Evaluation of Linear HPMA-Doxorubicin Conjugates with pH-Sensitive Drug Release: Efficacy, Safety, and Immunomodulating Activity in Murine Model', *Pharm. Res.*, vol. 27, no. 1, p. 200, Nov. 2009, doi: 10.1007/s11095-009-9999-7.
[89] T. Etrych, M. Šírová, L. Starovoytova, B. Říhová, and K. Ulbrich, 'HPMA Copolymer Conjugates of Paclitaxel and Docetaxel with pH-Controlled Drug Release', *Mol. Pharm.*, vol. 7, no. 4, pp. 1015–1026, Aug. 2010, doi: 10.1021/mp100119f.
[90] T. Etrych *et al.*, 'High-molecular weight star conjugates containing docetaxel with high anti-tumor activity and low systemic toxicity in vivo', *Polym. Chem.*, vol. 6, no. 1, pp. 160–170, Dec. 2014, doi: 10.1039/C4PY01120A.
[91] B. Říhová and M. Kovář, 'Immunogenicity and immunomodulatory properties of HPMA-based polymers', *Adv. Drug Deliv. Rev.*, vol. 62, no. 2, pp. 184–191, Feb. 2010, doi: 10.1016/j.addr.2009.10.005.
[92] K. Ulbrich, K. Holá, V. Šubr, A. Bakandritsos, J. Tuček, and R. Zbořil, 'Targeted Drug Delivery with Polymers and Magnetic Nanoparticles: Covalent and Noncovalent Approaches, Release

Control, and Clinical Studies', *Chem. Rev.*, vol. 116, no. 9, pp. 5338–5431, May 2016, doi: 10.1021/acs.chemrev.5b00589.
[93] L. W. Seymour *et al.*, 'Phase II studies of polymer-doxorubicin (PK1, FCE28068) in the treatment of breast, lung and colorectal cancer', *Int. J. Oncol.*, vol. 34, no. 6, pp. 1629–1636, Jun. 2009, doi: 10.3892/ijo_00000293.
[94] B. Rihova *et al.*, 'Induction of Systemic Antitumour Resistance with Targeted Polymers', *Scand. J. Immunol.*, vol. 62, no. s1, pp. 100–105, 2005, doi: https://doi.org/10.1111/j.1365-3083.2005.01617.x.
[95] M. Sirova *et al.*, 'Treatment with HPMA copolymer-based doxorubicin conjugate containing human immunoglobulin induces long-lasting systemic anti-tumour immunity in mice', *Cancer Immunol. Immunother.*, vol. 56, no. 1, pp. 35–47, Jan. 2007, doi: 10.1007/s00262-006-0168-0.
[96] T. Mrkvan *et al.*, 'Chemotherapy based on HPMA copolymer conjugates with pH-controlled release of doxorubicin triggers anti-tumor immunity', *J. Controlled Release*, vol. 110, no. 1, pp. 119–129, Dec. 2005, doi: 10.1016/j.jconrel.2005.09.028.
[97] S. M. *et al.*, 'HPMA Copolymer-Bound Doxorubicin Induces Immunogenic Tumor Cell Death', *Curr. Med. Chem.*, vol. 20, no. 38, pp. 4815–4826, Nov. 2013.
[98] L. Apetoh *et al.*, 'Toll-like receptor 4–dependent contribution of the immune system to anticancer chemotherapy and radiotherapy', *Nat. Med.*, vol. 13, no. 9, Art. no. 9, Sep. 2007, doi: 10.1038/nm1622.
[99] M. Obeid *et al.*, 'Calreticulin exposure dictates the immunogenicity of cancer cell death', *Nat. Med.*, vol. 13, no. 1, Art. no. 1, Jan. 2007, doi: 10.1038/nm1523.
[100] D. H. Lee, G. B. Iwanski, and N. H. Thoennissen, 'Cucurbitacin: Ancient Compound Shedding New Light on Cancer Treatment', p. 7, 2010.
[101] Y. Cai *et al.*, 'Cucurbitacins: A Systematic Review of the Phytochemistry and Anticancer Activity', *Am. J. Chin. Med.*, vol. 43, no. 07, pp. 1331–1350, Jan. 2015, doi: 10.1142/S0192415X15500755.
[102] X. Chen *et al.*, 'Biological activities and potential molecular targets of cucurbitacins: a focus on cancer', *Anticancer. Drugs*, vol. 23, no. 8, pp. 777–787, Sep. 2012, doi: 10.1097/CAD.0b013e3283541384.
[103] O. Molavi *et al.*, 'Polymeric micelles for the solubilization and delivery of STAT3 inhibitor cucurbitacins in solid tumors', *Int. J. Pharm.*, vol. 347, no. 1–2, pp. 118–127, Jan. 2008, doi: 10.1016/j.ijpharm.2007.06.032.
[104] S. Gitter, R. Gallily, B. Shohat, and D. Lavie, 'Studies on the Antitumor Effect of Cucurbitacins', *Cancer Res.*, vol. 21, no. 4, pp. 516–521, May 1961.
[105] R. Gallily, B. Shohat, J. Kalish, S. Gitter, and D. Lavie, 'Further Studies on the Antitumor Effect of Cucurbitacins', *Cancer Res.*, vol. 22, no. 9, pp. 1038–1045, Oct. 1962.
[106] B. Jayaprakasam, N. P. Seeram, and M. G. Nair, 'Anticancer and antiinflammatory activities of cucurbitacins from Cucurbita andreana', *Cancer Lett.*, vol. 189, no. 1, pp. 11–16, Jan. 2003, doi: 10.1016/S0304-3835(02)00497-4.
[107] N. Ding *et al.*, 'Apoptosis induction through proteasome inhibitory activity of cucurbitacin D in human T-cell leukemia', *Cancer*, vol. 117, no. 12, pp. 2735–2746, 2011, doi: https://doi.org/10.1002/cncr.25711.
[108] N. Takahashi, Y. Yoshida, T. Sugiura, K. Matsuno, A. Fujino, and U. Yamashita, 'Cucurbitacin D isolated from Trichosanthes kirilowii induces apoptosis in human hepatocellular carcinoma cells in vitro', *Int. Immunopharmacol.*, vol. 9, no. 4, pp. 508–513, Apr. 2009, doi: 10.1016/j.intimp.2009.01.006.
[109] M. Sikander *et al.*, 'Novel Mechanistic Insight into the Anticancer Activity of Cucurbitacin D against Pancreatic Cancer (Cuc D Attenuates Pancreatic Cancer)', *Cells*, vol. 9, no. 1, Art. no. 1, Jan. 2020, doi: 10.3390/cells9010103.
[110] M. Sikander *et al.*, 'Cucurbitacin D Reprograms Glucose Metabolic Network in Prostate Cancer', *Cancers*, vol. 11, no. 3, Art. no. 3, Mar. 2019, doi: 10.3390/cancers11030364.
[111] S. Jing *et al.*, 'Cucurbitacins: Bioactivities and synergistic effect with small-molecule drugs', *J. Funct. Foods*, vol. 72, p. 104042, Sep. 2020, doi: 10.1016/j.jff.2020.104042.

[112] T. Ishii, N. Kira, T. Yoshida, and H. Narahara, 'Cucurbitacin D induces growth inhibition, cell cycle arrest, and apoptosis in human endometrial and ovarian cancer cells', *Tumor Biol.*, vol. 34, no. 1, pp. 285–291, Feb. 2013, doi: 10.1007/s13277-012-0549-2.
[113] S. A. Spear *et al.*, 'Natural Compounds as Potential Treatments of NF2-Deficient Schwannoma and Meningioma: Cucurbitacin D and Goyazensolide', *Otol. Neurotol. Off. Publ. Am. Otol. Soc. Am. Neurotol. Soc. Eur. Acad. Otol. Neurotol.*, vol. 34, no. 8, pp. 1519–1527, Oct. 2013, doi: 10.1097/MAO.0b013e3182956169.
[114] T. Nakanishi *et al.*, 'Autophagy is associated with cucurbitacin D-induced apoptosis in human T cell leukemia cells', *Med. Oncol.*, vol. 33, no. 4, p. 30, Feb. 2016, doi: 10.1007/s12032-016-0743-y.
[115] Y. Wang, Y. Shen, S. Wang, Q. Shen, and X. Zhou, 'The Role of STAT3 in Leading the Crosstalk between Human Cancers and the Immune System', *Cancer Lett.*, vol. 415, pp. 117–128, Feb. 2018, doi: 10.1016/j.canlet.2017.12.003.
[116] S. R. Kim *et al.*, 'Trichosanthes kirilowii Ethanol Extract and Cucurbitacin D Inhibit Cell Growth and Induce Apoptosis through Inhibition of STAT3 Activity in Breast Cancer Cells', *Evid. Based Complement. Alternat. Med.*, vol. 2013, p. e975350, Sep. 2013, doi: 10.1155/2013/975350.
[117] M. Sikander *et al.*, 'Cucurbitacin D exhibits potent anti-cancer activity in cervical cancer', *Sci. Rep.*, vol. 6, no. 1, Art. no. 1, Nov. 2016, doi: 10.1038/srep36594.
[118] Y. Xia, S. Shen, and I. M. Verma, 'NF-κB, an active player in human cancers', *Cancer Immunol. Res.*, vol. 2, no. 9, pp. 823–830, Sep. 2014, doi: 10.1158/2326-6066.CIR-14-0112.
[119] J. M. Ku *et al.*, 'Cucurbitacin D induces cell cycle arrest and apoptosis by inhibiting STAT3 and NF-κB signaling in doxorubicin-resistant human breast carcinoma (MCF7/ADR) cells', *Mol. Cell. Biochem.*, vol. 409, no. 1–2, pp. 33–43, 2015, doi: 10.1007/s11010-015-2509-9.
[120] J. M. Ku *et al.*, 'Cucurbitacin D exhibits its anti-cancer effect in human breast cancer cells by inhibiting Stat3 and Akt signaling', *Eur. J. Inflamm.*, vol. 16, p. 1721727X17751809, Jan. 2018, doi: 10.1177/1721727X17751809.
[121] M. R. Tavares *et al.*, 'HPMA-Based Copolymers Carrying STAT3 Inhibitor Cucurbitacin-D as Stimulus-Sensitive Nanomedicines for Oncotherapy', *Pharmaceutics*, vol. 13, no. 2, Jan. 2021, doi: 10.3390/pharmaceutics13020179.
[122] J. Abdulghani *et al.*, 'Stat3 Promotes Metastatic Progression of Prostate Cancer', *Am. J. Pathol.*, vol. 172, no. 6, pp. 1717–1728, Jun. 2008, doi: 10.2353/ajpath.2008.071054.
[123] J. Schust, B. Sperl, A. Hollis, T. U. Mayer, and T. Berg, 'Stattic: A Small-Molecule Inhibitor of STAT3 Activation and Dimerization', *Chem. Biol.*, vol. 13, no. 11, pp. 1235–1242, Nov. 2006, doi: 10.1016/j.chembiol.2006.09.018.
[124] M. Ouzounova *et al.*, 'Monocytic and granulocytic myeloid derived suppressor cells differentially regulate spatiotemporal tumour plasticity during metastatic cascade', *Nat. Commun.*, vol. 8, Apr. 2017, doi: 10.1038/ncomms14979.
[125] L. Sivak *et al.*, 'Overcoming multidrug resistance via simultaneous delivery of cytostatic drug and P-glycoprotein inhibitor to cancer cells by HPMA copolymer conjugate', *Biomaterials*, vol. 115, pp. 65–80, Jan. 2017, doi: 10.1016/j.biomaterials.2016.11.013.
[126] E. Randárová *et al.*, 'Highly effective anti-tumor nanomedicines based on HPMA copolymer conjugates with pirarubicin prepared by controlled RAFT polymerization', *Acta Biomater.*, vol. 106, pp. 256–266, Apr. 2020, doi: 10.1016/j.actbio.2020.02.011.
[127] B. Říhová *et al.*, 'Synergistic Action of Doxorubicin Bound to the Polymeric Carrier Based on N-(2-Hydroxypropyl)methacrylamide Copolymers through an Amide or Hydrazone Bond', *Mol. Pharm.*, vol. 7, no. 4, pp. 1027–1040, Aug. 2010, doi: 10.1021/mp100121g.
[128] R. Pola *et al.*, 'Polymer Cancerostatics Targeted by Recombinant Antibody Fragments to GD2-Positive Tumor Cells', *Biomacromolecules*, vol. 20, no. 1, pp. 412–421, Jan. 2019, doi: 10.1021/acs.biomac.8b01616.
[129] M. Pechar *et al.*, 'Polymer Cancerostatics Targeted with an Antibody Fragment Bound via a Coiled Coil Motif: In Vivo Therapeutic Efficacy against Murine BCL1 Leukemia', *Macromol. Biosci.*, vol. 18, no. 1, p. 1700173, 2018, doi: https://doi.org/10.1002/mabi.201700173.
[130] W. Ge *et al.*, 'Synthesis of Cucurbitacin B Derivatives as Potential Anti-Hepatocellular Carcinoma Agents', *Molecules*, vol. 23, no. 12, Art. no. 12, Dec. 2018, doi: 10.3390/molecules23123345.

[131] U. Kaushik, V. Aeri, and S. R. Mir, 'Cucurbitacins – An insight into medicinal leads from nature', *Pharmacogn. Rev.*, vol. 9, no. 17, pp. 12–18, 2015, doi: 10.4103/0973-7847.156314.
[132] M. Studenovsky *et al.*, 'Polymer nitric oxide donors potentiate the treatment of experimental solid tumours by increasing drug accumulation in the tumour tissue', *J. Controlled Release*, vol. 269, pp. 214–224, Jan. 2018, doi: 10.1016/j.jconrel.2017.11.017.
[133] C. Ma, T. Kapanadze, J. Gamrekelashvili, M. P. Manns, F. Korangy, and T. F. Greten, 'Anti-Gr-1 antibody depletion fails to eliminate hepatic myeloid-derived suppressor cells in tumor-bearing mice', *J. Leukoc. Biol.*, vol. 92, no. 6, pp. 1199–1206, Dec. 2012, doi: 10.1189/jlb.0212059.
[134] J. S. Ko, R. M. Bukowski, and J. H. Fincke, 'Myeloid-derived suppressor cells: a novel therapeutic target', *Curr. Oncol. Rep.*, vol. 11, no. 2, pp. 87–93, Mar. 2009, doi: 10.1007/s11912-009-0014-6.
[135] M. K. Srivastava *et al.*, 'Myeloid Suppressor Cell Depletion Augments Antitumor Activity in Lung Cancer', *PLOS ONE*, vol. 7, no. 7, p. e40677, Jul. 2012, doi: 10.1371/journal.pone.0040677.
[136] A.-K. Noack, H. Lucas, P. Chytil, T. Etrych, K. Mäder, and T. Mueller, 'Intratumoral Distribution and pH-Dependent Drug Release of High Molecular Weight HPMA Copolymer Drug Conjugates Strongly Depend on Specific Tumor Substructure and Microenvironment', *Int. J. Mol. Sci.*, vol. 21, no. 17, Aug. 2020, doi: 10.3390/ijms21176029.
[137] B. Tomalova *et al.*, 'The structure-dependent toxicity, pharmacokinetics and anti-tumour activity of HPMA copolymer conjugates in the treatment of solid tumours and leukaemia', *J. Controlled Release*, vol. 223, pp. 1–10, Feb. 2016, doi: 10.1016/j.jconrel.2015.12.023.
[138] T. Etrych, P. Chytil, T. Mrkvan, M. Šírová, B. Říhová, and K. Ulbrich, 'Conjugates of doxorubicin with graft HPMA copolymers for passive tumor targeting', *J. Controlled Release*, vol. 132, no. 3, pp. 184–192, Dec. 2008, doi: 10.1016/j.jconrel.2008.04.017.
[139] A. Braunová *et al.*, 'Polymer nanomedicines based on micelle-forming amphiphilic or water-soluble polymer-doxorubicin conjugates: Comparative study of in vitro and in vivo properties related to the polymer carrier structure, composition, and hydrodynamic properties', *J. Controlled Release*, vol. 321, pp. 718–733, May 2020, doi: 10.1016/j.jconrel.2020.03.002.
[140] J. G. Navashenaq, P. Zamani, A. R. Nikpoor, J. Tavakkol-Afshari, and M. R. Jaafari, 'Doxil chemotherapy plus liposomal P5 immunotherapy decreased myeloid-derived suppressor cells in murine model of breast cancer', *Nanomedicine Nanotechnol. Biol. Med.*, vol. 24, p. 102150, Feb. 2020, doi: 10.1016/j.nano.2020.102150.
[141] D. Alizadeh *et al.*, 'Doxorubicin Eliminates Myeloid-Derived Suppressor Cells and Enhances the Efficacy of Adoptive T Cell Transfer in Breast Cancer', *Cancer Res.*, vol. 74, no. 1, pp. 104–118, Jan. 2014, doi: 10.1158/0008-5472.CAN-13-1545.

9 Appendix

Following results presented in this diploma thesis have already been published:

M. R. Tavares *et al.*, 'HPMA-Based Copolymers Carrying STAT3 Inhibitor Cucurbitacin-D as Stimulus-Sensitive Nanomedicines for Oncotherapy', *Pharmaceutics*, vol. 13, no. 2, Jan. 2021, doi: 10.3390/pharmaceutics13020179.